MASS. INST. OF TECHNOLOGY
SEP 15 1965
LIBRARIES

"ON THE MECHANICS OF TWIST INSERTION"

By

ALY H. M. EL-SHIEKH

B.Sc. University of Alexandria, U.A.R.
1956

S.M. Massachusetts Institute of Technology
1961

M.E. Massachusetts Institute of Technology
1964

Submitted in Partial Fulfillment
of the Requirements for the
Degree of Doctor of Science
at the
MASSACHUSETTS INSTITUTE OF TECHNOLOGY
May 1965

Signature of the Author.....
Department of Mechanical Engineering
Fibers and Polymers Division

Certified by.....
Thesis Supervisor

Accepted by.....
Chairman Departmental Committee on Graduate Students

ACKNOWLEDGMENT

I would like to express my sincere gratitude to Professor Stanley Backer for his guidance, criticism, encouragement and help during my graduate work at M.I.T.

I would also like to extend my thanks to Professor Brandon Rightmire and Professor Robert Mann for the interest they showed by serving on my doctoral committee and for their guidance during this investigation.

I am indebted to Professor John Hearle for his many valuable suggestions and discussions during the year he spent at M.I.T.

I would like to thank all my friends and colleagues in the Division for their help during the course of this investigation. Special thanks are due to Peter Popper, Franco Marzoli and Dieter Ender.

I wish to express my appreciation to Miss Dorothy Eastman for her many typing hours in the preparation of this thesis.

I am deeply indebted to the Government of the United Arab Republic whose financial support has made my graduate program possible.

Without the active encouragement, inspiration and patience of both my mother and wife during my graduate career, this thesis would not have been possible.

To Nina, a young lady of 3, who kept encouraging me every night I had to go to work with these words "Have a good luck, daddy", this thesis is dedicated.

ABSTRACT

ON THE MECHANICS OF TWIST INSERTION

by

ALY H. M. EL-SHIEKH

Submitted to the Department of Mechanical Engineering
Fibers and Polymers Division, on May 14, 1965 in
Partial Fulfillment of the Requirements for the Degree of
Doctor of Science in Mechanical Engineering

This investigation is directed toward an improved understanding of the mechanisms and actions taking place in the textile twisting process. During conventional twisting, material is fed into the system at a constant rate and in the form of a flat ribbon, composed either of continuous filaments or short discontinuous fibers such as cotton or wool. Upon passing the delivery point, the ribbon is continuously twisted into a compact yarn structure. During twisting, the different filaments comprising the ribbon compete for the central position in the yarn structure. The difference in fiber path lengths between inner and outer yarn layers leads to tension variation between the fibers and this, in turn, causes a continuous change of fiber position along the yarn length.

The mechanism of this fiber interchange, or migration, was studied theoretically and experimentally. It was found that in open structures outward migration occurs when predetermined slack develops in the pretwist zone. In closed structures, outward migration occurs when the central fiber buckles compressively against the surrounding fiber matrix. The experimentally measured migration frequencies agreed well (within 10-20%) with the theoretically predicted values.

Further downstream in the twisting zone the newly formed structure whirls around a rotating spindle in a twisting balloon. Twist distribution in this zone was analyzed, taking into consideration geometrical effects coupled with the torsional and bending rigidities of the yarn. Twist variation across both the twisting element (traveller) and the yarn guide (pig tail) was also computed. The resulting prediction of yarn twist distribution was verified by measurements using high speed photography on a specially constructed model twisting unit.

The twist distribution along the yarn and, in particular, the twist level developed at the point of yarn formation, affects not only the fiber migration pattern but also the overall efficiency of the twisting process. In this critical region the yarn was found to have approximately 60% of its final twist. It is essential that the fibers are twisted here at such a rate as to provide cohesive strength capable of withstanding the tensions arising from the rotating balloon. The interactions between yarn twist and strength and twist versus tension in the twisting operation were considered in detail. A method for predicting yarn breakage on the basis of these interactions is proposed.

In addition to the above-mentioned actions involved in twisting, several secondary effects were considered. They include twist variation with ring rail motion; fiber drafting in the twisting zone; and the changing geometry of the twist triangle.

The study focuses on important yarn structural effects which relate to twisting conditions and it leads to several suggestions for process improvements which should be considered in current mill practice.

Department of Mechanical Engineering
Massachusetts Institute of Technology
Cambridge, Massachusetts 02139

May 14, 1965

Professor William C. Greene
Secretary of the Faculty
Massachusetts Institute of Technology
Cambridge, Massachusetts 02139

Dear Professor Greene:

In accordance with the regulations of the Faculty, I herewith submit a thesis, entitled "On the Mechanics of Twist Insertion" in partial fulfillment of the requirements for the degree of Doctor of Science in Mechanical Engineering at the Massachusetts Institute of Technology.

Respectfully submitted

[illegible]
Fibers and Polymers Division

TABLE OF CONTENTS

I. GENERAL INTRODUCTION	1
A. Yarn Manufacturing	1
B. Purpose of Study	6
C. Earlier Studies on Ring Spinning Frames	6
II. EXPERIMENTAL APPARATUS	10
A. Twisting Machines	10
1. Ring Twisting Frame	10
2. Model Twister	14
B. Tensile and Torsion Testing	17
1. Tensile Testing Device	17
2. Torque Measuring Device	17
C. Photographic Equipment and Accessories	21
III. THE TWIST TRIANGLE	25
A. Factors Affecting the Geometry of the Twist Triangle	25
1. Introduction	25
2. Experiments	27
3. Results	28
4. Discussion	28
5. Conclusions	33
B. Fiber Migration	36
1. Introduction	36
2. Mechanisms of Migration	37
3. Theory of Migration	38
4. Experiments	78
5. Results	85
6. Discussion	89
7. Conclusions	101
IV. THE TWISTING AND WINDING ZONE	104
A. Variation of Twist with Ring Rail Motion	104
1. Introduction	104
2. Theory	105

3. Experiments 109
4. Results 111
5. Discussion 113
6. Conclusions 113
B. Twist Distribution in the Twisting and Winding Zone 114
1. Introduction 114
2. Theory 119
3. Experiments 132
4. Results 139
5. Discussion 143
6. Conclusions 148
V. APPLICATION OF RESEARCH 152
A. Effect of Angle of Wrap on Draft 152
1. Introduction 152
2. Experiments 152
3. Results 154
4. Discussion 155
5. Conclusions 158
B. Twist Distribution as a Cause of End Breakage 160
1. Introduction 160
2. Balloon Theory 161
3. Experiments 167
4. Results 167
5. Discussion 171
6. Conclusions 173
VI. GENERAL SUMMARY, CONCLUSIONS AND RECOMMENDATIONS 175
A. Summary and Conclusions 175
B. Recommendations 178
VII. APPENDICES 180
1. Appendix A 180
Variation of Twist Triangle Height in Static Twisting 180

2. Appendix B 185
Method of Calculation of Tensions in the Twisting Zone 185
3. Appendix C 187
Method of Calculations of Friction Caused Moments 187
4. Appendix D 189
Variation of Twist along an Irregular Yarn 189
VIII. REFERENCES 192

I. GENERAL INTRODUCTION

A. Yarn Manufacturing

The key process in the manufacture of textile yarns is that of spinning, the art of converting fibrous materials to a continuous yarn possessing strength, extensibility, and abrasion resistance sufficient to withstand subsequent manufacturing operations (such as weaving or knitting). In producing a yarn made up of relatively short staple fibers there is a continuous operation for drawing the fibers into a thin parallelized structure. This structure is then twisted so as to provide yarn coherence and strength.

The spinning process in its most general meaning covers the entire production of the twisted strand of fibers, although in what follows below we will designate the spinning process in its more narrow sense, that of performing the final stages of drafting and then inserting twist into the drafted strand.

In general, yarn manufacturing consists of several processes for staple fibers:

1. Opening. This process is intended to open the compressed fibrous material. It also provides a valuable function in cleaning dirt and trash included in the raw fiber.

2. Carding. A process designed to achieve a high degree of fiber separation (breaking down of clumps and also to provide an additional thorough cleaning of the fiber assembly.

3. Drawing. (Sometimes referred to as drafting). This operation is carried on to reduce the fiber assembly, termed a sliver, to smaller proportions--corresponding to the yarn diameter. The resulting attenuation by fiber

slippage in the early drawing operation improves the fiber parallelization and establishes a structure more suitable for final drafting and twisting which takes place in the formal spinning operation.

4. Combing. This operation may or may not be used in the yarn preparation sequence. Its purpose is to achieve further straightening of the fibers, removal of short fibers, and also maximum separation.

5. Spinning. The process generally termed spinning in the textile industry is conducted in two separate stages on the conventional spinning frame. The first stage of the operation is a final drafting or drawing of the fiber assembly down to the final yarn dimension. The second stage is that of twist insertion.

There are many types of spinning frames, including the Mule-, the Cap- and the Ring-spinning frames. We will deal only with the ring-spinning frame in the considerations of this study.

The conventional ring-spinning frame generally has about 100 spindles or spinning stations, arranged on both sides of the machine and driven by a common tape. Specifically, this frame can be described according to two functions.

a. Drafting. The drafting area is established between two or more pairs of rollers as shown in Fig. 1.1. In the two-set drafting assembly shown, the back roller set operates at a speed slower than that of the front roller set. The ratio of speeds represents the machine-draft of the unit. The fibrous material is reduced in its lateral dimension because of the speed difference between these two sets of follers. In some spinning systems there are

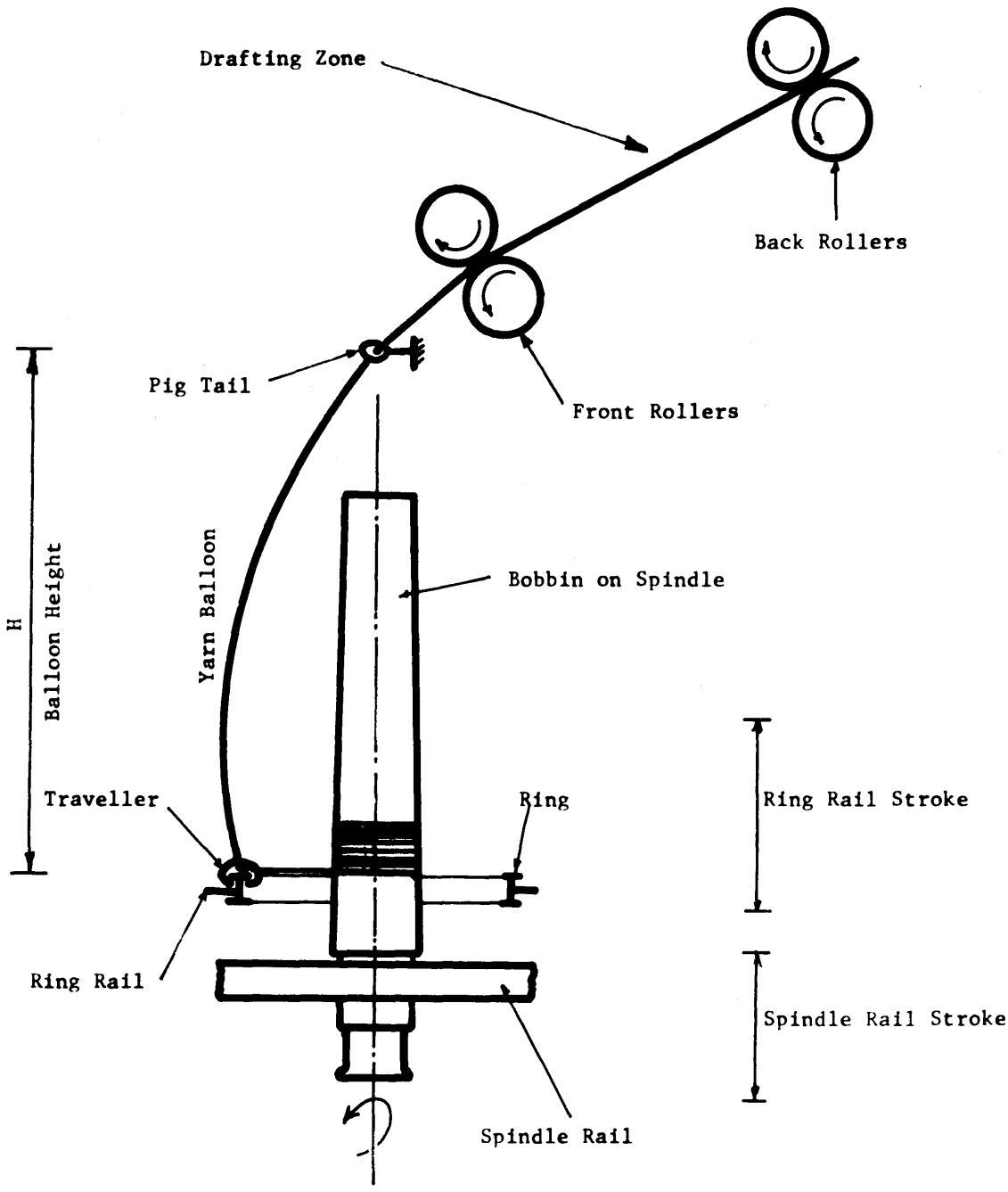

Fig. (1•1)

Diagramatic Representation of
The Spinning Frame.

controlling devices provided between the rollers in the drafting zone. These devices are intended to increase the control of short fibers in the drafting zone. On woolen spinning frames the drafting takes place between two pairs of rolls, while in cotton spinning three sets are generally used.

b. Twisting and Winding. These actions take place between the front roller and the bobbin. In this area twist is inserted into the flat relatively twist-less ribbon of fibers emerging from the front roller and serves to form it into a round, compact, strong, twisted structure. Twist is continuously inserted into the yarn passing through the traveller as it is being wound on the positively driven bobbin. The length of the yarn between the yarn guide and the traveller whirls about with a speed equal to that of the traveller. The centrifugal effect resulting from this rotation causes the yarn to bulge away from the bobbin, forming what is known as the spinning balloon, Fig. 1.1. The yarn package is built up by the vertical reciprocation of the ring-rail and/or the spindle rail which serve to place uniform layers of yarn on the bobbin.

Before any form of investigation of the twisting and winding process is begun, it is convenient to divide it into different zones according to the action taking place in each region. These zones (Fig. 1.2) will be defined as:

(1) The twist triangle which is bounded by the front roller nip and the point of yarn formation, or the twist point.

(2) The twisting and winding zone which

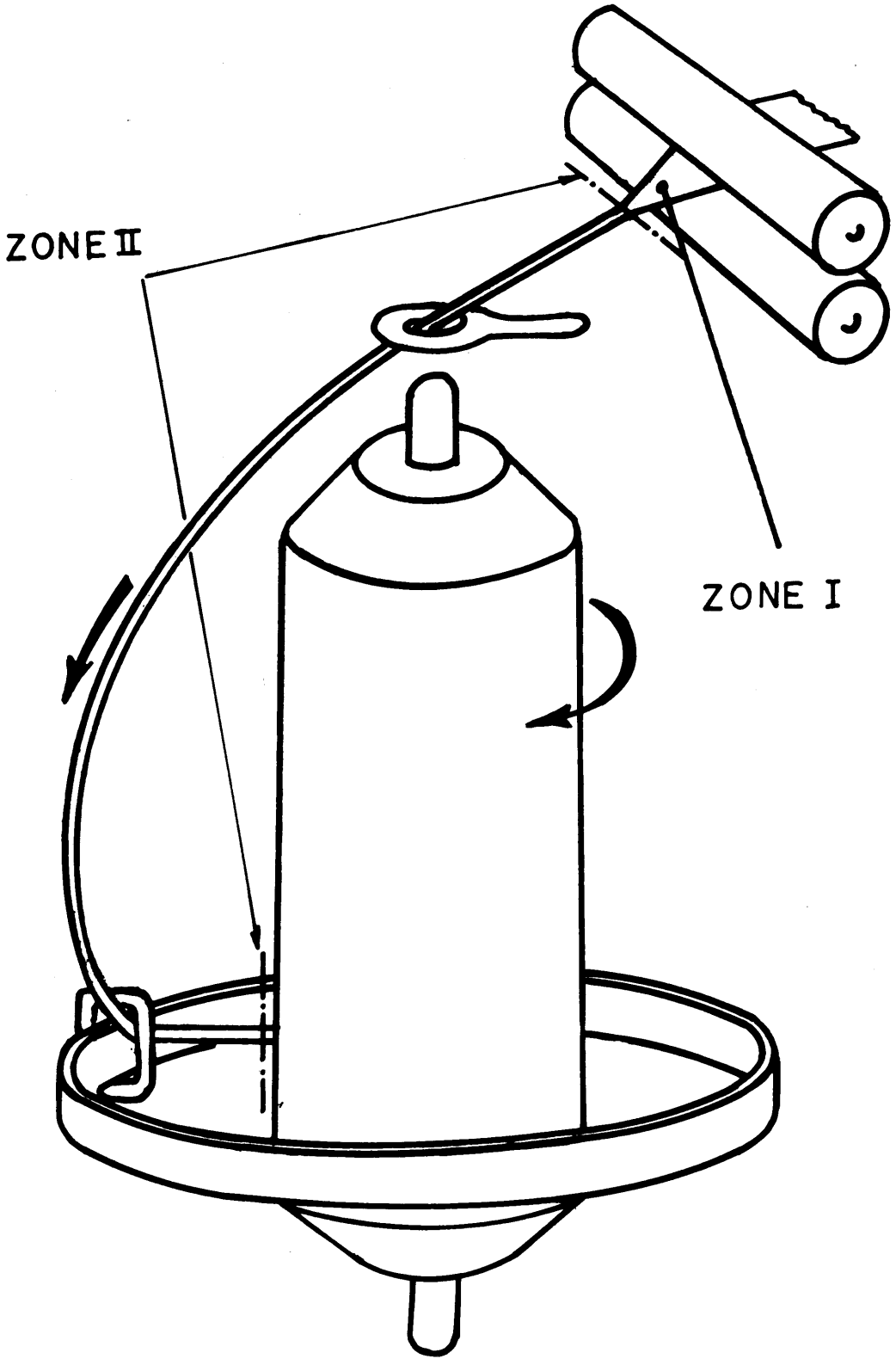

Fig. 1-2

Different Zones in the Twisting
And Winding Process

includes the region between the point of yarn formation, and the wind-on point at the bobbin.

B. Purpose of the Study

The object of this work is to investigate the interaction between the fibrous material ribbon delivered by the front roller and the twisting action of the ring frame. In particular, we will investigate the following:

1. The behavior or interaction between the fibers in the twist triangle as they are being twisted, so as to understand the mechanisms of fiber migration, to be able to predict its frequency and to define the factors affecting it.

2. The effect of ring rail motion on the final twist level in the yarn on the bobbin.

3. To express theoretically the twist distribution in the yarn across the traveller and along the balloon in order to predict end breakage during spinning on a primarily mechanical rather than statistical basis.

C. Earlier Studies on Ring Spinning Frames

There is considerable literature on the subject of spinning and, in particular, on the mechanics of ring spinning. This literature is too extensive to permit complete review here, but we will in later sections review the work done in our specific area of interest. In general, the reports published on the subject of ring spinning can be classified into three areas as follows:

General study of yarn irregularity
Study of the mechanics of drafting
Study of the mechanics of twisting.

In this section we will point out some of the work (and some of the problems) reported in each of these areas. However, it is only the third area relating to the twisting zone which we will consider in some detail.

1. Causes of Yarn Irregularity. Martindale[1], Cox et al[2] and others[3] reviewed the causes of yarn irregularity. These can be generally listed as follows:

a. Non-uniformity of raw materials.
b. Non-uniformity in mixing fibers.
c. Inherent drafting mechanisms.
d. Mechanically defective machinery.
e. External causes due to lack of operator efficiency.

The last three of these causes occur in the spinning frame, while the others take place in operations prior to spinning. But it should be pointed out that the twisting operation itself can introduce some yarn irregularity.

2. Investigations in the drafting area. The inherent drafting mechanism itself is considered to be one of the main causes of yarn irregularity. Such drafting irregularities, when periodic, are termed drafting waves and they are due primarily to lack of control of the shorter fibers during their passage through the drafting zone. These fibers tend to issue from the front rollers in clumps, thus causing an alternation of thick and thin places in the drafted ribbon.

Numerous attempts have been made to control these short fibers. One recent example of efforts to reduce yarn irregularities introduced in the drafting zone, is the AMBLER super draft system, discussed by Hannah et al[4].

Using this high draft system, Audivert et al[5] has recently studied the effect of roving twist on yarn irregularities.

It has been also established[3] that defective drafting rollers and fiber slippage at the roller nip cause irregularities in the drafted ribbon.

3. Investigations in the Twisting and Winding area. The major problems investigated in the twisting and winding area can be identified as: spindle vibration, traveller behavior, balloon dynamics and yarn tension. These topics point to ways of significantly increasing yarn production by operating at higher speeds with larger packages.

The writer[6] treated the problem of spindle vibration and found that as the package mass increases, the package-spindle natural frequency decreases, thus limiting the operation to relatively low speeds. Nissan[7] has studied spindle vibration at an earlier date.

Considerable[8] work has been done on the mechanics of traveller behavior. It has been established that the main restriction[9][10] to high speed spinning is the burning of the traveller due to contact friction with the ring.

The problem of balloon dynamics has attracted the attention of more investigators than any other phase of the entire spinning process. In a later section the theoretical results obtained by De Barr[14] which are considered to be of significant value in this area of study will be reviewed. It has also been observed[6][12] that misalignment in the spinning frame will produce changes in yarn tension. An example of such defects is the eccentricity of spindles in the ring. Such an eccentricity will produce a repeating change in the winding angle, resulting in a quick

periodic (having spindle frequency) change in the yarn tension.

Although there have been many reports on the above cited regions on the spinning frame, only a few papers [13, 14, 15] have considered the general mechanisms by which twist flows back to the flat, relatively twistless ribbon emerging from the front roller and forms it into a round, compact, twisted structure.

II. EXPERIMENTAL APPARATUS

During the course of this investigation, several instruments and devices were used. These may be classified into the following categories according to their functions and uses:

Twisting Machines
Force and Torque Measuring Devices
Photographic Equipment and Accessories.

In this chapter, each device will be described so as to give the reader a clear picture of its function, use, specification and capability.

A. Twisting Machines

Two different twisting machines were used--a single spindle continuous ring twisting frame and a model discontinuous twisting apparatus.

1. Ring Twisting Frame. The single spindle ring frame shown in Fig. 2.1 was designed and built during the course of this work. It consists of two connected steel frames (1) forming the main structure of the apparatus, with an overall dimension of 46" x 30" x 21". The frame is driven by a 3/4 H.P., 220 volt, single phase electric motor, (2). The motor (2) belt-drives a shaft (3) which, in turn, drives a vertical drum (4) and a horizontal shaft (7). The spindle, together with the bobbin,(5) is driven from the drum (4) by means of a tape. The spindle (5) is mounted on the spindle rail (6) which is bolted to the main frames (1) and its position can be changed vertically to provide complete winding of the bobbin. The shaft (7) is coupled at one end to a speed reducer (8) with a 1/50 ratio, and at the other end it drives the shaft (13) by means of a chain and sprocket

Fig. 2.1 Twisting Frame

arrangement (in the back of the figure.) The other end of the speed reducer (8) drives the two-cam shaft (9). The cams (10) provide the ring rail (12) with its reicprocating motion along two guide rods, with a maximum displacement of 3.0". The cams (10) were designed to give the ring rail a constant speed during winding.

The shaft (13) drives the bottom roller of the front roller set (14) of the drafting unit (15), through a chain and sprocket arrangement as shown. Finally, the back roller (16) is driven by the front roller via chains and sprockets. The drafting unit is mounted on a horizontal tube and is free to tilt around it. The back support (17) of the drafting unit is used to change its inclination.

a. Methods of Changing Twisting Conditions on the Ring Frame

(1) Spindle Speed. The spindle speed, together with the speed of all parts of the frame can be altered by changing the ratio of the two pulleys on motor (2) and on shaft (3).

(2) Twist. The twist level may be controlled by setting the ratio of the sprockets on shaft (13) and the bottom roller in the front roller set (14).

(3) Draft. Draft can be varied by changing the ratio of the sprockets on the back and front roller sets.

(4) Ring Rail Speed. Changing of the cam shaft sprocket controls the ring rail speed.

b. Cam Profile Equation. The equation of the cam profile based on a lift of three inches and a minimum radius of one inch is

$$r = \frac{3}{\pi}\theta + 1$$

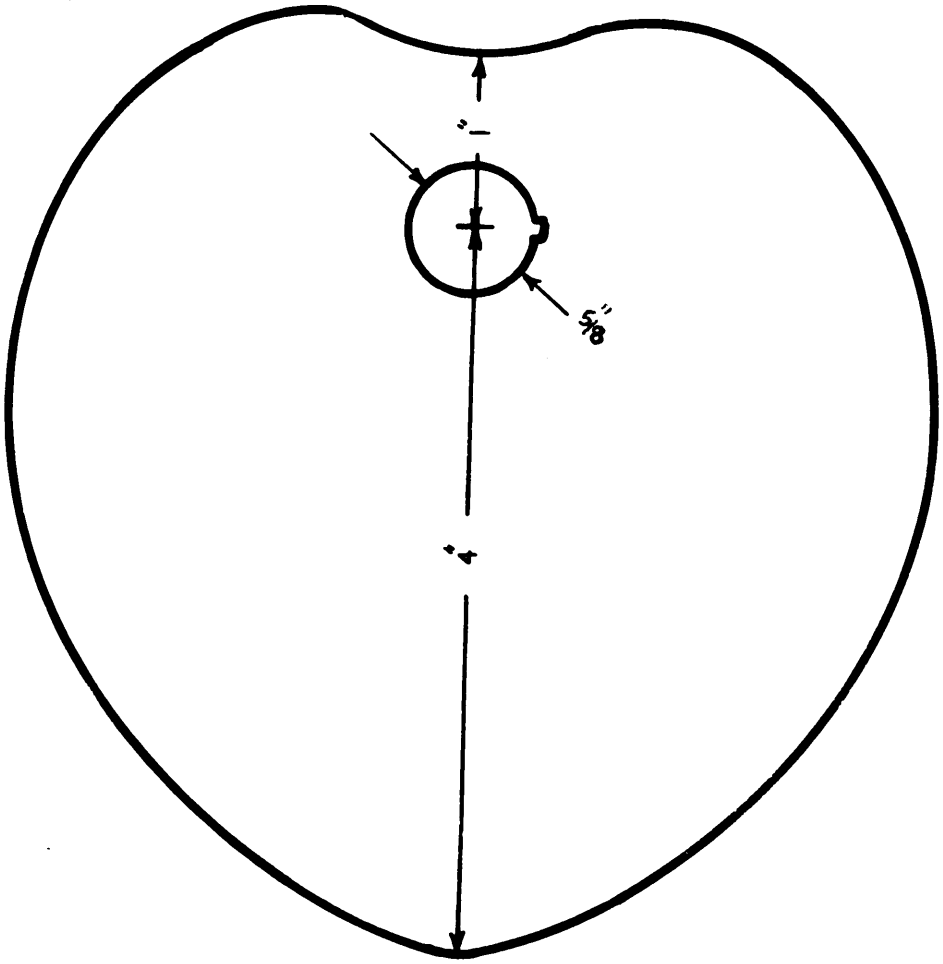

Fig. 2.2

Cam Contour

where

r = local radius

Θ = angle between local and minimum radii.

The cam provides a constant change in lift per unit time, except at the extremes of the traverse.

2. Model Twister. The model twister (Fig. 2.3) was designed by the writer for a study on the mechanics of wool yarns[23]. The machine was used briefly during work on fiber migration, and is being used now for an extensive experimental study on this same subject. This apparatus is capable of producing model yarns 40" long. It consists of three basic parts--the delivery head, the twisting head and the driving mechanism.

The delivery head consists of two sets of rollers--the back roller (1) and the front roller (2), connected by sprockets and a chain mechanism. The twisting head (4) is synchronous motor, mounted on a carriage (5) which slides horizontally on two guiding rods (6). The driving mechanism consists of a variable speed electric motor (8) which drives a (48:1) speed reducer (9). The low speed shaft of the reducer is coupled to the front roller set (2). The high speed shaft of the reducer is geared to a synchronous generator, which electrically drives the synchronous twisting motor (4).

As the yarn is delivered by the front roller (2), it passes through a thread spacer (3), then is grabbed by the jaw of the twisting head (4). Different spacers are shown in Fig. 4. The twisting head (4) on its carriage (5) moves backward under the tension supplied by the weight (7). This tension in effect determines the twisting tension.

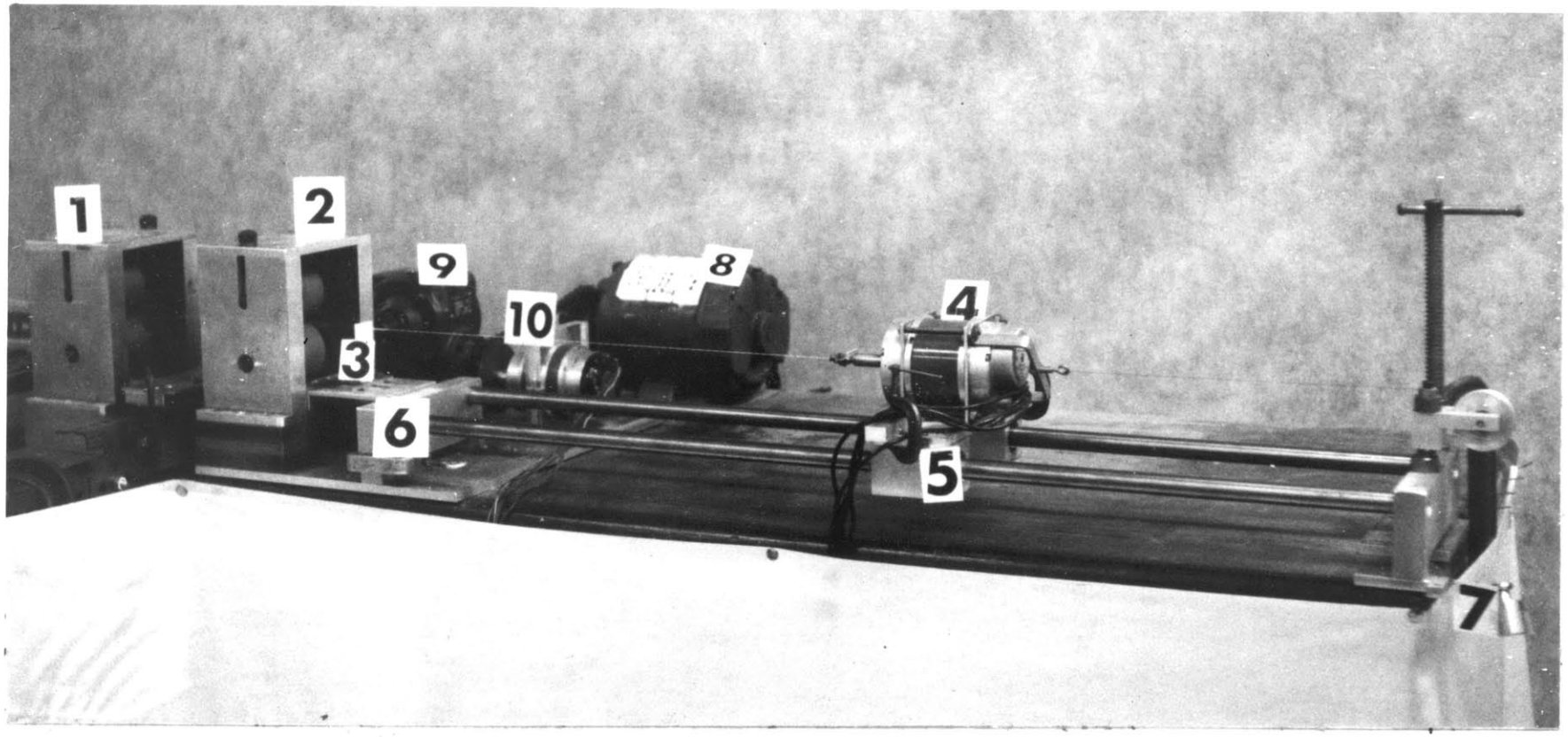

Fig. 2.3 Model Twister

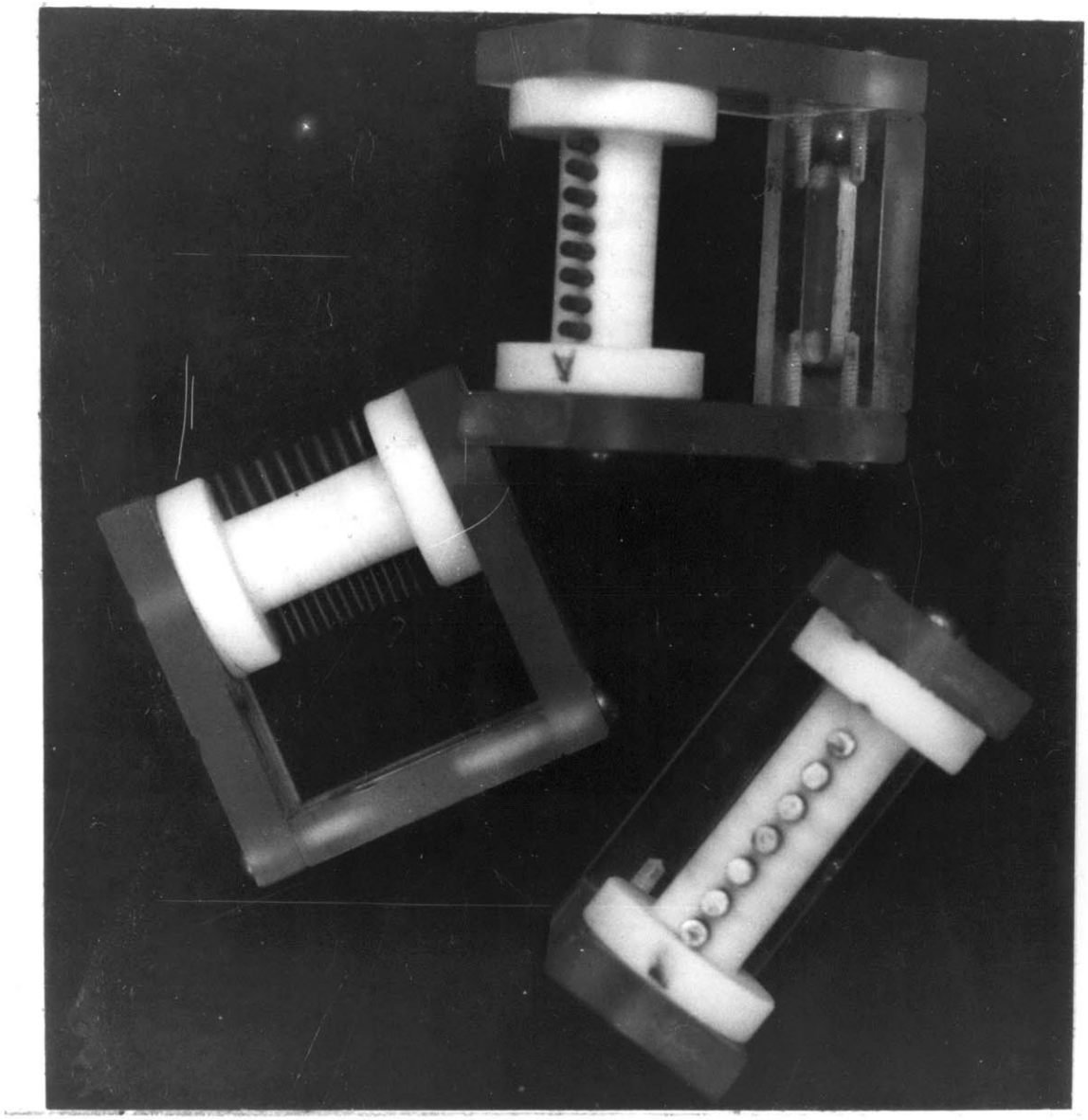

Fig. 2.4 Thread Spacers

a. Methods of Changing the Twisting Conditions

(1) Operating Speed. The driving motor is provided with a variac for changing the overall operating speed of the apparatus.

(2) Twist. Twist can be altered by changing the gear ratio connecting the speed reducer (9) and the synchronous generator.

(3) Draft. Draft can be varied by means of changing the sprockets on the feeding rollers.

B. Tensile and Torsion Testing

1. Tensile Testing Device. All load-elongation measurements were carried out on a standard Instron tensile testing machine (Fig. 2.5) Model TT.B. The specimen to be tested was held between two jaws, the top of which is attached to the load cell, while the bottom one moves with the cross-head of the machine, thus introducing the strain to the specimen. The machine is designed for testing at constant strain rates.

2. Torque Measuring Device. The torque-twist measurements were made using a torque measuring device (Fig. 2.6). This apparatus was designed by the writer during an investigation on the torsional buckling of textile yarns and was used during this work to obtain the torsional rigidity of yarns. The apparatus (Fig. 2.6) consists of two main parts--the twisting head and the load measuring part.

The specimen (1) to be twisted is held in the two jaws (2) and (3), as shown. The jaw (2) is fixed to a shaft (4) which can rotate and is free to slide. This sliding permits yarn contraction during twisting. The motor (7) drives the shaft (8) (by means of a belt as shown) which is geared to

Fig. 2.5 Instron Testing Machine

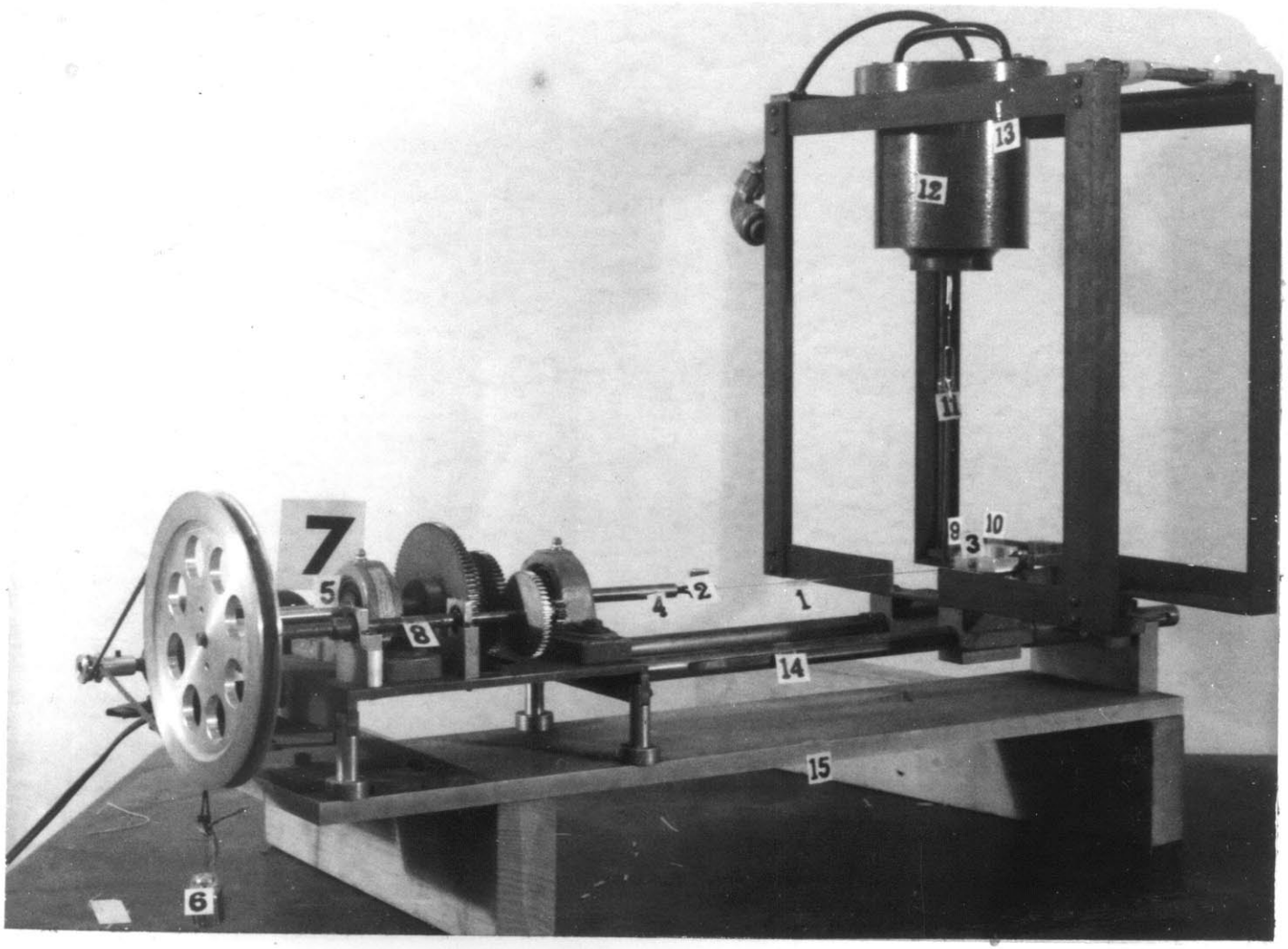

Fig. 2.6 Torque Measuring Apparatus

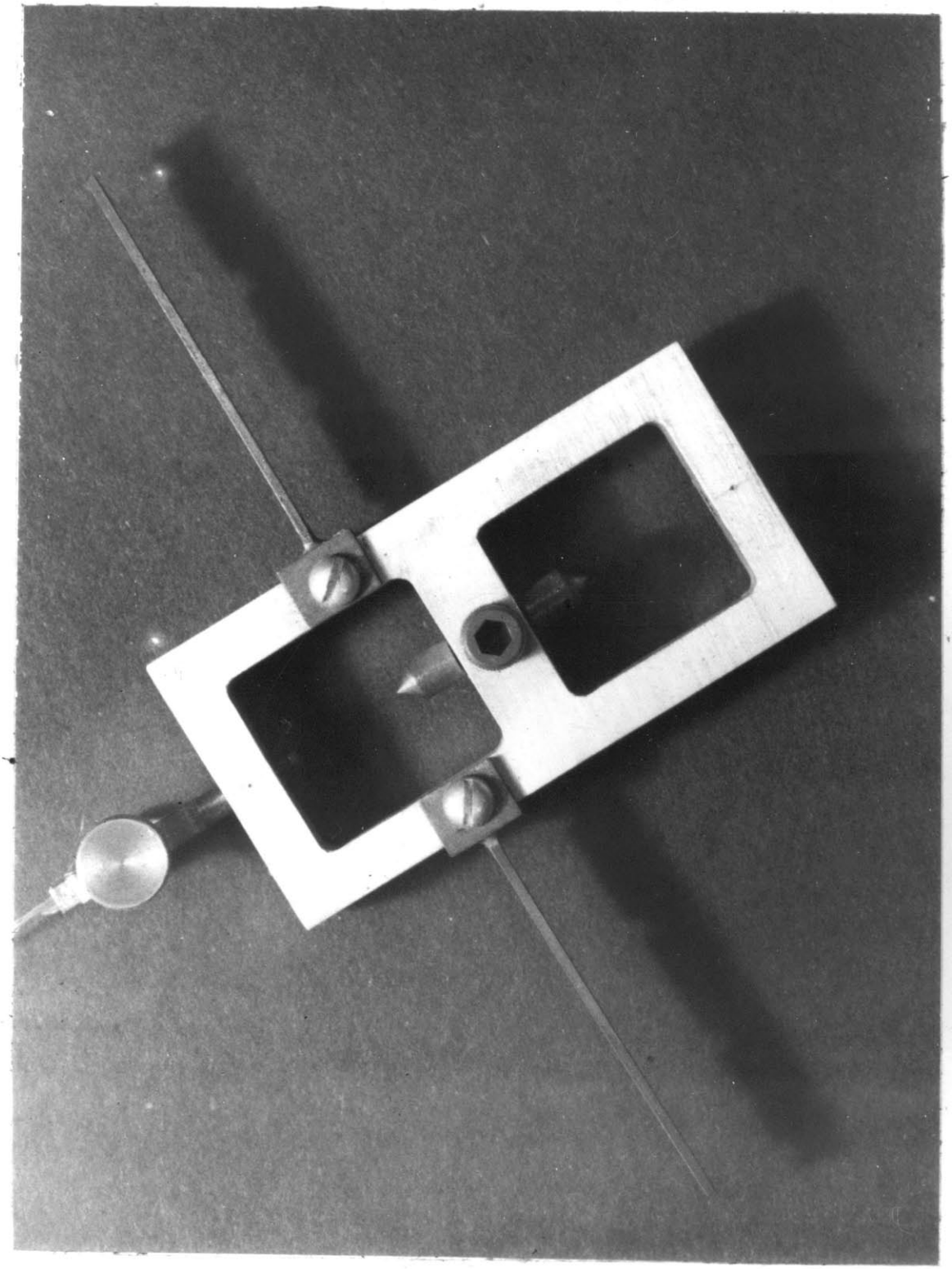

Fig. 2.7 Oscillating Cage

the hollow shaft (5) thus introducing twist to the specimen (1). The torque developed in the yarn being twisted is converted to a tensile force by means of the oscillating cage (9) (supported by two jewel bearings (10)) through the vertical level (11). The lead then is measured by the load cell (12) connected to an Instron recorder. The load cell is mounted on the frame (13) which together with the jewel bearings supports can slide on the two rods (14) as a provision of changing specimen length.

The apparatus is equipped with three gears on shaft (5) corresponding to three twisting rates, namely 23, 90 and 144 turns/min. Fig 2.7 shows a picture of the oscillating cage (9).

C. Photographic Equipment and Accessories

Fig. 2.8 shows the layout of the high speed photographic equipment used for taking the pictures of the yarn in the twisting zone. A photoelectric pickoff* (1) is mounted on the ring rail, facing the traveller and one-quarter inch away from the ring. The pickoff contains its own light source, together with a photocell. The light reflected from the traveller (which is painted white) as it passes in front of the pickoff generates a pulse to trigger the flash delay unit** (2). The flash delay unit (2), when triggered, generates amplified pulses at the same rate as the electrical impulses received from the pickoff. The unit is provided with a circuit which can vary the delay before the pulses are passed to the "Strobotac" unit*** (3). The unit also can be triggered

* Type 1536-A by General Radio Company

** Type 1531-P2 by General Radio Company

*** Type 1531-A by General Radio Company

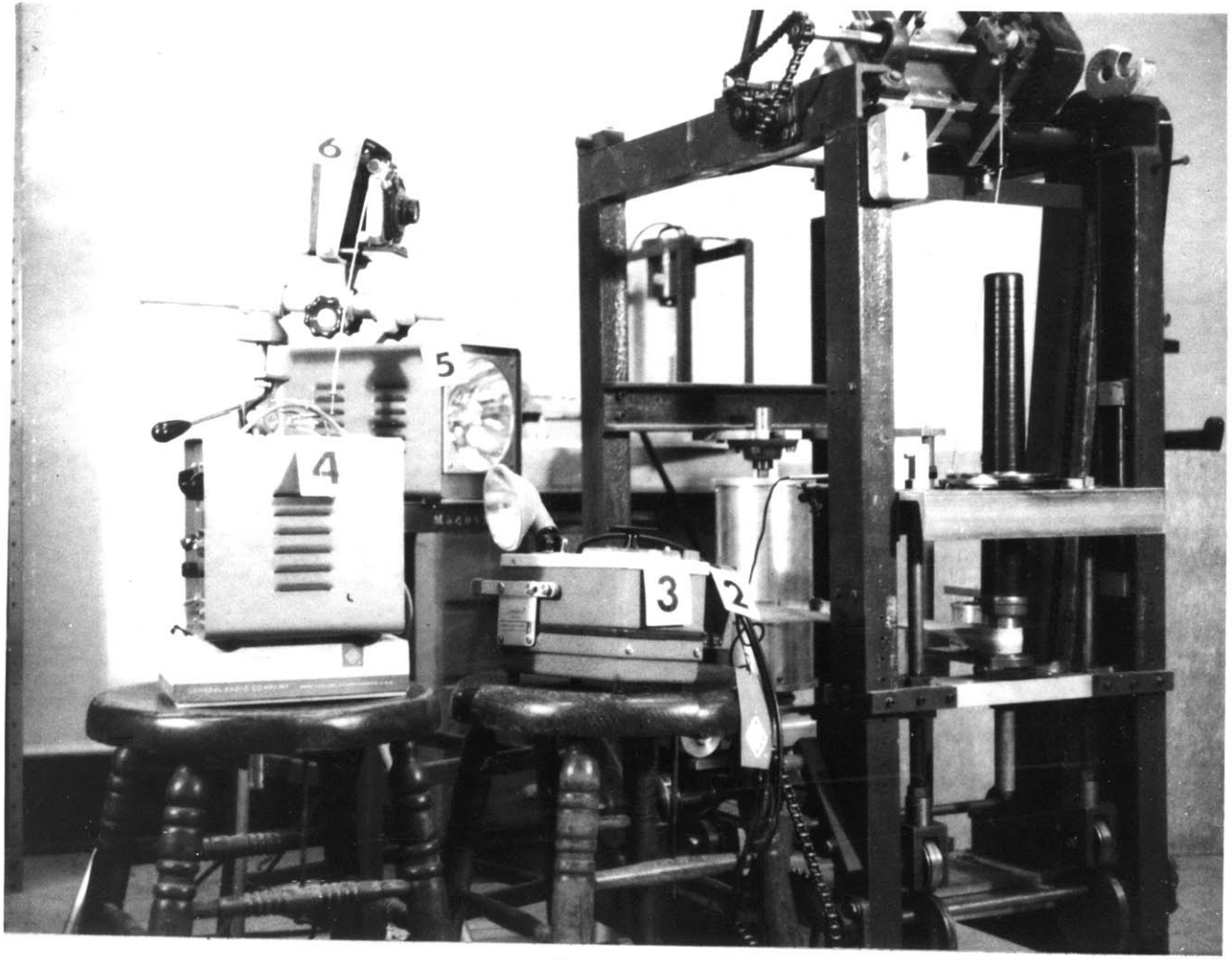

Fig. 2.8 Photographic Equipments

to give a single pulse. The "Strobotac" unit (3) produces flashes with a frequency varying from 110 to 250,000 cycles/min. The Strobotac is triggered by means of the pulse generated from the delay unit (2).

The microflash driver (4) is in turn triggered by the flashing light of the "Strobotac" unit (3), and it generates a pulse to trigger the micro flash (5). The micro flash (5) is capable of producing a flash of duration 0.4 μ sec with a peak light of 5 million candle power. (More information about the micro flash unit can be found in reference (16)). Finally, the picture of the balloon is taken by means of the camera (6) which is a Linhof 4 x 5" press camera.

Embedding Device. The device used for embedding the twist triangle is shown in Fig. 2.9. The filaments (1) to be twisted were first passed through the seven holes in the thread spacer or guide (2), which is fixed to the main frame (3). After twist is inserted and the required conditions are obtained, the twisted yarn and the seven filaments are clamped to the frame (3) by means of the two pieces (4) (one at each side). The two side plates (5) (front one is not shown) are then fixed to the frame by means of three screws. The embedding of the twist triangle was then carried following the procedure described in Chapter III.

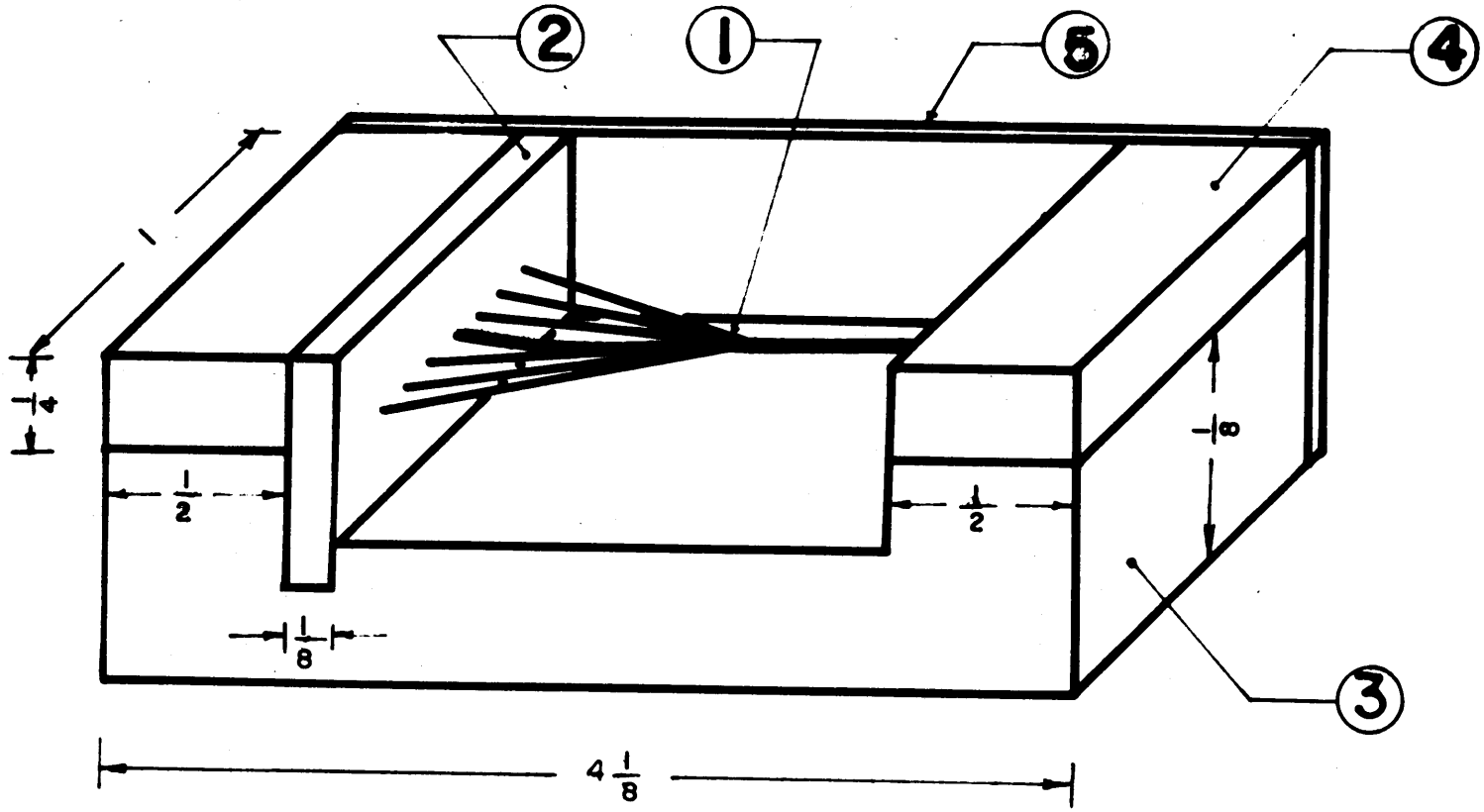

Fig. 2.9 Embedding Device

III. THE TWIST TRIANGLE

A. Factors Affecting the Geometry of the Twist Triangle

1. Introduction: As twist is inserted by the rotation of the traveller, it will flow back in the yarn balloon and past the pig tail to a point very close to the front roller nip. This point is defined as the twist point, the limit of twist propagation, or the point of yarn formation. The area between the twist point and the front roller nip is the twist triangle.

The flat ribbon of fibers delivered by the front rolls forms the base of the twist triangle. This ribbon is gathered into a compact round structure at the twist point corresponding to the apex of the triangle. The twist triangle, Fig. 3.1, is characterized by its base (w) and its height (h), which are of great importance because of their effect on the process of yarn manufacturing. For example, Hearle[17] showed that the frequency of fiber migration during twisting depends to a great extent on the free length of the fiber above the twist point. In the case of staple fiber spinning, the height of the twist triangle will affect both end breakage and post front roller drafting, as will be discussed in later chapters.

Very little attention had been paid to study the variation of the height of the twist triangle and the factors affecting it. Fujino[13] et al recognized the problem and investigated theoretically the effect of yarn tension on the height of the twist triangle. The authors assumed that the strain in a fiber in the triangle depends on its position at the roller nip or that strain is proportional to the distance of the fiber from the center line of the yarn. This assumption, however, has no justification because the line of the yarn will continuously move because of fiber migration, as will be discussed later.

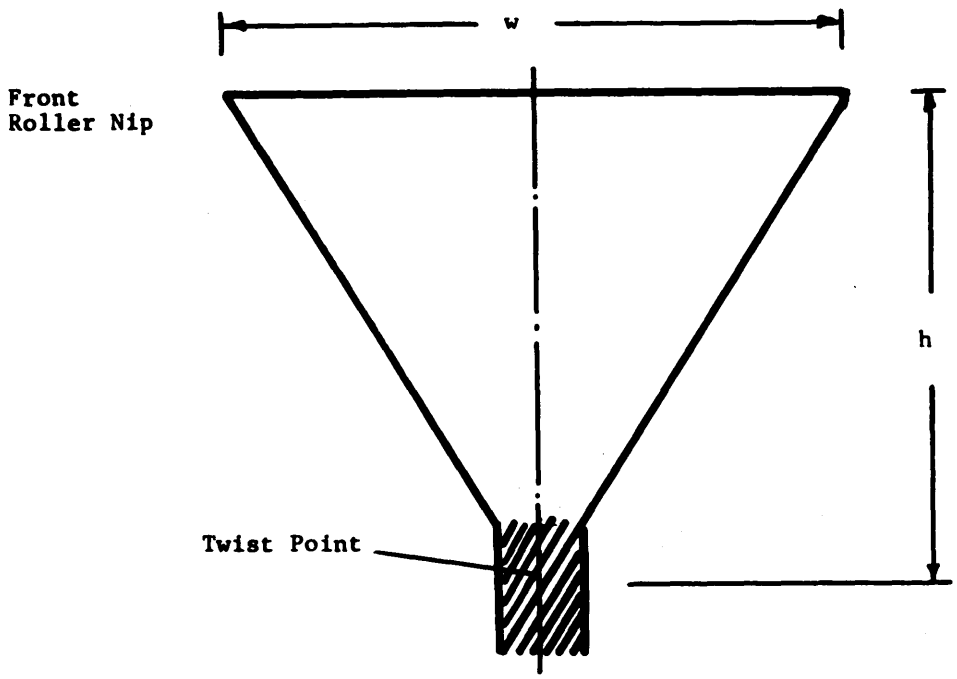

Fig. 3.1 The Twist Triangle

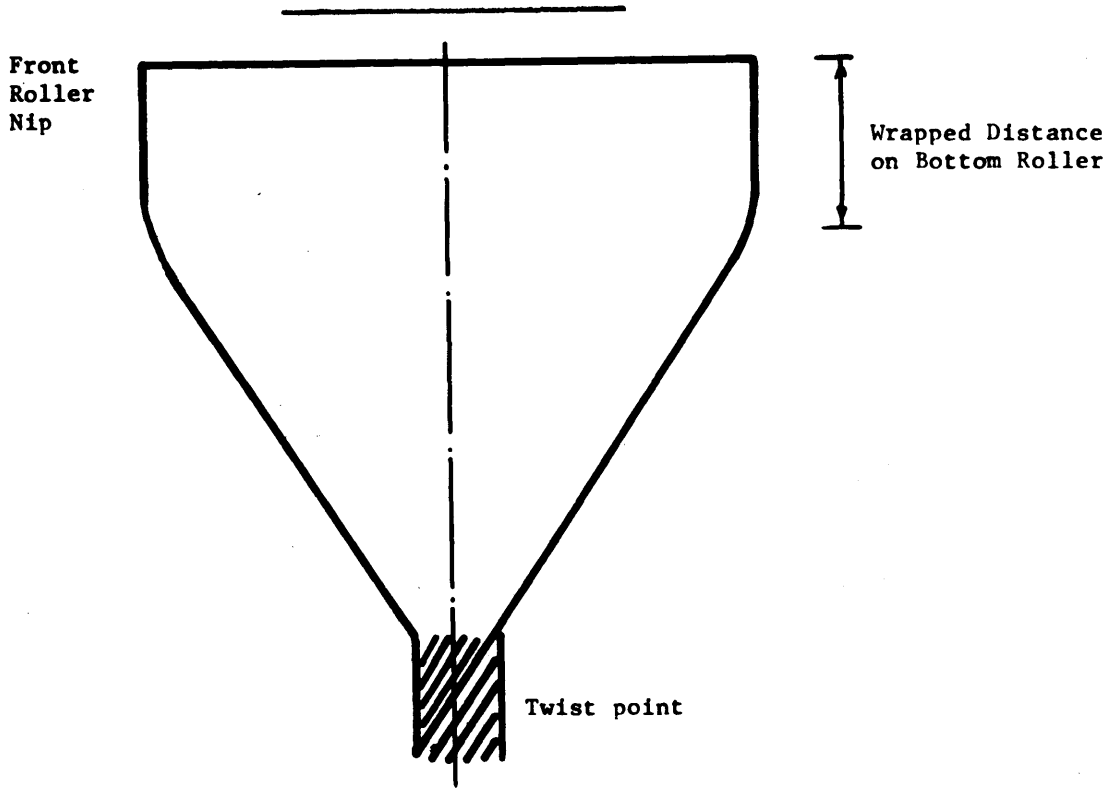

Fig. 3.2 Twist Triangle with Ribbon Wrapped on Bottom Roller.

During the course of this investigation various attempts were made to establish a theoretical relation between the factors affecting the geometry of the twist triangle. But, it was only possible to obtain such a relation for the static twisting case (twisting at constant length) which will be discussed in Appendix A. However, qualitative treatment of the factors influencing twist triangle geometry was possible and experiments were undertaken to establish the order of magnitude of their effect. In this section, the results obtained from these experiments will be presented.

2. Experiments. The following set of experiments were designed to investigate the factors affecting the twist triangle height. In particular, it was of interest to observe and measure: (1) the maximum height of the twist triangle; (2) the path of the twist point; (3) the relation between the helix angle of the yarn and the apex angle of the triangle.

a. Material Used

(1) 7 Viscose Rayon yarns with the following properties:
EA = 24800 gms (fractional modulus or initial slope of the load-elongation curve.)
No. of filaments/yarn: 60
Producer's Twist: 3 T.P.I. S
Yarn Denier: 300

(2) 7 Viscose Rayon yarns with the following specifications:
EA = 5820 grams (fractional modulus)
No. of filaments/yarn: 14
Producer's Twist = 2.5 T.P.I. S
Yarn Denier = 75

The load-elongation curves of these yarns are shown in Fig. 3.29.

b. Twisting Conditions

(1) The 300 denier yarns were twisted on the single spindle ring frame (Fig. 2.1) under the following conditions:

(a) Twist levels: 2.5, 5.0, 9.0 TPI

(b) Traveller weights: 159, 340, 570 mg

(c) Balloon height: 12"

(d) Spacer widths = 1.1" and .75"

(2) Both the 300 and 75 denier yarns were twisted on the model twister (Fig. 2.3) under the following conditions:

(a) Twisting tension: 100, 200, 300 grams

(b) Twist level = 5, 12 TPI.

c. Procedure. While twisting on both ring spinning frame and the model twister, the location of the twist point was observed against a small ruler. The height of the twist triangle was measured when the twist point was located below the center of the spacer. The locus of the twist point was observed and was marked on a card placed under the twist triangle.

3. Results. Fig. 3.3 shows the variation of the height of the twist triangle with respect to both twisting tension (traveller weight) and twist. Fig. 3.4 shows the locus of the path of the twist point. Fig. 3.5 shows the effect of twist triangle height as a function of EA and Tension. Fig. 3.7 shows the relation between the helix angle as measured on the yarn and the apex angle of the twist triangle.

4. Discussion.

a. Effect of twisting tension (traveller weight). From Fig. 3.3 it is clear that as the twisting tension

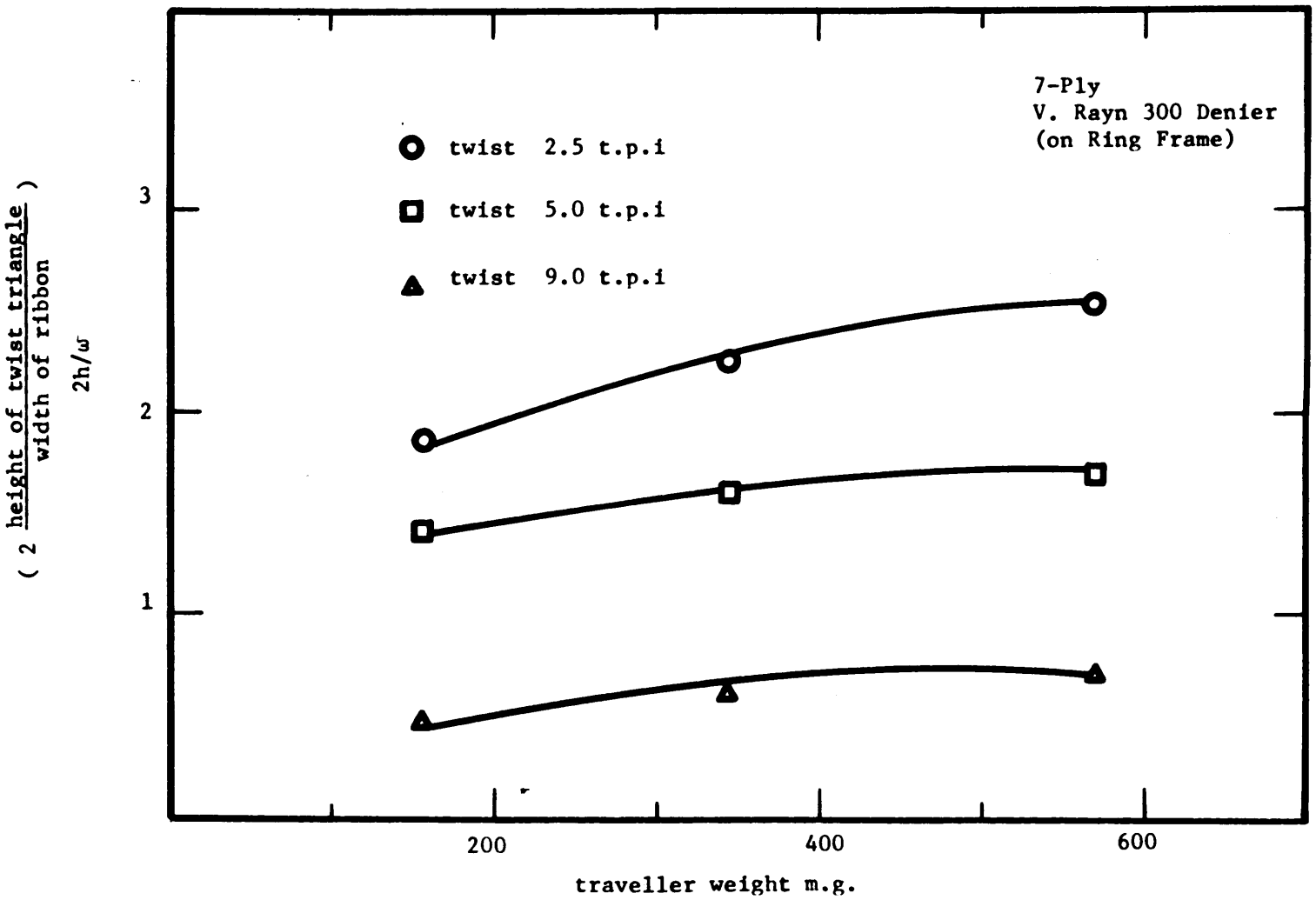

Fig. 3.3 Effect of Traveller Weight on Twist Triangle Height

(Experimental)

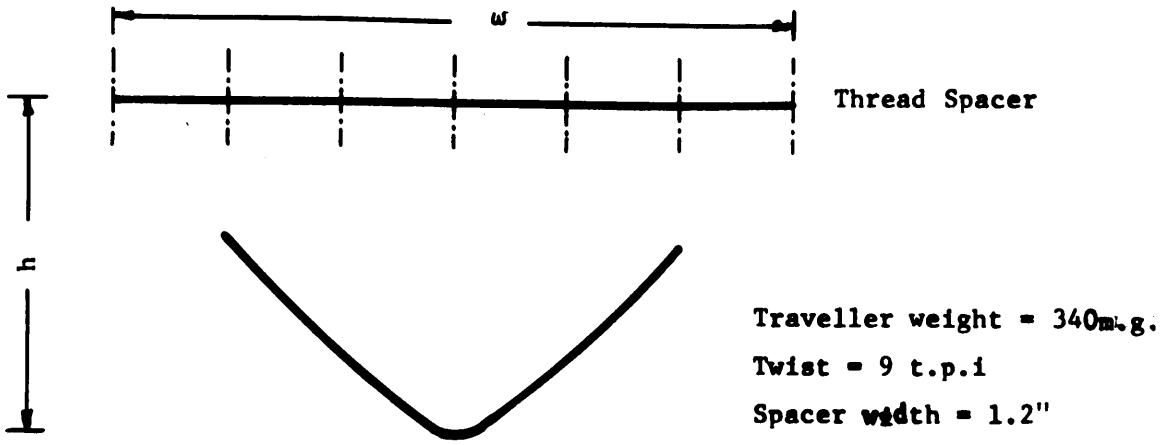

Locus of Twist Point

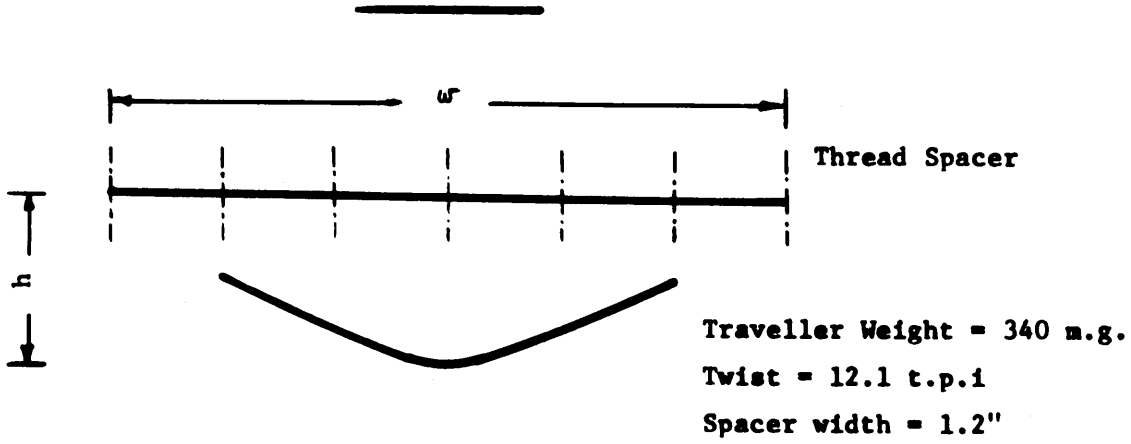

Locus of Twist Point

Fig. 3.4 Effect of Migration on the Location of the Twist Point

increases, the twist triangle height increases. This is due to three factors:

(1) the increase in strain level in the material due to high yarn tension,

(2) the increase in both the torsional rigidity and bending stiffness of the filaments in the ribbon to be twisted,

(3) the reduction of twist level above the pig tail due to increase of friction between the yarn and the latter.

b. Effect of Twist Level. As the twist increases, the triangle height decreases, since more twist now propagates closer to the front roller nip.

c. Effect of Fractional Modulus. As the modulus increases, the height of the twist triangle at a given twisting tension decreases due to the reduction in strain in the material in the twist triangle.

d. Effect of Fiber Migration. Fiber migration will cause the twist point to move sideways taking a path as shown in Fig. 3.4. This effect may be explained by the fact that when a filament migrates into the inner layer, it loses its tension and hence the overall twisting tension will be supported only by the remaining components. In effect, the twist point will be located under the center of force of the tensioned filaments.

e. Effect of Cross-Sectional Shape of the Ribbon Input. If no migration takes place, the twist point will be located below the center of gravity of the ribbon. However, when migration does occur, the twist point will oscillate within the principal region of fiber concentration.

f. Effect of Ribbon Width. Fig. 3.6 shows the effect

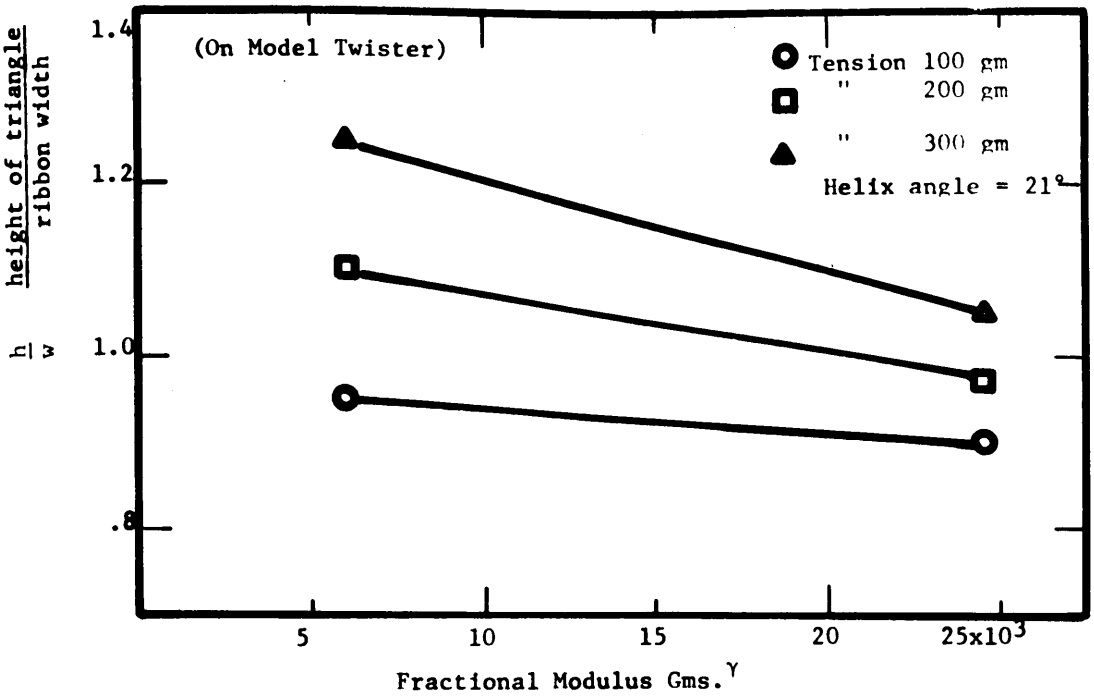

Fig. 3.5 Effect of Fractional Modulus on Twist Triangle Height (Experimental)

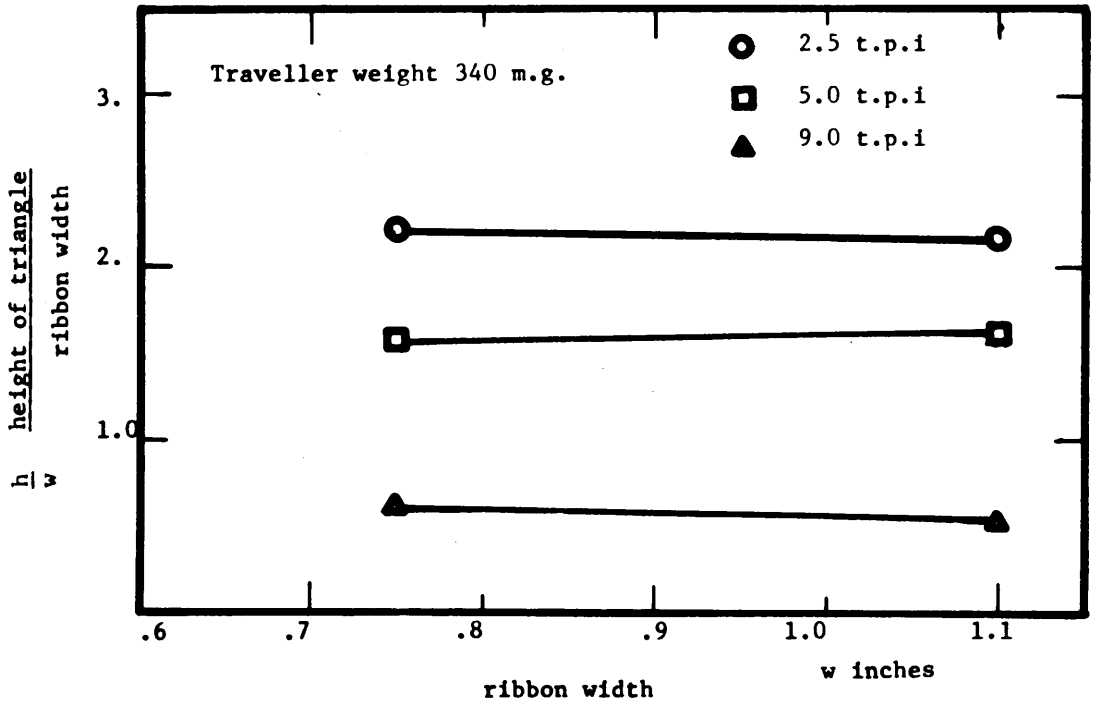

Fig. 3.6 Effect of Ribbon Width on Twist Triangle Height

(Experimental)

of spacer width on the twist triangle height. It is apparent that the apex angle of the twist triangle remains constant under each twisting condition with different spacer widths, thus keeping the apex angle constant.

g. Effect of Angle of Wrap of Yarn around Bottom Delivery Roller. It was observed during spinning that as the angle of wrap of yarn around the bottom delivery roller increases, the distance between the roller nip and the twist point increases. The twist triangle in this case will have a flat (rectangular) portion between the roller nip and the line of contact at which the material leaves the rollers. Fig. 3.2 shows the shape of the twist triangle, including the yarn wrap around the front roller. This effect is due to the friction between the bottom roller and the fibers, which restrains the twist point from moving back closer to the roller nip.

5. Conclusions. From the study of the change in the dimensions of the twist triangle and the location of the twist point, it may be concluded that the location of the twist point and the geometry of the twist triangle depend on:

a. Twisting Tension. As the tension increases, the twist triangle height increases.

b. Twist Levels. As twist increases, the height of the twist triangle decreases.

c. Elastic (Fractional) Modulus. As the fractional modulus increases, the height of the triangle will decrease at a given tension.

d. Fiber Migration. Migration causes the twist point to move sideways away from the fiber running into the inside layer. This effect is shown in the cross-sections of the twist triangle shown in Figs. 3.32, 3.33, 3.34.

e. Fiber Distribution at the Front Roller. When

twisting non-uniform ribbon (in cross-section), the twist point will tend to oscillate sideways (due to fiber migration) around the line passing through the center of gravity of the cross section.

f. Ribbon Width. As the ribbon width increases, the height of the twist triangle increases keeping the apex angle of the triangle constant. In general, the apex angle of the triangle was found approximately to be equal to twice the helix angle of the yarn as shown in the plot of helix angle against the apex angle (Fig. 3.7).

g. Angle of Wrap between Yarn and Bottom Roller. As the angle of wrap increases, the height of the twist triangle (i.e., distance between front roller nip and twist point) will increase. Fig. 3.2.

In general, the relation between the helix angle and the geometry of the twist triangle can be given in the following empirical relation

$$\tan \alpha = \tan \frac{2w}{h}$$

where h is the maximum height of the twist triangle, w is the ribbon width and α is the helix angle measured on the yarn.

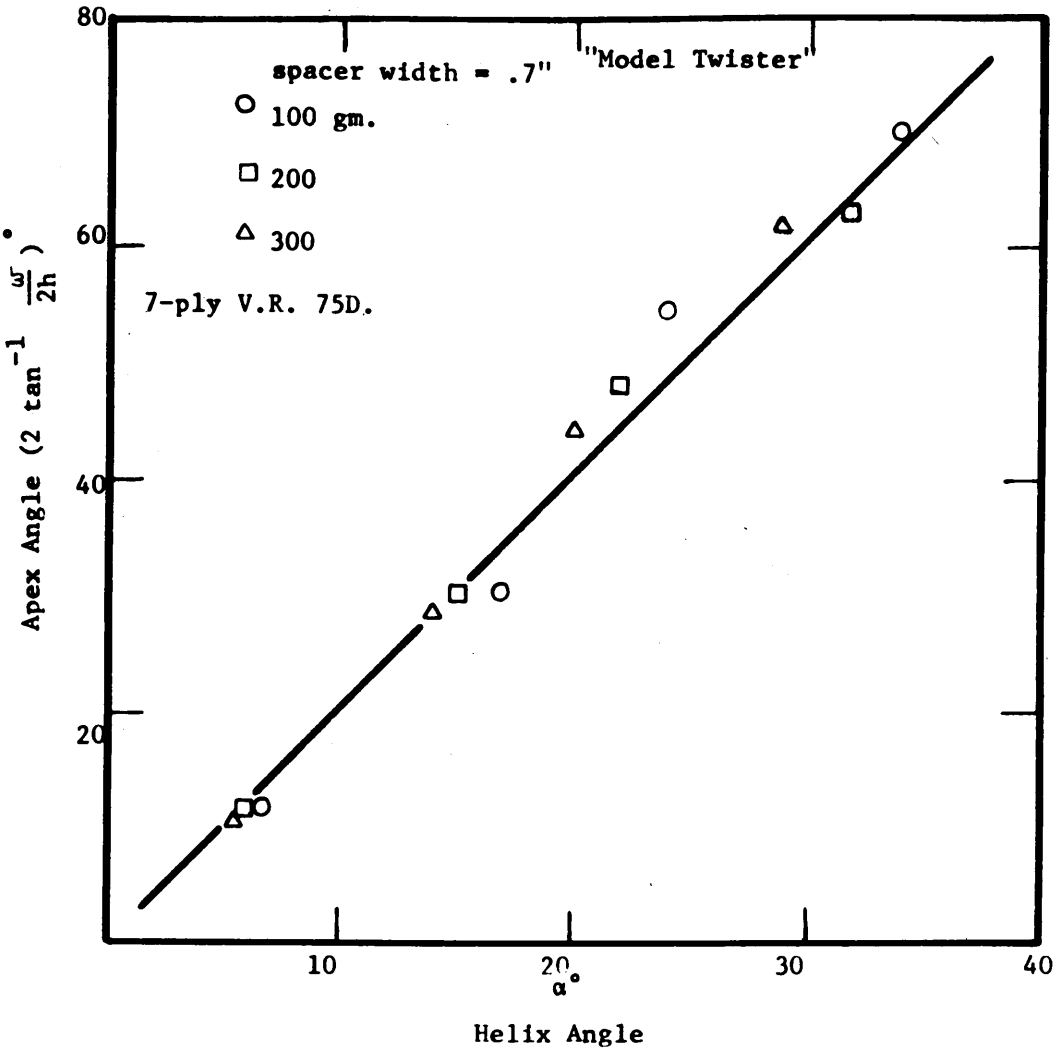

Fig. 3.7 Relation Between Apex Angle of Twist Triangle and Helix Angle

(Experimental)

B. Fiber Migration.

1. Introduction. During the last 15 years, the mechanics of twisted yarns had been the subject of many researches. Most of the theories developed on the subject were based on the assumption that a yarn is composed of a series of concentric cylinders of different radii, with each of the components in the yarn taking a helical path around one of these cylinders. The component or fiber which occupies the central layer is considered to follow a straight path along the yarn axis. Although this idealized structure is very simple for mathematical analysis, it is impossible to achieve in practical spinning. And even if it could be made, it would be useless in the case of staple fiber yarns.

The difficulty in producing a yarn with such a structure arises because of the differences in lengths of the path of the fibers at different yarn radii. Fibers in the outside layers will follow a much longer path than those occupying the inside. Since in actual spinning all fibers are supplied at the same rate, we can achieve this idealized structure only by having the fibers in the outside layers subjected to high compressive strains causing them to buckle in the yarn.

The idealized structure is of no value in the case of spun yarns because of the lack of cohesion of fibers on the surface, and hence lack of cohesion in the yarn as a whole. The relatively short staple fibers on the outside will be unable to support any tensile forces because they cannot develop interfiber friction. Without tension buildup they, in turn, will not exert any transverse pressure to aid in mutual gripping of the fibers in the inside layers and hence the entire yarn will not be able to support any tensile load. It is likely that the fibers in the outside

layer would peel off due to lack of cohesion and the whole yarn would subsequently disintegrate. In practical spinning, fibers change their radial position along the yarn length, thus leading to a mutual gripping of the fibers which in effect gives spun yarns strength and cohesion.

The tucking, or change of fiber position along the yarn length was recognized by Peirce[18] who suggested that it is due to the random tangle of the fibers in the yarn. Morton[19] proposed the regular migration of each fiber from the outside to the inside due to the tension differences developed in fibers following different paths. Morton[20] in another publication described the use of tracer fiber technique for the study of staple fiber yarns. Later, Riding[21] applied this technique to study the migratory behavior of continuous filament.

Hearle[22] assumed an ideal migration behavior and obtained theoretical expressions for the frequency of migration in yarns. Subsequently, he studied the mechanics of staple fiber yarns using his ideal migration behavior. Although qualitative observations show that migration occurs in an irregular manner, Hearle and the writer[23] experimentally verified the validity of the Hearle theory.

Riding[21] in his experimental study on continuous filaments found that there was a close correlation between the migration period and the period of producer's twist. This was explained by Hearle[24] to be due to the wrapped form of the yarn which develops the original producer's twist into a pseudo migration of equal period to the producer twist.

2. Mechanisms of Migration. Morton[19] suggested the differences of tension levels in fibers twisted in different layers of the yarn to be one mechanism of migration. Hearle[17]

suggested that the yarn form and its mode of twist provide another mechanism. Although we recognize that these mechanisms exist, we should emphasize the importance of the displacement action of the fiber occupying the center position. This fiber has to be laterally moved in order that another occupy its place. Hearle[17] suggested the development of slack to be one mechanism of outward migration. This is valid only for an open structure in which the fibers are separated from each other.

In practical spinning there is no place for slack to develop because of the mutual support of the fibers in the twist triangle. Instead, the migration mechanism will be initiated through fiber buckling. This buckling can be either static or dynamic (snapback). In short, migration will take place in actual twisting when a fiber in a certain layer buckles, either statically due to excessive compressive strains, or dynamically due to the sudden release of its tension as its tail end leaves the front roller nip.

3. Theory of Migration in a Seven-Ply Structure. To study the mechanism suggested by Hearle[17], i.e. the buildup of sufficient slack to initiate outward migration, we will analyze the case of twisting a 7-ply structure. This structure was found to be very convenient for analysis, since it packs into an arrangement with one single yarn forming the core, and the other 6 following helical paths in the outer layer. Hearle and Merchant[17] studied this structure for a certain input form. In their study they analyzed a case in which the material (the 7 singles) was delivered through a circular guide as shown in Fig. 3.8. This model does not actually simulate the case of actual twisting because in practice the material input is in the form of a flat ribbon.

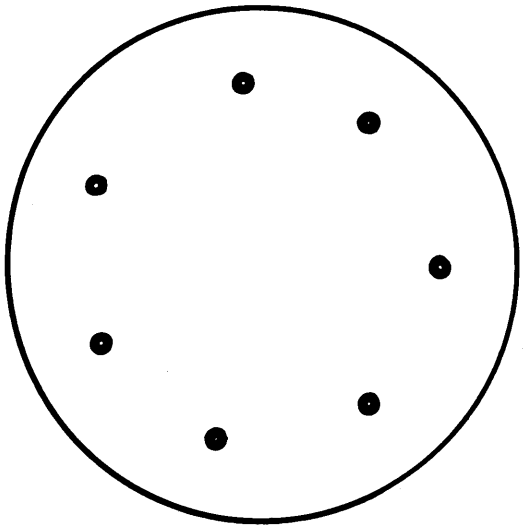

Fig. 3.8 Circular Thread Guide Used by Hearle

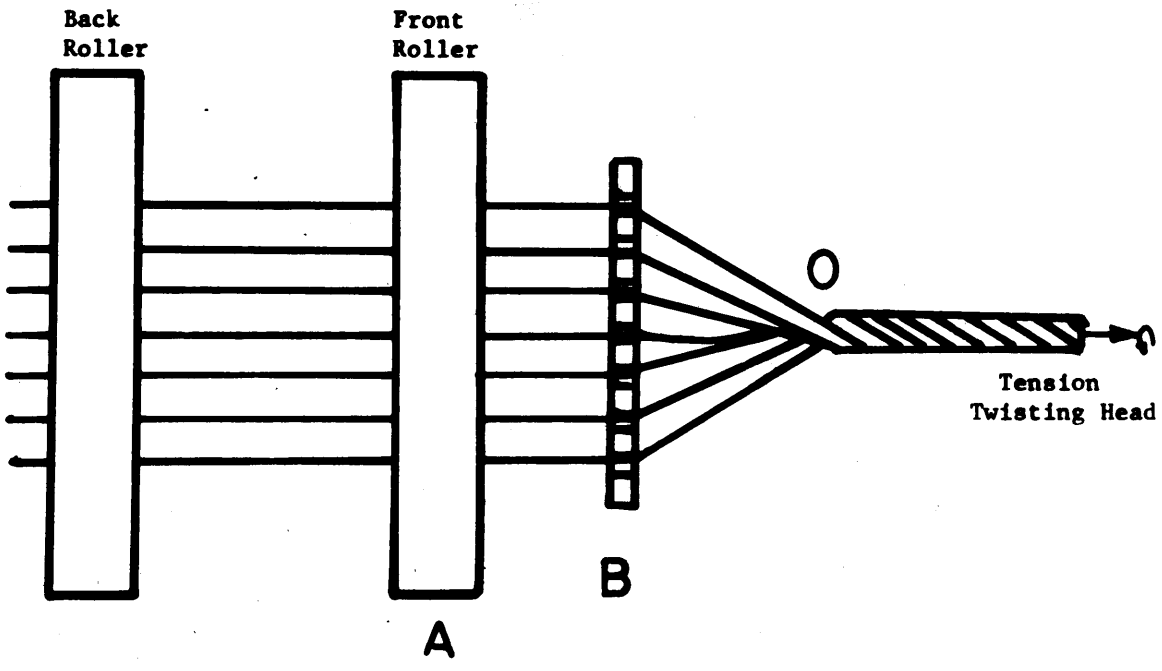

Fig. 3.9 Twisting of a 7-Ply
With a Flat Ribbon Input

The main features of the model considered here are shown in Fig. 3.9. The 7 ends (singles) are being supplied at the same rate by the front rollers (A) of the twisting machine to a yarn guide (B) containing 7 slots evenly spaced along its width. The 7 ends then brought together and twisted at the twist point "O" located as shown.

a. Nomenclature

a = semi-minor axis of the ellipse assumed by the slack yarn

d = diameter of single yarn

E = Young's Modulus of Material

f = number of migrations/single yarn/in.

h = height of twist triangle

I = cross sectional moment of inertia of fibers.

k = spring constant of matrix of fibers surrounding the central fiber in the twist triangle

L = free length

n = twist/unit length at the twist point

S = length along the ply yarn

S_c = length of ply yarn in which a single occupies the central position

S_o = length of ply yarn in which a single in the inside layer reaches zero tension

S_x = length of ply yarn required to develop the slack x (in the open structure) or the critical strain ϵ_1 (in the closed structure) in the single in the inside layer

S_y = length of ply yarn in which a single wraps around the other component as it moves to the outside.

T = tension in a single at any time

T_y = twisting tension

T_m = mean tension in a single in the outside layer

t = time

V_1 = delivery speed at front roller nip

V_2 = speed of yarn formation at the twist point

w = width of the ribbon to be twisted

x = slack needed to initiate outward migration of the central single

α = helix angle of twisted yarn

α_1 = angle of wrap of a single around the other components as it moves to the outside.

γ = fractional modulus or load/unit strain of singles used

δ = distance between singles along the front roller nip

ϵ_1 = critical strain required to develop static buckling of the central fiber or single, in the twist triangle

ϵ_c = strain in central single at any time

ϵ_o = strain in singles in outside layer at any time

ϵ_s = average strain in a single in the outside layer

ρ = linear density of the central fiber in the twist triangle at any time

ρ_1 = linear density of fibers upstream the front roller nip

b. Assumptions. During the course of this analysis we will assume that outward migration will take place when the

single occupying the center position of the structure loses its tension and develops a certain amount of slack. We will also assume that:

1. All the singles are completely elastic and uniform, having the same mechanical properties.

2. The singles are round and have the same diameter.

c. Conditions of Migration. Hearle and Merchant[17] obtained a theoretical expression for the conditions at which migration will occur (assuming that the central single will not buckle) in the form.

For migration to occur

$$T_y < 6\gamma (1 - \cos\alpha) \qquad 3.1$$

and if

$$T_y > 6\gamma (1 - \cos\alpha) \qquad 3.2$$

no migration will take place.

d. Period of Migration. At the instant of migration the tension in the central layer is zero and, subsequently, the twisting tension is supported by the yarns in the outer layer. We now have mean tension/single in outer layer

$$T_m = T_y \sec\alpha \qquad 3.3$$

After migration takes place, the yarn which has just moved into the central layer will begin to lose its tension. After its tension reaches a zero value, this yarn will continue in the central position until it develops an amount of slack needed to initiate outward migration. After the yarn migrates outward, it will begin to wrap around the other yarns until the slack is consumed. As soon as the slack is gone, the tension will build up in this yarn and it will then

take a place in the outer yarn layer during subsequent twisting.

Figs. 3.10 (A-F) represent a migration cycle for one single of a 7-ply structure. We fix our attention on the black single yarn occupying the central position in Fig. 3.10-A. At this point it has just enough slack to initiate outward migration. In B, the black yarn is being displaced to the outside layer, having been caught between two adjacent yarns. The slack yarn is now wrapped around the 7-ply structure. The black yarn is further twisted down into the surface layer as shown in D. Fig. 3.10-E shows a downstream picture of the 7-ply structure with the black yarn running in the outside layer. It is easy to see the difference between the wrapped portion involving removal of slack and the integral twisted portion involving buildup of tension. Finally, after a certain period of time, the tracer yarn will move into the central layer again, as shown in F. Figs. 3.11-3.16 show the same sequence with the tracer in different spacer positions.

Fig. 3.17 represents the tension history for one of the 7 singles during a migration cycle. The single will reduce its tension from a value $\frac{T_y \sec \alpha}{6}$ as given by equation (3) to a zero value during a length of ply yarn S_o. During the formation of the ply length S_x, the yarn will develop the slack needed to initiate outward migration. The length S_y is the duration of slack removal and with the elimination of slack, the tension will build up as shown. In the following section, we will obtain theoretical expressions for S_o, S_x and S_y, together with the form in which the tension will build up in a single as it occupies the outside.

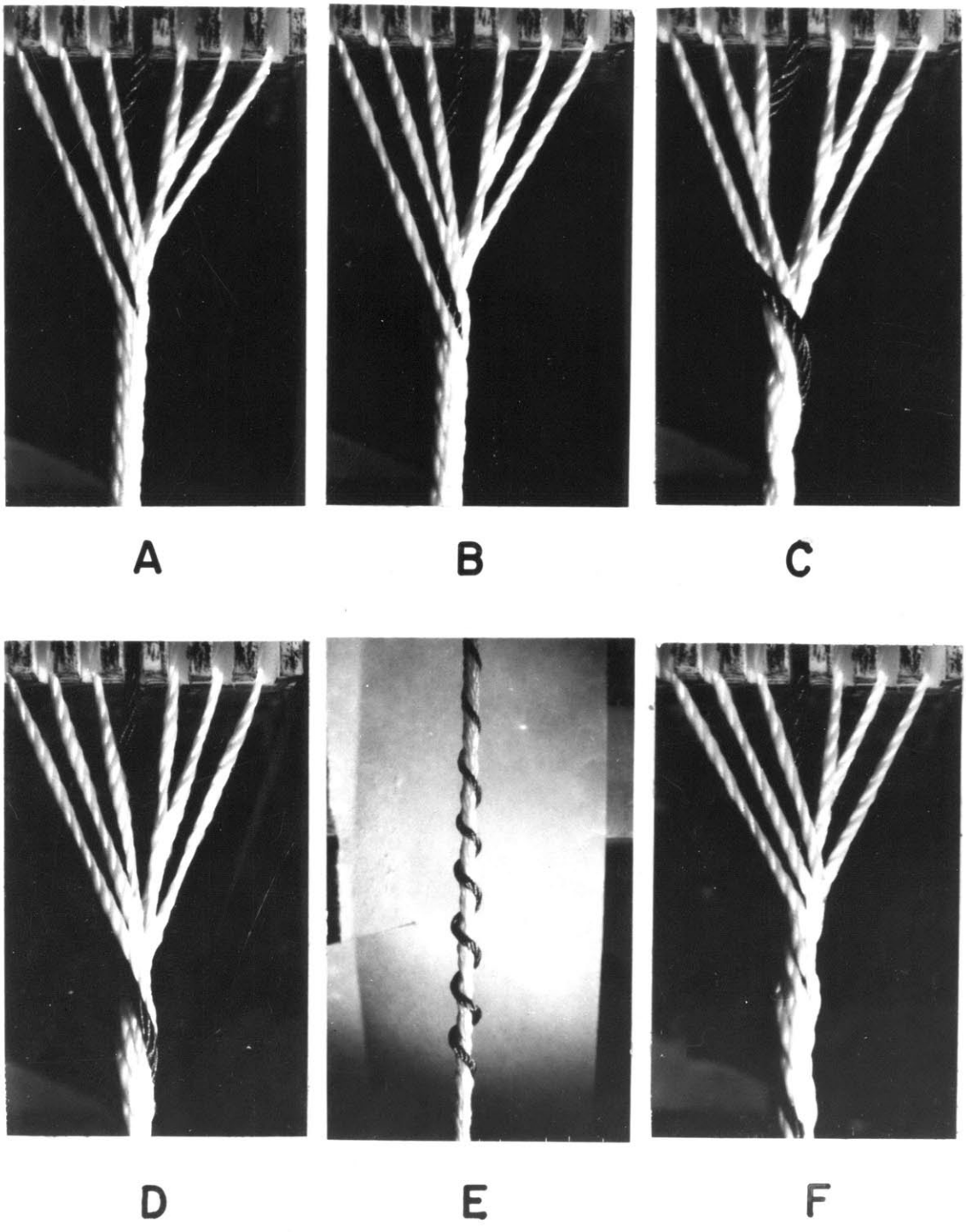

Fig. 3.10

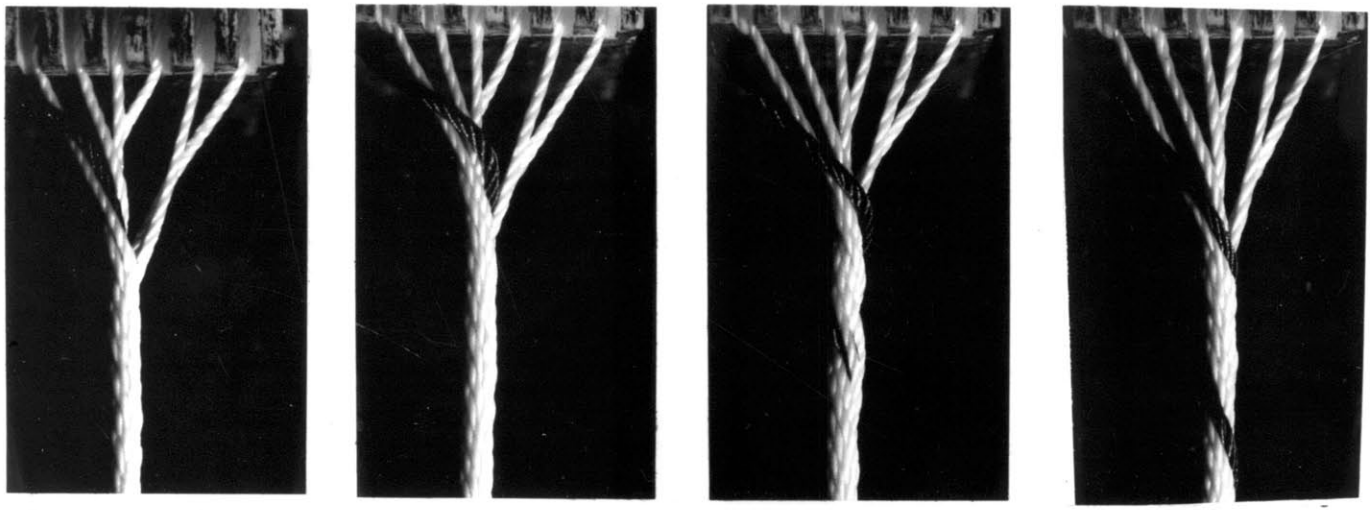

Fig. 3.11

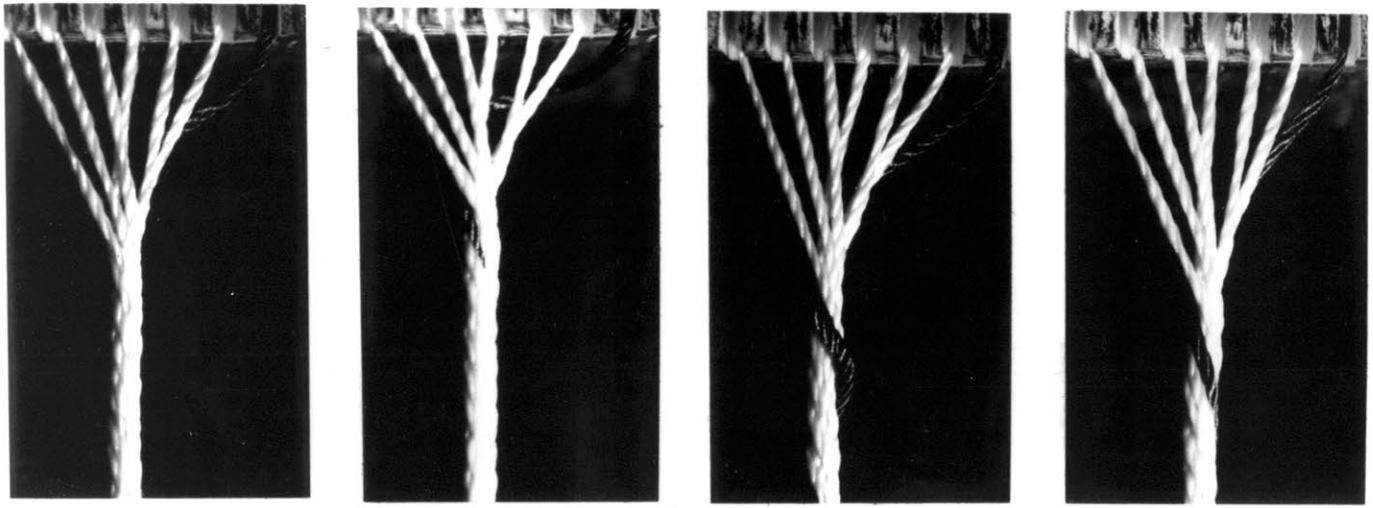

Fig. 3.12

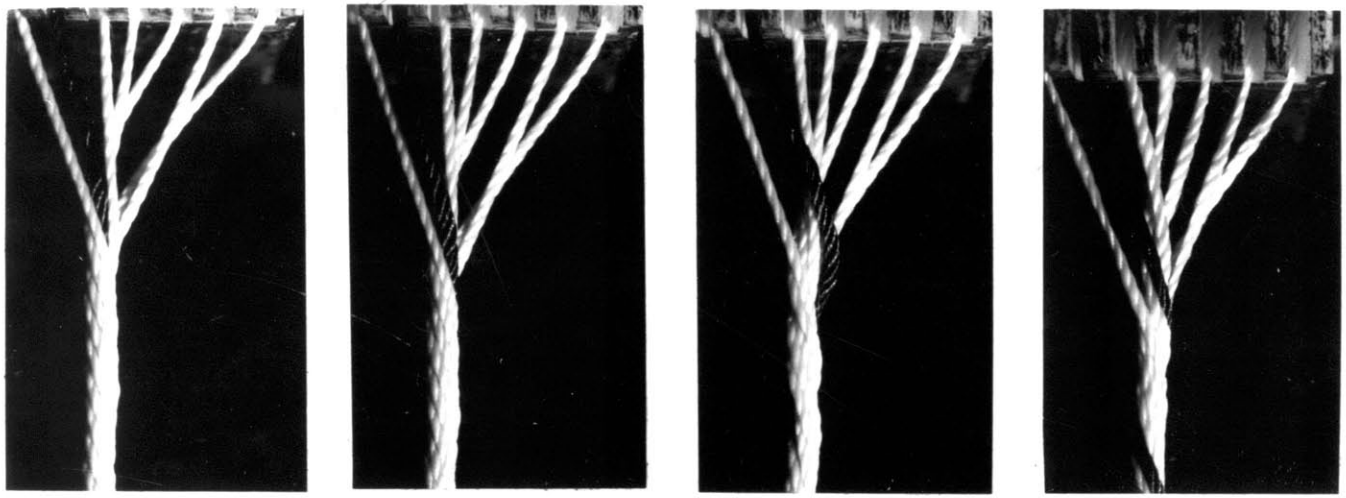

Fig. 3.13

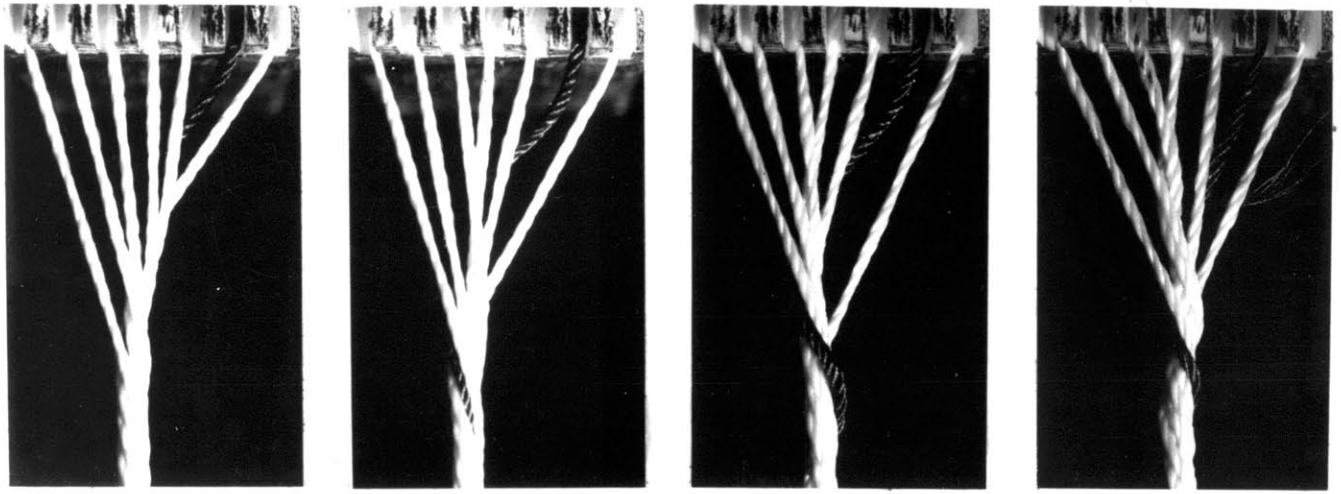

Fig. 3.14

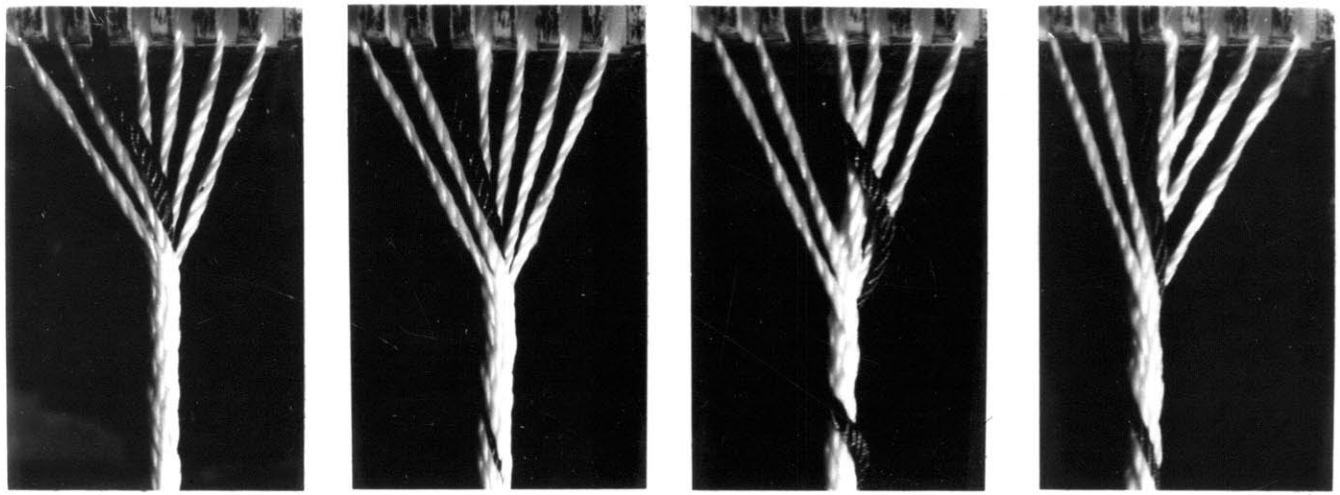

Fig. 3.15

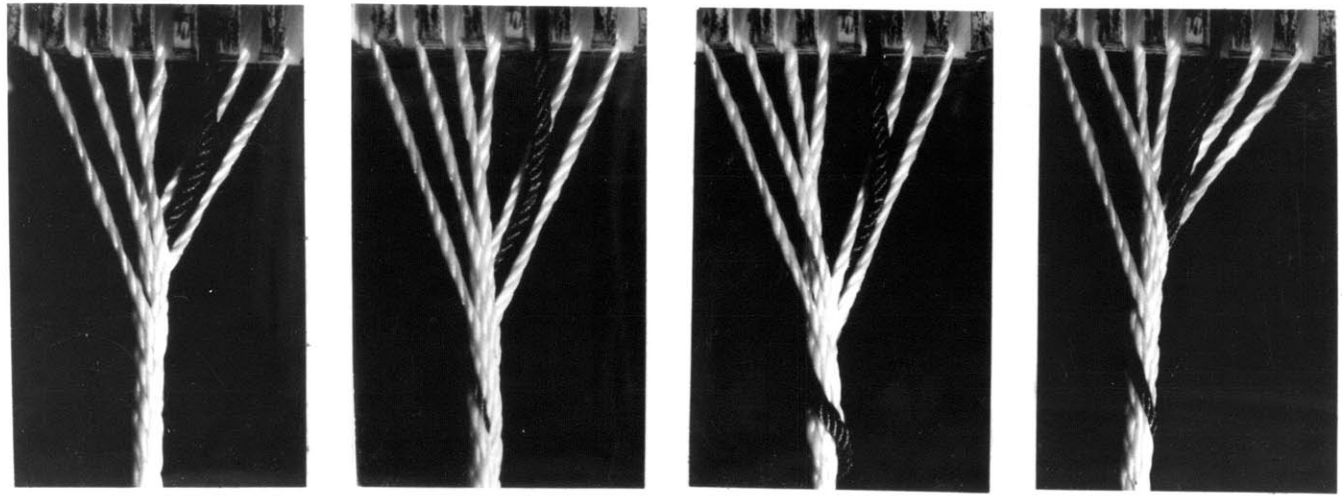

Fig. 3.16

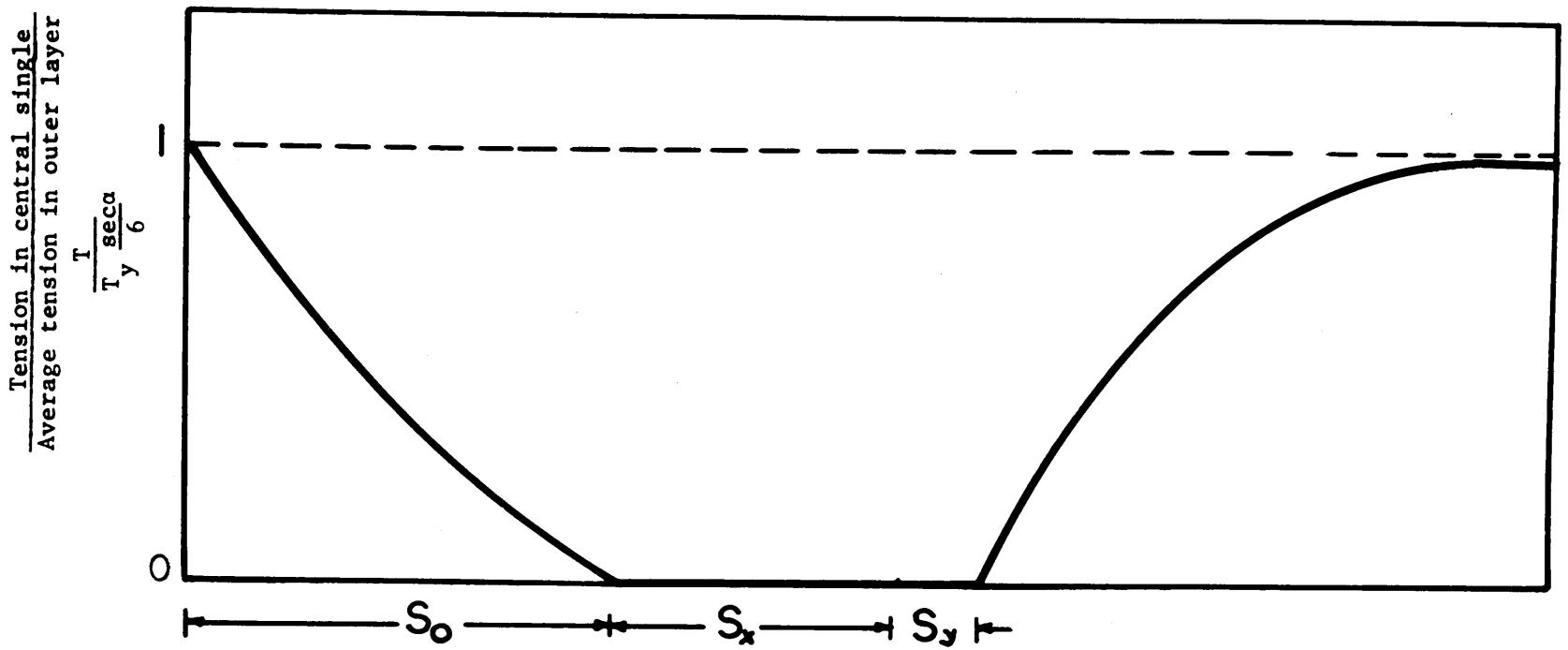

Fig. 3.17 Variation of Tension in a Single Yarn During a Migration Cycle

(1) Length of Ply Required for Loss of Tension (S_o). Let us consider the period in which the element of ply yarn of length dS shown in Fig. 3.18 is formed. Let the tension in the central yarn be T. Then the tension supported by the outer layer is given by

$$T_y - T \qquad 3.4$$

If we now assume that the tension in the outer layer is carried only by 5 yarns due to the fact that the yarn which just migrated outward is still wrapping around the ply structure with no tension, then the tension in one yarn in the outer layer during this period is

$$\frac{T_y - T}{5} \sec \alpha \qquad 3.5$$

and its strain is given by

$$\epsilon_o = \frac{(T_y - T) \sec \alpha}{5 \gamma} \qquad 3.6$$

It should be noted here that Hearle and Merchant used the mean strain given by equation 3.3 instead of equation 3.6.

Since the yarn in the outer layer is following a helical path, then the length of the outer layer in dS is dS sec α . This length (dS sec α) is actually the strained length, whereas the actual zero strain length supplied by the front rollers to form a length dS of ply yarn is given by

$$\frac{dS \sec \alpha}{1 + \epsilon_o}$$

or

$$\frac{dS \sec \alpha}{1 + \frac{T_y - T}{5 \gamma} \cdot \sec \alpha} \qquad 3.7$$

The strained length of the central yarn in dS is dS and the

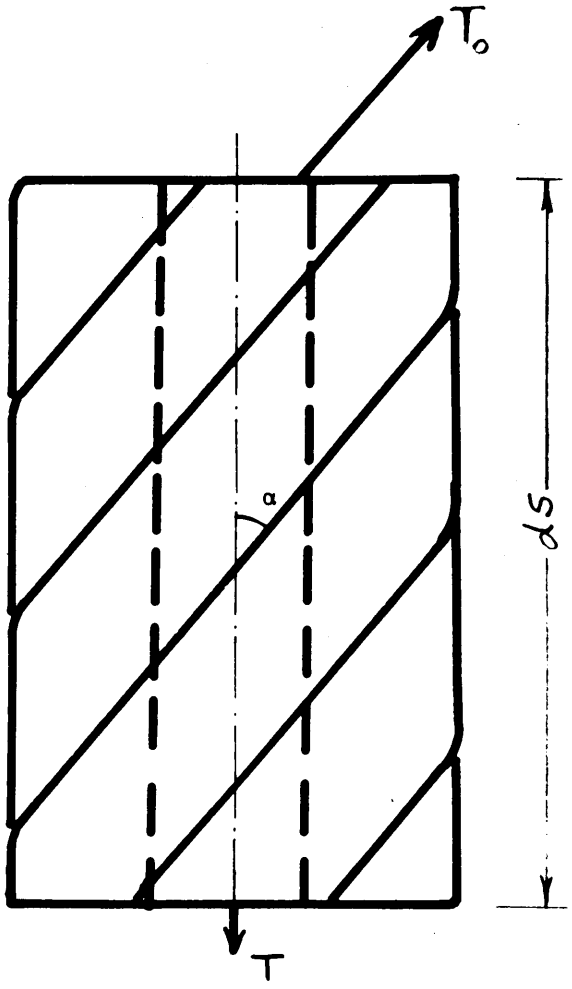

T_y = Ply Yarn Tension

T = Central Yarn Tension

T_o = Tension in outside Layer

$= \frac{T_y - T}{5}$ see α

Fig. 3.18 Element of Ply yarn

actual zero strain length supplied by the front rollers to form a ply yarn dS is

$$\frac{dS}{1 + \epsilon_c} = \frac{dS}{1 + T/\gamma} \qquad 3.8$$

where ϵ_c = strain in central yarn = $\frac{T}{\gamma}$ 3.9

The excess length supplied to the central yarn is given by the difference of equations 3.7 and 3.8, i.e.,

$$\frac{dS \sec \alpha}{1 + \frac{(T_y - T)\sec\alpha}{5\gamma}} - \frac{dS}{1 + T/\gamma} \qquad 3.10$$

This excess length is shared by the whole free length between the front roller nip A and the twist point O. If L_i is the strained free length (in the region A-B-O) of the yarn occupying the central position at that instant, then its free length (as measured under zero strain) is given by

$$\frac{L}{1 + T/\gamma} \qquad 3.11$$

Because of the excess length supplied to the central yarn, its tension will now be reduced. Let the reduction in tension during the formation of dS to be -dT.

Therefore, we have $-dT = \gamma$ x (reduction in strain in the free length) where the reduction in strain in free length is equal to

$$\frac{\text{excess length supplied to central yarn}}{\text{free length of central yarn as measured under zero tension}} \qquad 3.12$$

$$\therefore \quad -dT = \gamma \frac{\left[\frac{\sec\alpha}{1 + (T_y - T\sec\alpha)/5\gamma} - \frac{1}{1 + T/\gamma}\right] dS}{\frac{L}{1 + T/\gamma}}$$

or

$$\frac{dS}{L} = \frac{1}{\gamma}\left[1 - \frac{1 + T/\gamma}{\cos\alpha - (T_y - T)/5\gamma}\right] dT \qquad 3.13$$

If we now integrate equation 3.12 subject to the boundary conditions:

$$\text{at } S = o \qquad T = \frac{T_y \sec \alpha}{6}$$

and 3.14

$$\text{at } S = S_o \qquad T = 0$$

and using the notation that ϵ_s is the mean strain in outer layer as given by equation 3.3, we get

$$\frac{S_o}{L} = \frac{5}{36}\left\{1 + \cos\alpha(5 + 6\epsilon_s)\right\}\left[\ln\frac{(1-\cos\alpha)(5+6\epsilon_s)}{5(1-\cos\alpha) - 6\epsilon_s\cos\alpha}\right] - \frac{\epsilon_s}{6} \qquad 3.15$$

Fig. 3.19 represents the theoretical relation 3.15 for different helix angles, and it is seen that as the helix angle increases, the length S_o decreases.

(2) Length of Ply Yarn Required to Develop a Slack X in the Central Yarn. After the tension in the central yarn had reached a zero value, it will continue to occupy the central position until it develops a certain amount of slack in the free length zone of the twist triangle. If we identify such a slack by

$$X = \frac{\text{(slack/length of yarn in free length zone-projected length in free zone)}}{\text{(projected length in free zone)}}$$

then the length of ply yarn S_x (measured after the central yarn reaches a zero tension state) required to develop a slack X is given by Hearle[17] as:

$$\frac{S_x}{L} = \frac{X\cos\alpha(1+\epsilon_s)}{1 - \cos\alpha(1+\epsilon_s)} \qquad 3.16$$

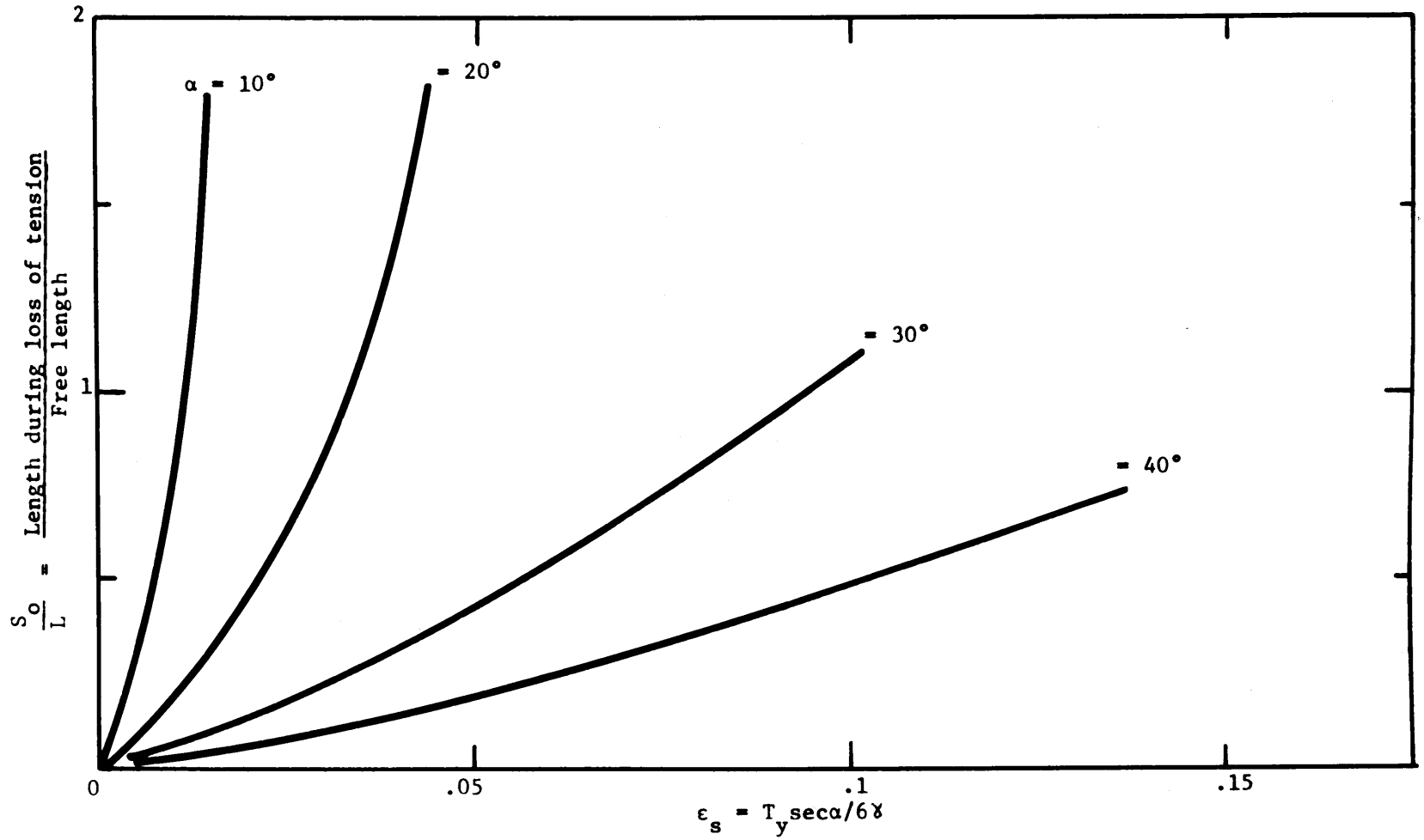

Fig. 3.19 Effect of Tension and Twist on Length in the Central Position for a Fiber to Drop its Tension from the Average of $\frac{T_y \sec\alpha}{6}$ To a Zero Value

Fig. 3.20 represents equation 3.16 for different values of

3. Length of Ply Yarn in which a Single Occupies the Central Position. Combining 3.15 and 3.16 we get:

$$\frac{S_o + S_x}{L} = \frac{S_c}{L} = \frac{5}{36}\left\{1 + \cos\alpha(5+6\epsilon_s)\right\}\left[\ln\frac{(1-\cos\alpha)(5+6\epsilon_s)}{5(1-\cos\alpha)-6\epsilon_s}\right] + \frac{X\cos\alpha(1+\epsilon_s)}{1-\cos\alpha(1+\epsilon_s)} - \frac{\epsilon_s}{6} \qquad 3.17$$

where S_c is the total length of ply yarn in which a single will occupy the center position. The corresponding expression obtained by Hearle[17] is

$$\frac{S_c}{L} = \cos\alpha(1+\epsilon_s)\ln\frac{(1-\cos\alpha)(1+\epsilon_s)}{(1-\cos\alpha)-\epsilon_s\cos\alpha} - \frac{X\cos\alpha(1+\epsilon_s)}{1-\cos\alpha(1+\epsilon_s)} \qquad 3.18$$

The two theories 3.17 and 3.18 agree fairly well at low yarn tensions, but at higher yarn tensions equation 3.17 shows values which exceed by 10-15% those obtained by Hearle[17] via equation 3.18. It should also be noted that in Hearle's[17] theory the free length of all yarns was the same, while in this modified theory the free length differs from single to single.

4. Frequency of Migration. The length S_c, as given by equation 3.17, represents the average length of ply yarn in which a single will occupy the center position. For a given ply yarn, each single will occupy the central position for one-seventh of the total ply yarn length. Since for each time a single occupies the center position it has two migrations (one inward and one outward),

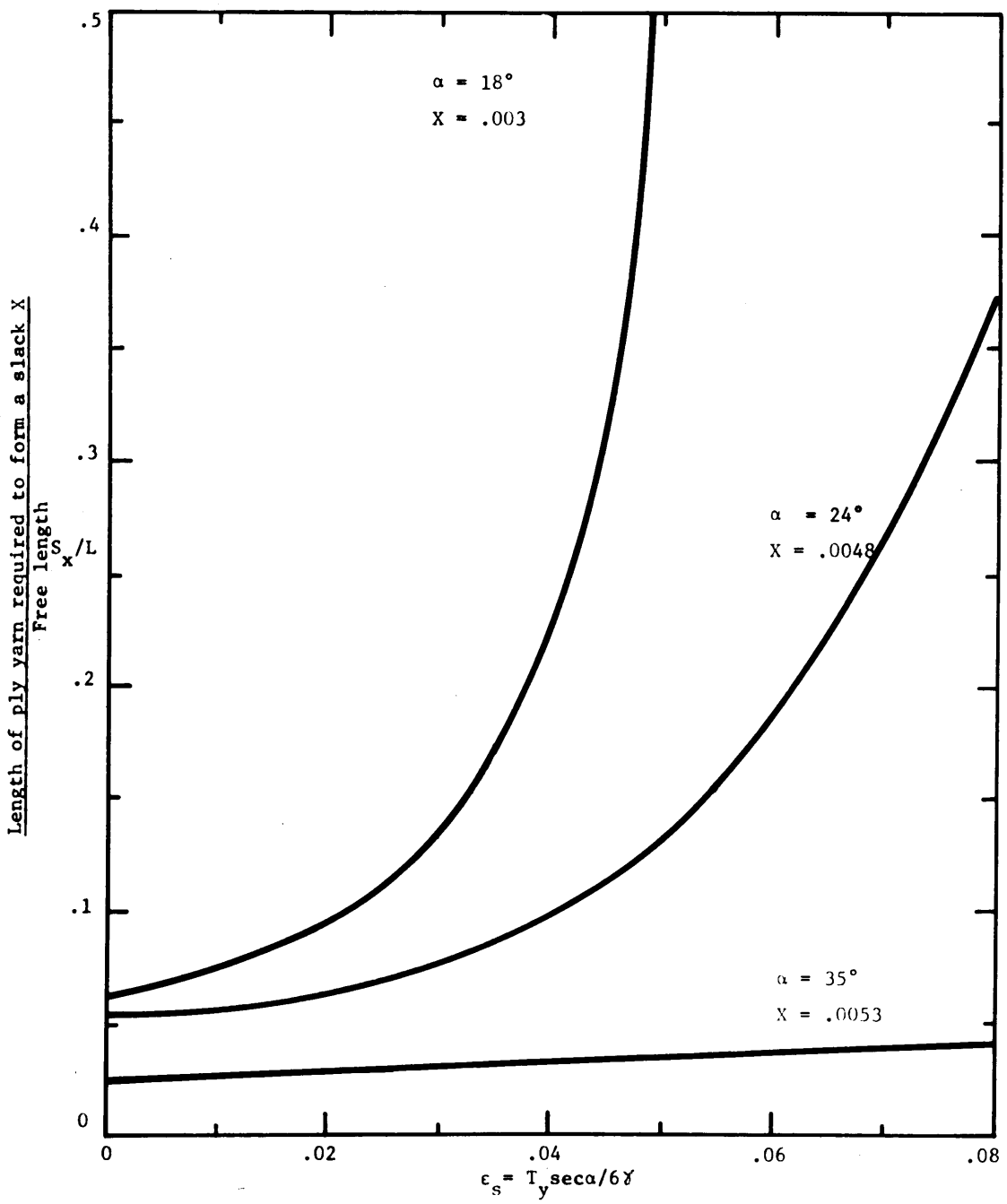

Fig. 3.20 Variation of Theoretical Ply Length for Developing a Slack X with Tension and Twist

then it follows that the number of migrations per single yarn per unit length of ply yarn is given by:

$$f = \frac{2}{7\,S_c} \qquad 3.19$$

Equations 3.17 and 3.19 indicate that the frequency of migration "f" depends on:

(a) The helix angle α

(b) The twisting tension T_y

(c) The fractional modulus

(d) The free length L

(e) The amount of slack needed to initiate outward migration X.

5. Calculation of Slack Needed to Initiate Outward Migration. After the central single reaches a zero state, it will continue in the central position until it develops a certain amount of slack. Let us consider the case where the 7-ply structure twists in an idealized form as shown in Fig. 3.21a with the middle single occupying the core position as shown. Now the free length of the core will increase due to the excess length supplied to it. The single then will assume the shape of a catenary or ellipse as shown. The twisting torque which is acting along the ply yarn axis will cause the slack single to rotate about that axis as a solid body. If the single has the sufficient amount of slack, it will be caught (while it is rotating) between two of the other singles and will be forced to move to the outside layer. This will take place when the center line of the single #2 cuts the surface of revolution generated by the rotation of the slack single.

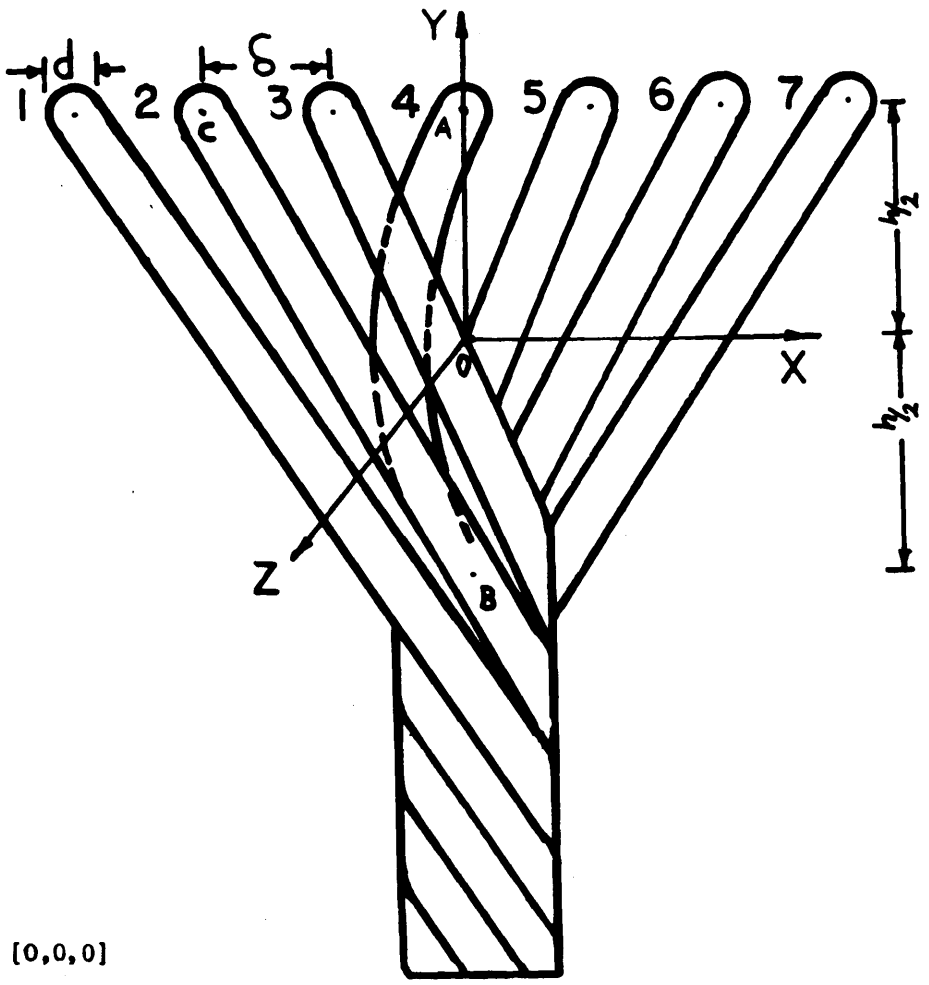

- a -

O ≡ [0,0,0]

A ≡ [0, $\frac{h}{2}$,0]

B ≡ [0,- $\frac{h}{2}$,0]

C ≡ [- 2δ, $\frac{h}{2}$, 0]

D ≡ [0,- $\frac{h}{2}$,d]

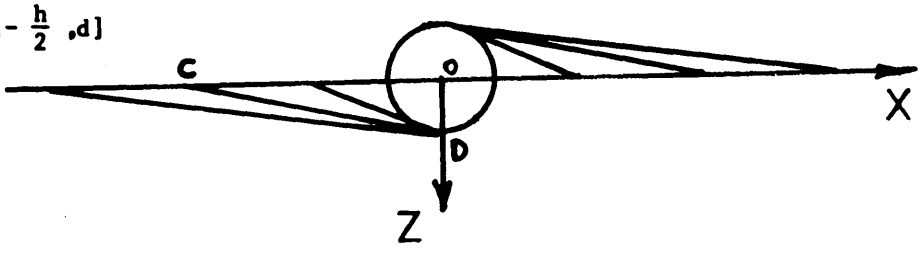

- b -

Fig. 3.21 Idealized Model of a 7-Ply Structure

"Development of Slack"

Let us pick the axes shown in Fig. 3.21 with the origin located on the ply yarn centerline midway between the roller nip and the twist point B. The Cartesian equation for the line CD is given by the interception of the plane passing through the points O (0, 0, 0), C $(-2\delta, \frac{h}{2}, d)$ & D $(0, -\frac{h}{2}, d)$, with the plane passing through A $(0, \frac{h}{2}, 0)$, C and D, where:

δ = distance between filaments along roller nip

h = height of twist triangle

d = diameter of singles

Now the equation of the plane passing through O, C and D is given by

$$\frac{d}{2\delta} x + \frac{2d}{h} y + z = 0 \qquad 3.20$$

and the equation of the plane through A, C and D is given by

$$\frac{2}{h} y + \frac{2}{d} z = 1 \qquad 3.21$$

The equation of the catenary is given by

$$u = b \cosh \frac{y}{b} \qquad 3.22$$

where

u is a dummy variable

b is a constant depending on the length of the catenary.

The equation of the body of revolution of the catenary (3.22) around the y-axis is given by

$$b \cosh \frac{y}{b} = \sqrt{x^2 + z^2} \qquad 3.23$$

Based on the assumption that the amount of slack required to initiate outward migration is achieved when the line given by equation 3.20 and equation 3.21 is a tangent to the body of revolution (3.23), one can obtain

the length of the catenary by solving 3.20, 3.21 and 3.23 with the conditions that they have a unique solution. So, by solving these equations with the requirements that there is one and only one solution, the constant b (which determines the catenary length) can be obtained and the slack is then given by

$$h\,(1 + X) = 2\int_{o}^{h/2} \sqrt{1 + u'^2}\, dy \qquad 3.24$$

where $u' = \frac{du}{dy}$ and u is given by equation 3.22.
The solution of the equations 3.20, 3.21 and 3.23, together with the evaluation of the integral 3.24 is quite difficult due to the presence of the hyperbolic function.

To simplify the analysis, let us assume that the slack yarn will take the shape of an ellipse (instead of a catenary) of semi-axis $\frac{h}{2}$ and a. The body of revolution generated by the rotation of the ellipse about its major axis (ply yarn axis) is an ellipsoid of the form

$$\left(\frac{x}{a}\right)^2 + \left(\frac{y}{h/2}\right)^2 + \left(\frac{z}{a}\right)^2 = 1 \qquad 3.25$$

The solution of the equations 3.20, 3.21 and 3.25 will result in an equation of the form

$$\left[\left(\frac{2\delta}{ad}\right)^2 + \left(\frac{2}{d}\right)^2 + \left(\frac{1}{a}\right)^2\right]\gamma^2 - \left[2\alpha\left(\frac{2\delta}{ad}\right)^2 + \frac{4}{d}\right]\gamma$$

$$+ \frac{4\delta^2}{a^2} = 0 \qquad 3.26$$

The solution of equation 3.26 leads to

$$\beta = \frac{\left[2\alpha\left(\frac{2\delta}{a\alpha}\right)^2 + \frac{4}{\alpha}\right]}{2\left[\left(\frac{2\delta}{a\alpha}\right)^2 + \frac{4}{\alpha^2} + \frac{1}{a^2}\right]} \pm \frac{\sqrt{\left[2\alpha\left(\frac{2\delta}{a\alpha}\right)^2 + \frac{4}{\alpha}\right]^2 - 16\left(\frac{\delta}{a}\right)^2\left[\left(\frac{2\delta}{a\alpha}\right)^2 + \left(\frac{2}{\alpha}\right)^2 + \frac{1}{a^2}\right]}}{2\left[\left(\frac{2\delta}{a\alpha}\right)^2 + \frac{4}{\alpha^2} + \frac{1}{a^2}\right]} \qquad 3.27$$

and for equation 3.27 to have one and only one solution (unique solution) we have

$$\left[2\alpha\left(\frac{2\delta}{a\alpha}\right)^2 + \frac{4}{\alpha}\right]^2 = 16\left(\frac{\delta}{a}\right)^2\left[\left(\frac{2\delta}{a\alpha}\right)^2 + \left(\frac{2}{\alpha}\right)^2 + \left(\frac{1}{a}\right)^2\right] \qquad 3.28$$

which can be reduced to

$$\frac{1}{\alpha^2} = \frac{\delta^2}{a^4}$$

or

$$a = \sqrt{\delta\alpha} \qquad 3.29$$

Knowing a (semi-minor axis of the ellipse) the slack X can be calculated by computing half the length of the ellipse with semi-axis (a and $\frac{h}{2}$), which is equal to h(1 + X) as follows

$$h(1+X) = 2\int_0^{h/2} \sqrt{1 + x'^2}\, dy$$

or

$$X = \frac{2}{h}\int_0^{h/2} \sqrt{1 + x'^2}\, dy - 1 \qquad 3.30$$

where

$$x' = \frac{dx}{dy}$$

&

$$x = \sqrt{a^2 - \frac{4a^2}{h^2}y^2} \qquad 3.31$$

The integration in (3.30) can be computed by the use of elliptical integral tables. Fig. 3.22 represents the slack X as a function of the factor K which is given by

$$K = \sin^{-1}\sqrt{1 - \frac{4a^2}{h^2}} \qquad 3.32$$

where a is given by Equation 3.29.

It is clear here that as K increases, the amount of slack decreases. Slack X vanishes when K reaches $\frac{\pi}{2}$. This will only take place when the quantity $\frac{4\alpha\delta}{h}$ becomes zero, which means that either h is ∞ or d is zero. The condition that $h \longrightarrow \infty$ can only exist when no twist is inserted. Since the diameter of the fiber is always finite, it is clear that for any practical case the value $\frac{4\delta d}{h}$ may become very small, but will never vanish, provided that the structure is an opened one, i.e. δ is not zero.

(6) Development of Tension in Yarns in Outer Layer. When a single migrates to the outside, its free length will have an amount of slack developed to initiate outward migration. The single then will wrap around the other components during the period of slack removal and will have a different helix angle as shown in Fig. 3.10E. When the slack is removed, the tension will start building up in the single. As the tension starts to build up, the single will take the twisted configuration as shown in Fig. 3.10E, and will have the same helix angle as the other components.

(a) Removal of Slack. The length of ply

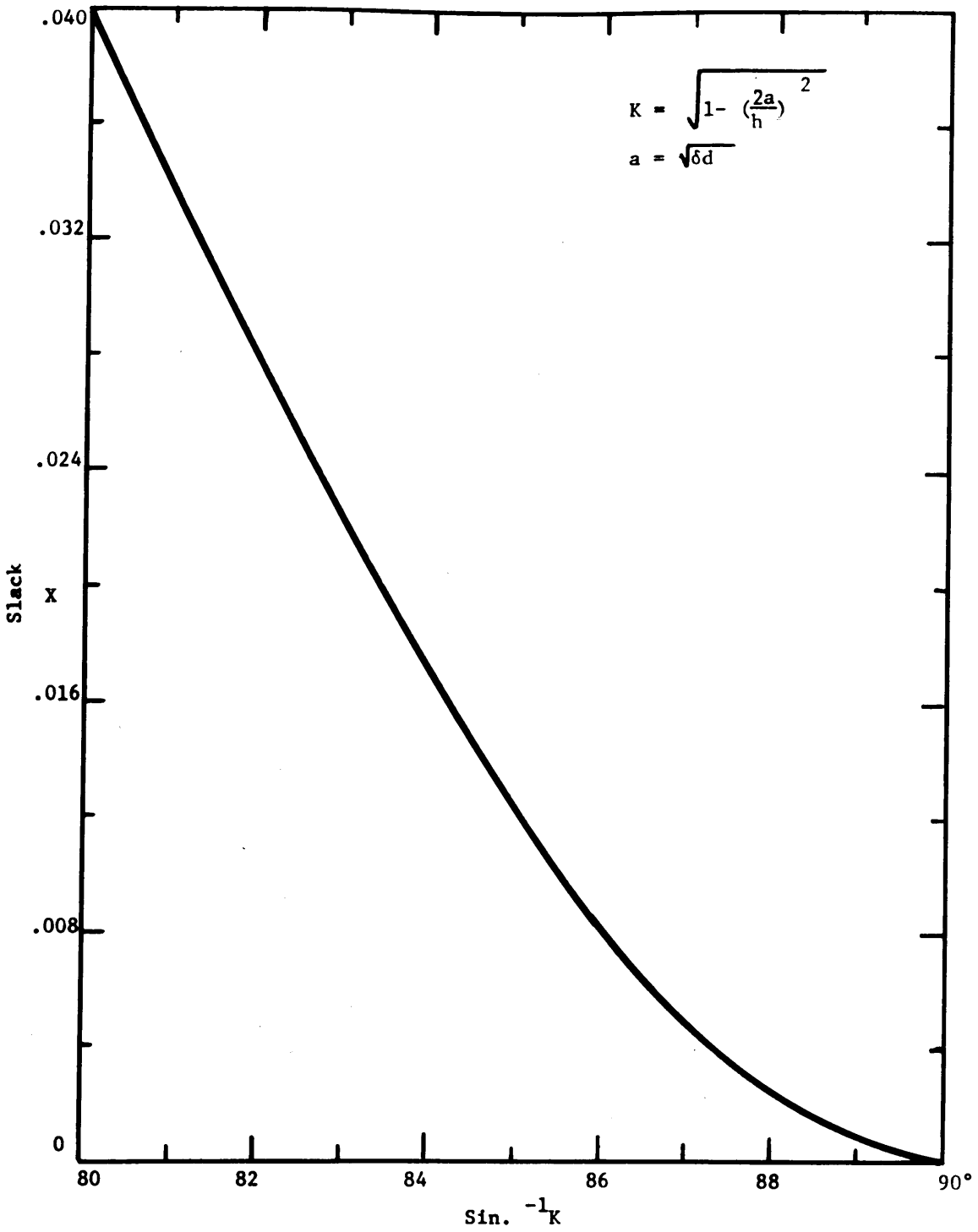

Fig. 3.22 Variation of Slack with Filament Diameter and Twist Triangle Dimensions.

yarn S_y necessary to remove the slack X from the free length zone can be calculated as follows. Let the helix angle of the wrapped single to be = α_1, and the helix angle of the other singles in the outer layer to be = α The length of singles in the outer layer (as measured under zero tension) to form a length S_y of ply yarn is given by:

$$\frac{S_x \sec \alpha}{1 + T_y \sec \alpha / 6\gamma} \qquad 3.33$$

For the single under consideration (the one which is wrapped around the structure) the length to form S_y is:

$$S_y \sec \alpha_1 \qquad 3.34$$

The difference between equations 3.34 and 3.33 is equal to the amount of slack to be removed, or

$$XL = S_y \sec \alpha_1 - \frac{S_y \sec \alpha}{1 + T_y \sec \alpha / 6\gamma} \qquad 3.35$$

and using the notation that $\epsilon_s = T_y \sec \alpha / 6\gamma$ we get:

$$\frac{S_y}{L} = \frac{X(1 + \epsilon_s)}{\sec \alpha_1 (1 + \epsilon_s) - \sec \alpha} \qquad 3.36$$

As discussed before, a single will, during its slack removal, wrap around the other 6 components. It can be easily shown, as will be discussed later in the experimental work, that the 6 components will be twisted in the most stable configuration with one in the center position and 5 around it, leaving an opening for the sixth single as shown in Figs. 3.23 and 3.24. In this case the radial distance measured from the ply yarn center to the center line of the singles (5 yarns) in the outer layer is equivalent to the diameter of a single. The single which,

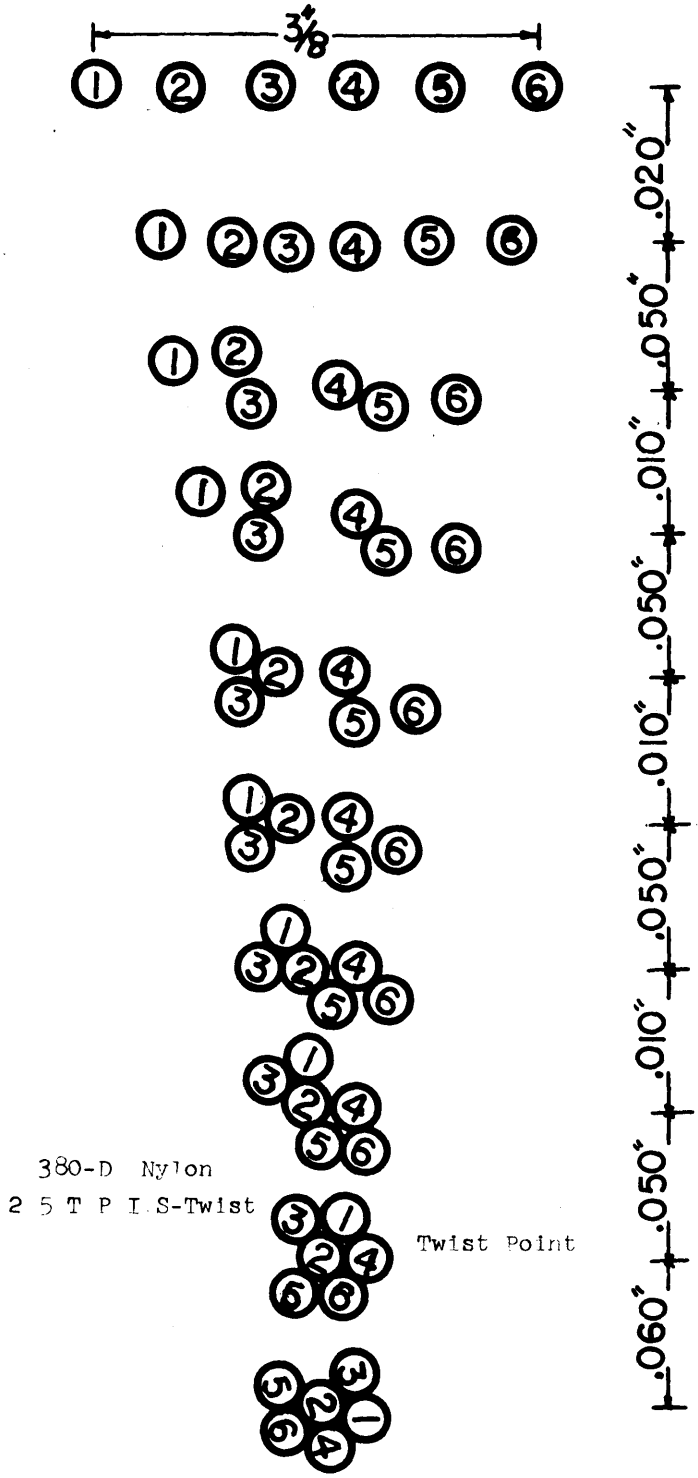

Fig 3 23 Twisting of a 6-Component Yarn
(At Constant Length)

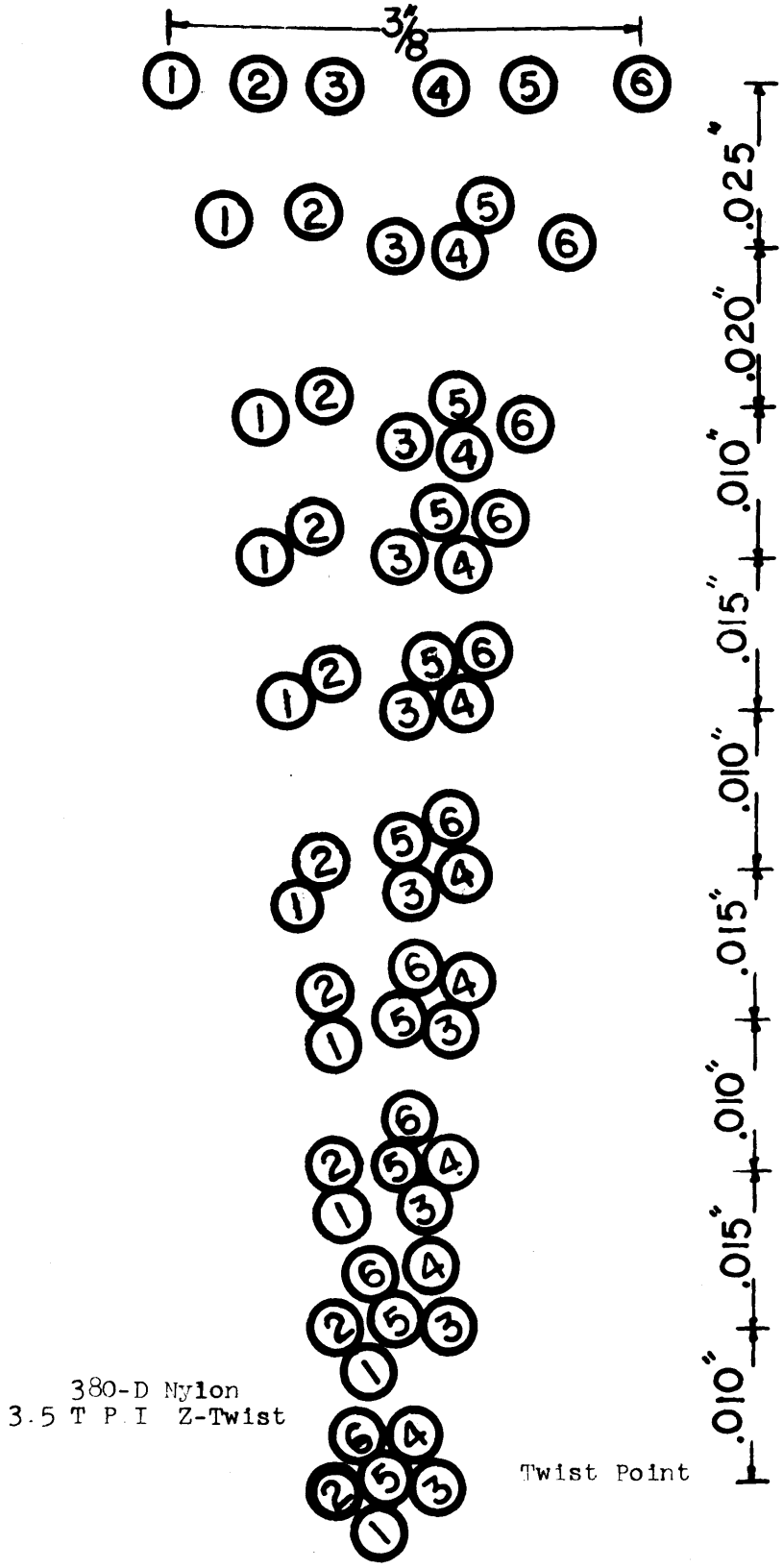

Fig 3 24 Twisting of a 6-Component Yarn
(At Constant Tension of 200gm)

losing its slack, will have its center line at a distance two singles diameters from the ply yarn center. Let us now assume the twist/unit length to be n, therefore, we have

$$\tan\alpha = \pi d.n \quad \& \quad \tan\alpha_1 = 2\pi d.n \qquad 3.37$$

from which we have

$$\alpha_1 = \tan^{-1} 2 \tan\alpha \qquad 3.38$$

Fig. 3.25 shows the variation of $S_y/_L$ as a function of ϵ_s for different values of X and α, while Fig. 3.26 represents the variation of α_1 with α.

(b) Tension Build up. After the slack had been completely removed from the free length of the single which has migrated to the outside, tension will start to build up in that single. Let us consider the instance when the tension in the single under consideration has reached the value T. Now the tension carried by other components in outer layer (neglecting the tension in the core) is given by:

$$T_y - T\cos\alpha \qquad 3.39$$

The tension in each one of 5 singles in outer layer is

$$\frac{T_y - T\cos\alpha}{5\gamma} \sec\alpha \qquad 3.40$$

Consider the formation of length ds of ply yarn during this tension build up. The length of each of the 5 singles in the outer layer measured under zero tension to form the ply length ds is:

$$\frac{ds \sec\alpha}{1 + \frac{T_y - T\cos\alpha}{5\gamma} \sec\alpha} \qquad 3.41$$

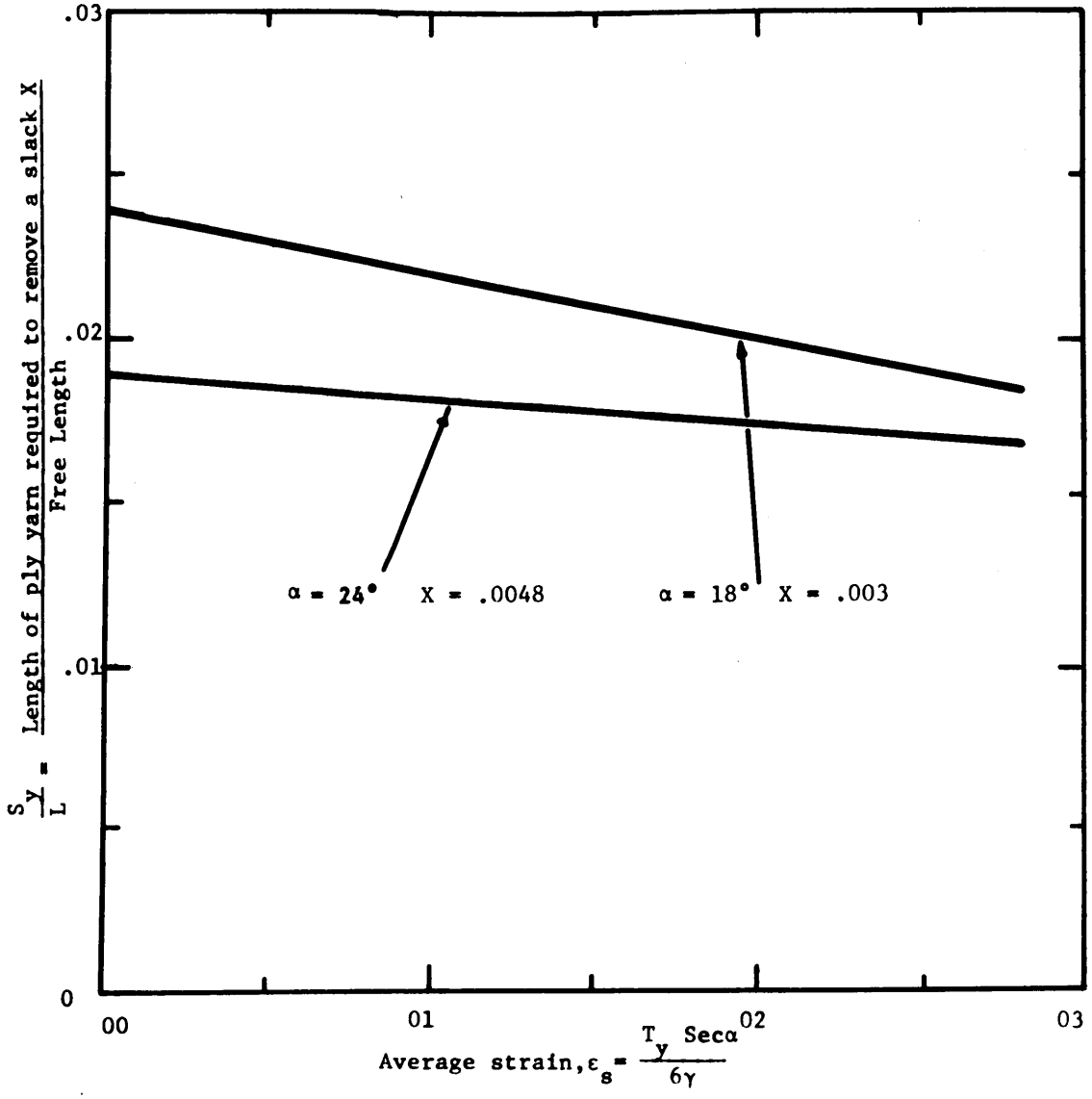

Fig. 3.25 Theoretical Variation of Ply Length for Slack Removal With Twisting Tension

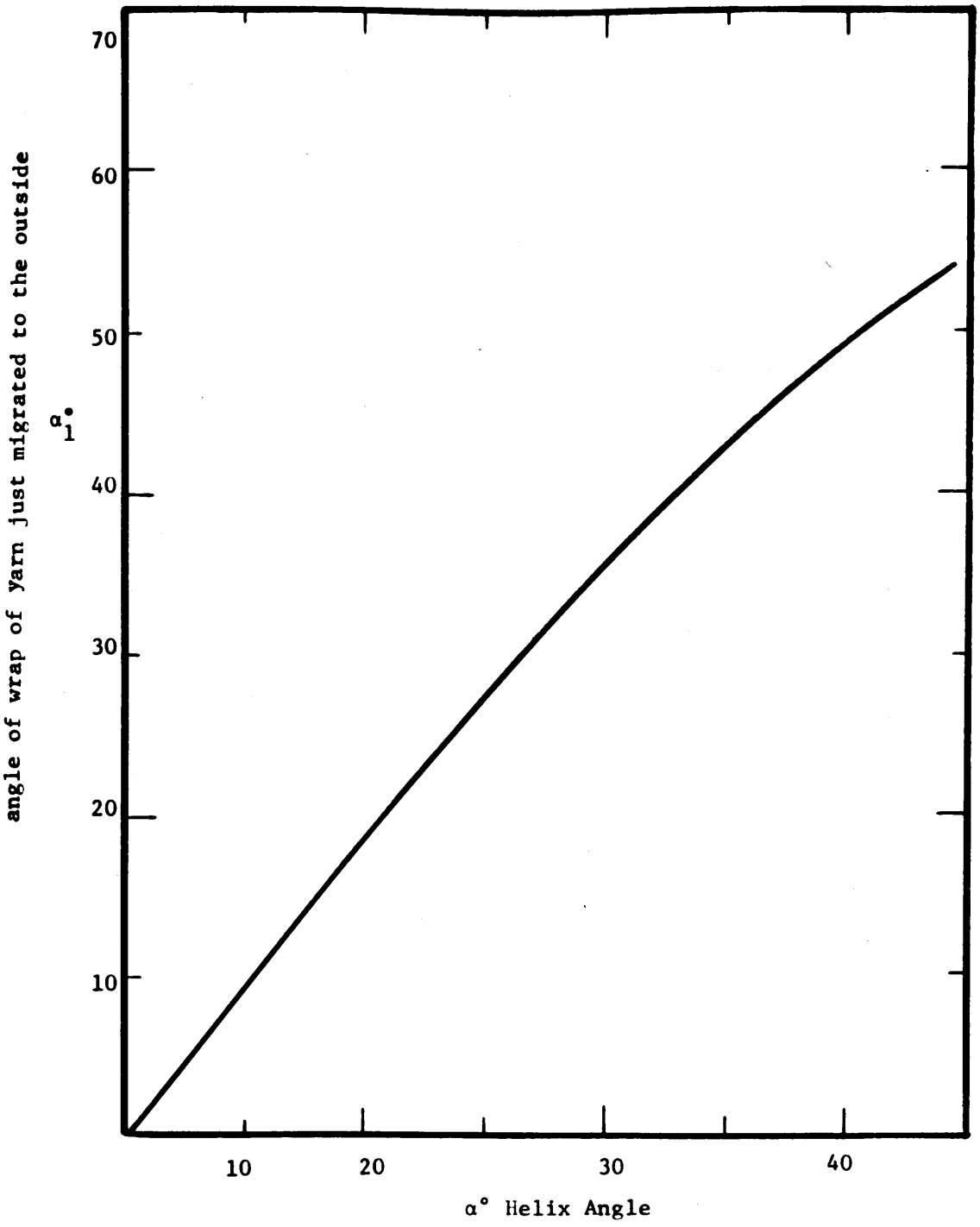

Fig. 3.26 Variation of angle of wrap with helix angle

The length of the single yarn under consideration (measured under zero tension) used to form a length ds of ply yarn is

$$\frac{dS \cdot \sec\alpha}{1 + T/\gamma} \qquad 3.42$$

The free length of the single under consideration as measured under zero tension is

$$\frac{L}{1 + T/\gamma} \qquad 3.43$$

The difference between 3.42 and 3.41 is the increase in actual elongation of the single.

If the increase in tension in the single during the formation of ds is dT, then we have

$$\frac{dT}{\gamma} = \frac{\text{increase in elongation}}{\text{Free length of single measured under zero tension}}$$

or

$$\frac{dT}{\gamma} = \frac{\dfrac{dS\sec\alpha}{1 + T/\gamma} - \dfrac{dS\sec\alpha}{1 + \dfrac{T_y - T\cos\alpha}{5\gamma}\sec\alpha}}{\dfrac{L}{1 + T/\gamma}}$$

which can be written in the form:

$$\frac{dS}{L\cos\alpha} = \frac{5\gamma + T_y\sec\alpha - T}{T_y\sec\alpha - 6T} \cdot \frac{dT}{\gamma} \qquad 3.44$$

Integrating in accordance with the boundary conditions

$T = o$ when $S = o$

and using $\epsilon_s = T_y \sec\alpha / 6$ we get

$$\frac{S}{L} = \frac{5}{6}\cos\alpha(1+\epsilon_s)\ln\frac{\epsilon_s}{\epsilon_s - T/\gamma} + \frac{T\cos\alpha}{6\gamma} \qquad 3.45$$

The last term in this equation is quite small compared to

the other terms and can be neglected so as to give:

$$\frac{S}{L} = \frac{5}{6}\cos\alpha(1+\epsilon_s)\ln\frac{\epsilon_s}{\epsilon_s - T/\gamma} \qquad 3.46$$

which leads to

$$\frac{T}{\gamma} = \epsilon_s\left(1 - e^{-\frac{6\,S/L}{5\cos\alpha(1+\epsilon_s)}}\right)$$

or

$$\frac{T}{T_y\frac{\sec\alpha}{6}} = 1 - e^{-\frac{6/5\;S/L\sec\alpha}{1+\epsilon_s}} \qquad 3.47$$

The corresponding expression derived by Hearle[17] is

$$\frac{T}{T_y\frac{\sec\alpha}{6}} = 1 - e^{-\frac{S/L\sec\alpha}{6(1+\epsilon_s)}} \qquad 3.48$$

The difference between the two expressions 3.47 and 3.48 is that in Hearle's[17] expression the tension will rise more rapidly than in the expression given here. Based on his expressions Hearle[17] showed that the yarn which has just migrated to the outside will have a certain probability to move back again before the other ones. According to our expression, this probability will be smaller than that obtained by Hearle. It should be noticed here that there are other factors which could influence the probability of a single to move back into the center before the other singles, such as

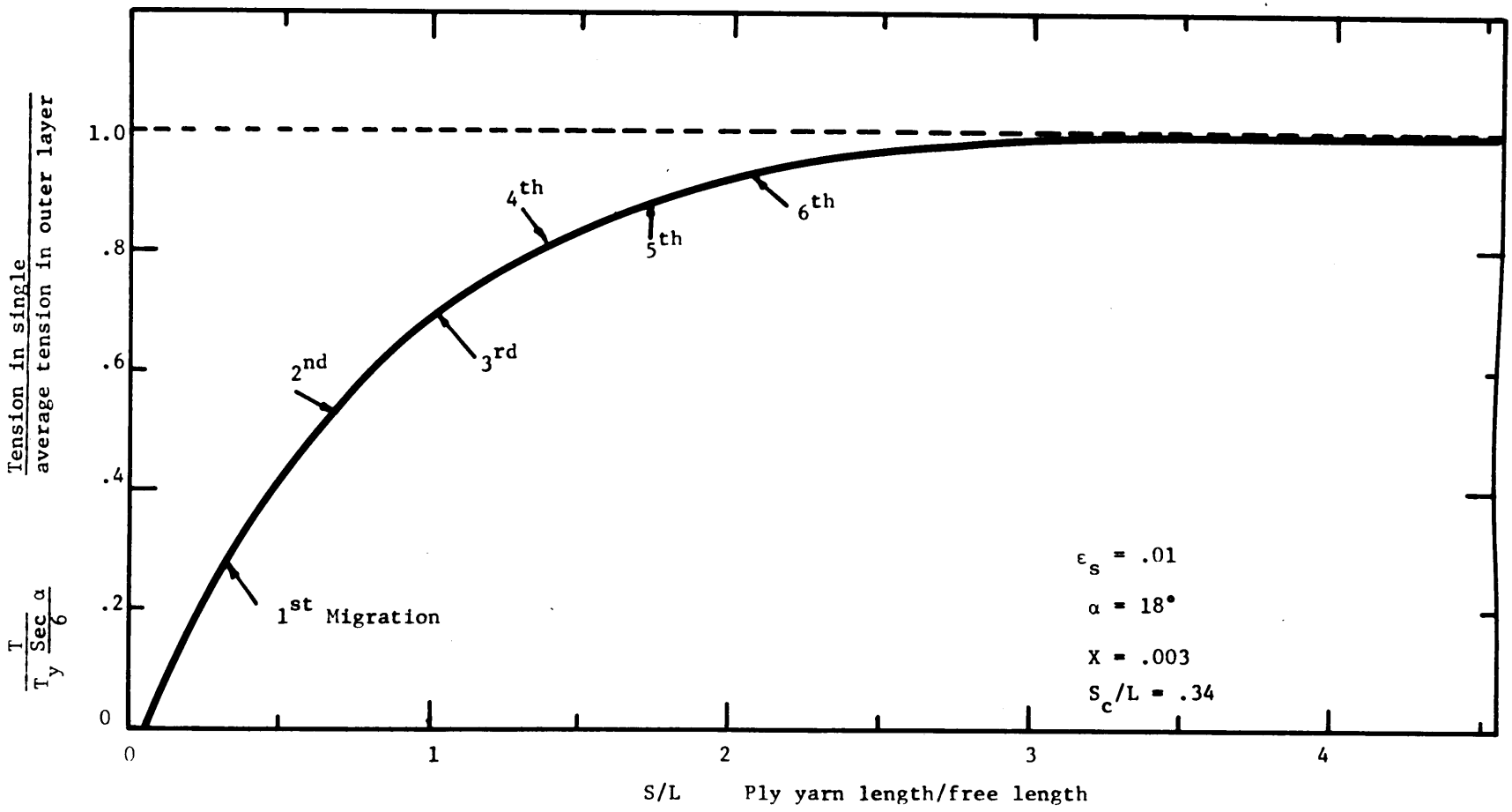

Fig. 3.21 Theoretical Build Up of Tension in Outer Layer

(i) vibration of system

(ii) group twisting of singles in the twisting triangle.

Fig. 3.27 represents the build up of tension in the single as given by equation 3.47.

e. Outward Migration in Practical Spinning

1. Static Buckling. In practice no sagging will take place because of the fact of mutual support of the fibers. Any one fiber can be considered as if embedded or supported by an elastic foundation consisting of the matrix of fibers in the roving to be spun. In this case, outward migration will take place when the fiber running in the inner or central position buckles out of its plane of motion. The buckling will take place due to the accumulation of its length in the twisting (triangle) zone because of the excess in length supplied to it. The critical load to initiate buckling in an elastic beam (Fig. 3.28-a) supported by an elastic foundation with an elastic constant k is given by

$$P_{crit.} = k \left(\frac{L}{\pi}\right)^2 + EI \left(\frac{\pi}{L}\right)^2 \qquad 3.49$$

where

$P_{crit.}$ = critical load for buckling to take place

k = spring constant of the fiber matrix/unit length

L = length of fiber in twist triangle

E = elastic modulus of fiber

I = area moment of inertia of fiber

But the critical strain, ϵ, is given by

$$\epsilon_1 = P_{crit.}/EA = \frac{P_{crit.}}{\gamma} \qquad 3.50$$

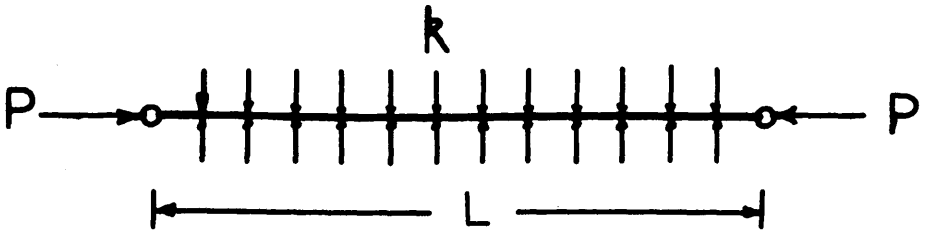

Fig.3.28.a
Beam on Elastic Foundation

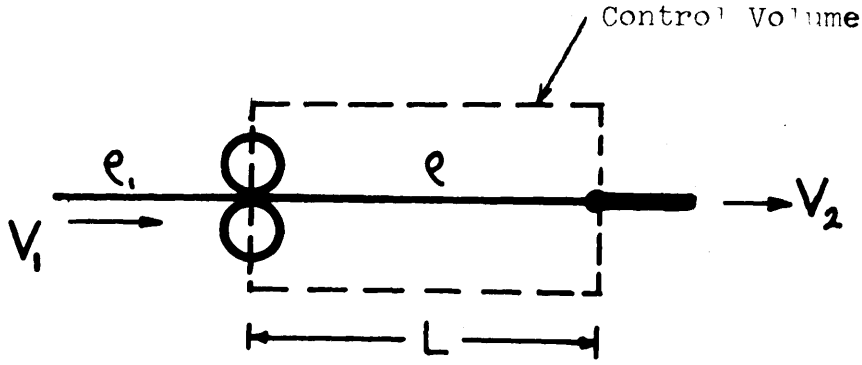

Fig.3.28.b
Mathematical Model for the
Buckling of the Center Fiber

$$\epsilon_1 = \frac{k}{\gamma}\left(\frac{L}{\pi}\right)^2 + \frac{I}{A}\left(\frac{\pi}{L}\right)^2 \qquad 3.51$$

where A = cross sectional area of fiber.

(a) Calculation of length of Spun Yarn (S_x) Necessary to Develop the Critical Strain (ϵ_1). Consider the twisting zone between the front roll and the twist point to be a control volume of a system as shown in Fig. 3.28-b. In time, dt, the material input into that system is

$$\rho_1 V_1 dt \qquad 3.52$$

the output is

$$\rho V_2 dt \qquad 3.53$$

where

V_1 = front roller speed

V_2 = speed of formation of ply

the increase inside the system is

$$d\rho L \qquad 3.54$$

Continuity gives

$$(\rho_1 V_1 - \rho V_2)\, dt = L d\rho \qquad 3.55$$

where

ρ_1 = linear density (or denier) of material prior to front roller

ρ = density of material inside control volume

V_1 = front roller speed

V_2 = spun yarn speed at twist point

From Equation 3.55 we have

$$dt = \frac{d\rho}{\rho_1 V_1 - \rho V_2} \qquad 3.56$$

Integrating, we get

$$t = \frac{L}{V_2} \ln \frac{1}{\rho_1 V_1 - \rho V_2} + C \qquad 3.57$$

but at $t = o$ $\rho = \rho_1$ then equation 3.57 gives

$$t = \frac{L}{V_2} \ln \frac{\rho_1 (V_1 - V_2)}{\rho_1 V_1 - \rho V_2} \qquad 3.58$$

or

$$\frac{\rho}{\rho_1} = \frac{V_1}{V_2} + (1 - \frac{V_1}{V_2}) \bar{e}^{V_2 \cdot t/L} \qquad 3.59$$

Now, if we assume that ϵ_1 will be at $P_{critical}$, then we have

$$\frac{(\epsilon_1 + 1) L}{L} = \frac{\rho_{crit}}{\rho_1} \qquad 3.60$$

$$(1 + \epsilon_1) = \frac{V_1}{V_2} + (1 - \frac{V_1}{V_2}) e^{-V_2 t_c/L} \qquad 3.61$$

from which the time, t_c, necessary to develop the critical strain for buckling is given by

$$t_{crit} = \frac{L}{V_2} \ln \frac{V_2 - V_1}{(1 + \epsilon_1) V_2 - V_1} \qquad 3.62$$

and the length of spun yarn (S_x) required to initiate buckling is given by

$$S_x = V_2 \, t_{crit} \qquad 3.63$$

where

$S_x = o$ at $\rho = \rho_1$, i.e. at $t = o$

S_x is measured from the point when the tension in the fiber in the center position had reached a zero state. Finally, using Equations 3.62 and 3.63 we get

$$\frac{S_x}{L} = \ln \frac{1 - V_2/V_1}{1 - (1+\epsilon_1) V_2/V_1} \qquad 3.64$$

For a 7-ply structure the ratio V_{2/V_1} can be easily seen

to be approximately equal to cos , i.e.

$$\frac{V_2}{V_1} \cong \cos \alpha \qquad 3.65$$

Using Equation 3.65, then Equation 3.64 can be written as

$$\frac{S_x}{L} = \ln \frac{1 - \cos \alpha}{1 - (1+\epsilon_1) \cos \alpha} \qquad 3.66$$

Equation 64 shows that the length required to initiate outward migration in staple fiber yarns (or closed structures) is dependent on: free length; ratio of take-up to delivery speeds (or helix angle); the critical strain to initiate static buckling. The critical strain is dependent on the free length, the fractional modulus of the fibers and the elastic modulus of the matrix around the fiber under consideration, which, in turn, is dependent on yarn tension. As tension increases, the modulus of matrix will increase. This elastic modulus will depend on the yarn tension and the elastic properties of the fibers in the matrix.

The value of the critical strain will increase as both helix angles and tension increase. This can be explained as follows: Elastic beams buckle easily when their length is longer, and as is known, the twist triangle height decreases with increasing twist, then static buckling requires high strain levels in such cases.

The effect of the twisting tension on the critical strain (increasing strain with tension) is due to the increase in the modulus of the matrix of fibers around the central one.

b. Length of yarn in Center Position in 7-Ply Closed Structures. Using Equations 3.15 and 3.66, the length of single yarn occupying the center position in a closed 7-ply structure is then given by

$$\frac{S_c}{L} = \frac{5}{36}\left[1+\cos\alpha\,(5+6\epsilon_s)\right]\ln\left[\frac{(1-\cos\alpha)(5+6\epsilon_s)}{5(1-\cos\alpha)-6\epsilon_s}\right]$$

$$+\ln\frac{1-\cos\alpha}{1-(1+\epsilon_1)\cos\alpha} - \frac{\epsilon_s}{6} \qquad 3.67$$

2. Dynamic Buckling or Snap Back. As discussed above, outward migration will occur if the central fiber buckles from its straight configuration. It has been shown that the application of a tensile force to a long slender rod will cause lateral buckling if the force is suddenly released. This phenomenon is known as dynamic buckling, or snap back. This case of buckling will take place in staple fiber spinning, when the tail of a fiber running in a central layer is suddenly released from the front roller nip (provided that the fiber still is under tension). This sudden release of the tail end from the front roller nip will result in a sudden release of fiber tension and snap back of the fiber. This snap back will result in a deformation of the fiber configuration from a straight one to a bent one, resulting in outward migration of the fiber under question. This mechanism will explain the experimental observation reported by Morton, that trailing ends appear on the surface much more than leading ends in staple fiber spinning.

In staple fiber spinning, the leading ends of the fibers have to be tucked in the yarn at the twist point, so that the tension will be developed in these fibers to support the twisting tension. On the other hand, as the trailing ends leave the roller nip, the tension in the fibers will be suddenly released and the fibers will migrate to the outside causing their trailing ends to appear on the yarn surface.

Dynamic buckling in snap back has been studied by Anderson[25] in the Division of Fibers and Polymers at M.I.T. The phenomenon is a most complex one, and its treatment for the simple case of one fiber is rather difficult and involves both linear and non-linear differential equations. It would be expected that the study of the snap back phenomenon in the case of actual spinning where the fiber under consideration is supported by a matrix of other fibers exerting lateral forces on it will be much more complex. We will make no attempt to analyze this phenomenon since it is outside the scope of this work.

4. Experiments. The following experimental work was designed to verify the theories obtained. In particular it was of interest to measure the length of ply yarn in which each of the seven components of a 7-ply structure occupies the central position; to observe the effect of spacer width on the frequency of migration; to observe the effect of migration on the horizontal location of the twist point; to observe the formation of slack in the twist triangle; to observe the twisted form of a 6-component yarn.

To measure the length of ply yarn in which a single occupies the central position, a tracer fiber technique was used. In this case the 6 grey singles, together with 1 brown yarn, were twisted to obtain the required 7-ply structure, using 75 denier viscose rayon yarn. In the case of the ply constructed of 300 denier viscose rayon, seven different colors were used.

a. Twisting Machines. The machines used for twist insertion during the course of this investigation were described in a previous section, i.e., the single spindle

ring frame, and the model twister shown in Figs. 2.1 and 2.3.

b. Material to be Twisted

(1) During the research on frequency of migration, continuous filaments viscose rayon yarns were used to measure the period of migration. Two yarn counts were used:

(a) The 75 denier viscose rayon yarns had 14 filaments/yarn, producer "S" twist of 2.5 t.p.i. and initial slope of its load elongation curve of 5800 gms/unit strain.

(b) 300 denier viscose rayon yarns chosen to be of 7 different colors (black, red, blue, green, yellow, tan and light blue.) These yarns had the following specifications:

Number of filaments in each yarn = 60
Producer twist S = 3 t.p.i.
Yarn count = 300 denier
EA = fractional modulus = 24800 gms.

(2) To study the interaction in the twist triangle 7 different colored nylon monofilaments 380 denier each having an EA = 17200 gm/unit strain were used.

Fig. 3.29 represents an average load-elongation curve of each of these yarns obtained on the Instron testing machine at a

Strain rate of 10%/min, a gauge length 10", and with 5 sample replicates.

c. Yarn Preparation. The 7 yarns to be twisted into a ply yarn were first wound on 7 spools (35 mm Kodak film spools 1" in diameter) to about 2" in diameter. The yarns were transferred from the producer's cones (3 lbs. each) to the spools by rotating the latter on a drill press. The

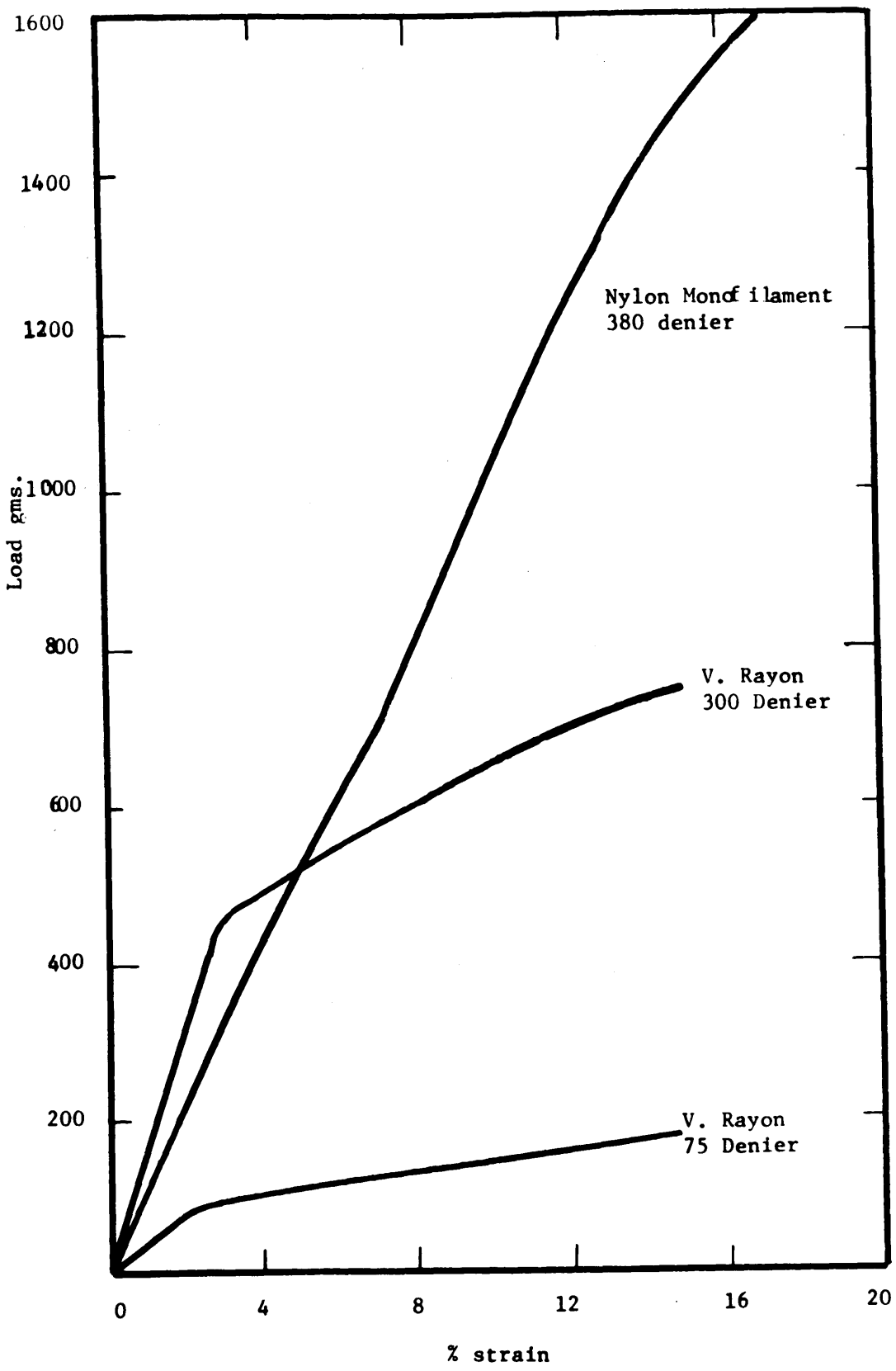

Fig. 3.29 Load-Elongation of Material Used

change in twist during this transferal due to the unwinding of the yarns from the cones may be considered negligible, being in the order of 1/10 t.p.i.

d. Twisting Procedure. The 7 spools (1) on which the yarns were wound, were free to rotate on pins (2) placed on a horizontal rack (3) as shown in Fig. 3.30. The 7 ends (4) passed through a thread spacer (5), to 2 sets of rollers (6) (back and front rollers) to another spacer (7) where they were twisted by either a twisting head (8) in the case of the model twister, or by the traveller in the case of the ring frame. The pre-tension developed in the yarns as they were pulled off the spools was measured by determining the weight required to overcome the inertia and friction of the spools on the pins. It was found to be in the order of 9-11 gms. The twisting tension was varied by changing the weight (7) (Fig. 2.3) pulling the twisting head in the model twister, or the traveller weight when twisting on the ring frame.

e. Twisting Conditions

(1) On the Ring Frame. When twisting on the ring frame, the following conditions were used:

(a) Spindle speed = 2620 rpm

(b) Balloon height (constant) = 14"

(c) Nominal T.P.I. = 11, corresponding to a measured helix angle of 21° for the 75 denier yarns.

(d) Traveller weights of 160, 340 and 570 m.g. corresponding to twisting tension of 14, 30 and 50 gms. at the delivery rollers. These tensions were computed using the theoretical expressions developed by DeBarr[11] with the conditions listed in Appendix B.

(e) The spacer (7), (Fig. 3.30) was placed at a distance of 3.75" from the front roller nip.

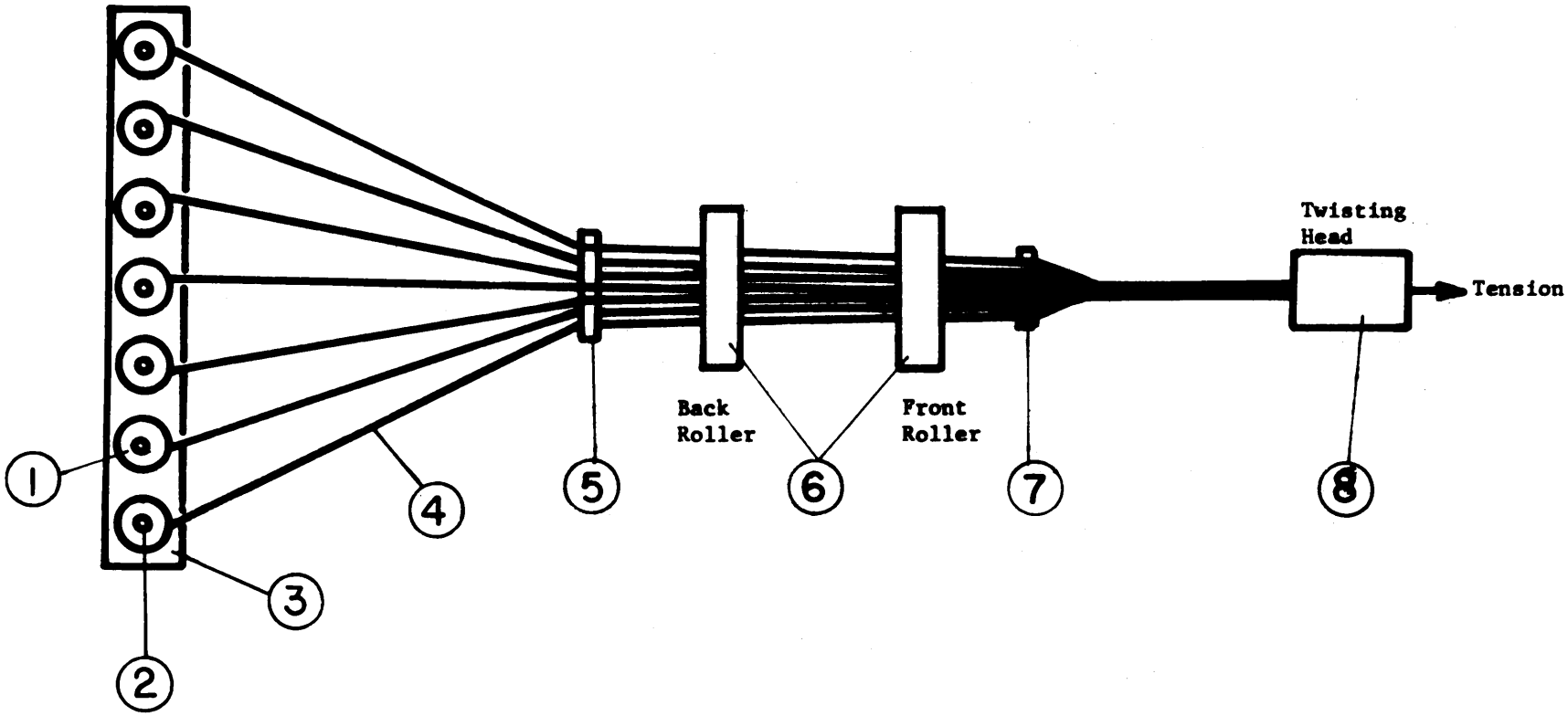

Fig. 3.30 Layout for Twisting The 7-Ply Structure

One spacer (0.7" wide) was used when twisting the 75 denier, while 4 different spacers were used in the case of the 300 denier at a twist of 12 t.p.i.

(2) On the Model Twister. The experimental conditions were:

(a) Twisting tensions of 100, 200 and 300 gms.

(b) Twisting levels of 8.1, 12.1 and 18.3 t.p.i., corresponding to helix angles of 18°, 24°, and 35° respectively.

(c) A spacer (.7" wide) was used when twisting at the three twist levels mentioned above, and was located at a distance of 3.8" from the front roller. In addition, the 7-ply yarn was formed using no spacer (contiguous yarns) at a twist level of 12.1 t.p.i.

f. Examination of the Twisted Yarn. To measure the length during which any of the 7 components occupies the center position, the tracer fiber technique was used. The ply yarn formed was observed under the microscope and the length of ply yarn in which the tracer yarn (brown) did not appear on the surface of the structure was recorded. The average of thirty readings was taken as the representative value of the measured quantity (Sc) at each twisting tension.

g. Measurements of Free Length. The geometrical free length L is the sum of the distance between front roller nip and the centerline of the spacer, and the height of the twist triangle. The height of the twist triangle was measured with a ruler when the free length of the tracer yarn was slack, that is, when the central yarn is under zero tension and the twist point is along the centerline of the

spacer.

h. Measurements of the Diameter of the Singles. The single yarns were twisted to different helix angles (using a hand twister) under different tension levels corresponding to the tension per single used during the ply yarn formation. The diameter measurements were made using a travelling microscope at five locations 3" apart for each sample. The tension levels used were 14.0, 28 and 43 gms. and the twist levels were (helix angles) 18, 24 and 35°.

i. Embedding of the Twist Triangle

(1) Purpose of the Experiments. The embedding of the twist triangle was intended to illustrate and observe the twisted form of a 6-component yarn, the formation of the slack and the effect of migration on the horizontal location of the twist point.

(2) Embedding Media. The embedding medium was a mixture of 99% Paraplex and 1% Lupersol DDM by volume.

(3) Embedding Procedure. After a length of ply yarn was formed on the model twister under the desired twisting conditions (which will be discussed with the results in a later section) with the embedding apparatus in place, the twist triangle was held by the clamps shown in Fig. 2.9, The embedding mixture was then poured slowly over the twist triangle to prevent air bubbles. The apparatus was then heated at 80°C in an oven for 15 minutes to speed up polymerization. The apparatus was left to cool for 10 minutes, then the solid resin was removed from it. Thin sections were then cut from the resin using a 15 mil. circular saw blade on a milling machine. The cross sections were then observed under a microscope and the resulting pattern was traced over the length of the twist triangle.

5. Results

a. Determination of Migration Amplitude:

1. On the Ring Frame. Table 3.1 shows the experimental results for the length (S_c) in which a single yarn occupies the central position obtained on the ring spinning frame, when twisting the 75 denier viscose rayon yarns.

Table 3.1

Effect of Twisting Tension on S_c

Material: V R 75, t.p.i.= 11.0, γ = 5800 gms, α = 21° (final helix angle)

Traveller Weight (mg)	Tension at FR (gms)	L (in.)	S_c^* (in.)	S_c/L	S_c/L_{AV}**	C_v (%)
159	14	4.44	.28	.063	.061	53
340	30	4.63	.29	.063	.063	51
570	50	4.75	.32	.067	.069	44

*average of 30 readings.

L_{AV}** = free length of the 3 values of L given above = 4.61".

When twisting the 300 denier viscose rayon with different spacers (thread guides), it was observed that the formed yarn was in a wrapped rather than a twisted configuration. This wrapping of the filament yarns around each other followed a distinctive repetitive pattern in which the singles on one side of the delivered ribbon occupied the center position with the remaining singles (on the other side) wrapping around them in a certain length of ply yarn. At the end of that length, the yarns changed position with the ones in the outside layer moving into the inside and those in the inside moving to the outside. This pattern was very noticeable when the singles were delivered by the

front rollers with the dark colored ones (black, blue and green) on one side, and the light colored ones (yellow, light blue and tan) on the other side, and the red one running along the center line of the ribbon. Fig. 3.31 shows a picture of a sample of these yarns, with the pattern clearly defined.

Table 3.2 represents the experimental results obtained for the amplitude of these patterns as they vary with the spacer width.

Table 3.2

EFFECT OF SPACER WIDTH ON MIGRATION

Spacer Width (in.)	(Amplitude* (in.)
.6	3.7
.92	5.3
1.1	6.7
1.3	7.3

Material 300 denier viscose rayon

*Average of 10 readings

(2) Model-Twister. Tables 3.3 and 3.4 represent the experimental results obtained for S_c on the model twister. Table 3.3 shows the result when twisting the 75 denier with no spacer, i.e., the yarns were delivered adjacent to each other. In this case, the twist triangle height (equal to the free length) was estimated, using the expression

$$\tan \alpha = w/2h$$

and

$$w = 10d$$

where w = width of the ribbon, h is triangle height, α is the helix angle and d = filament diameter.

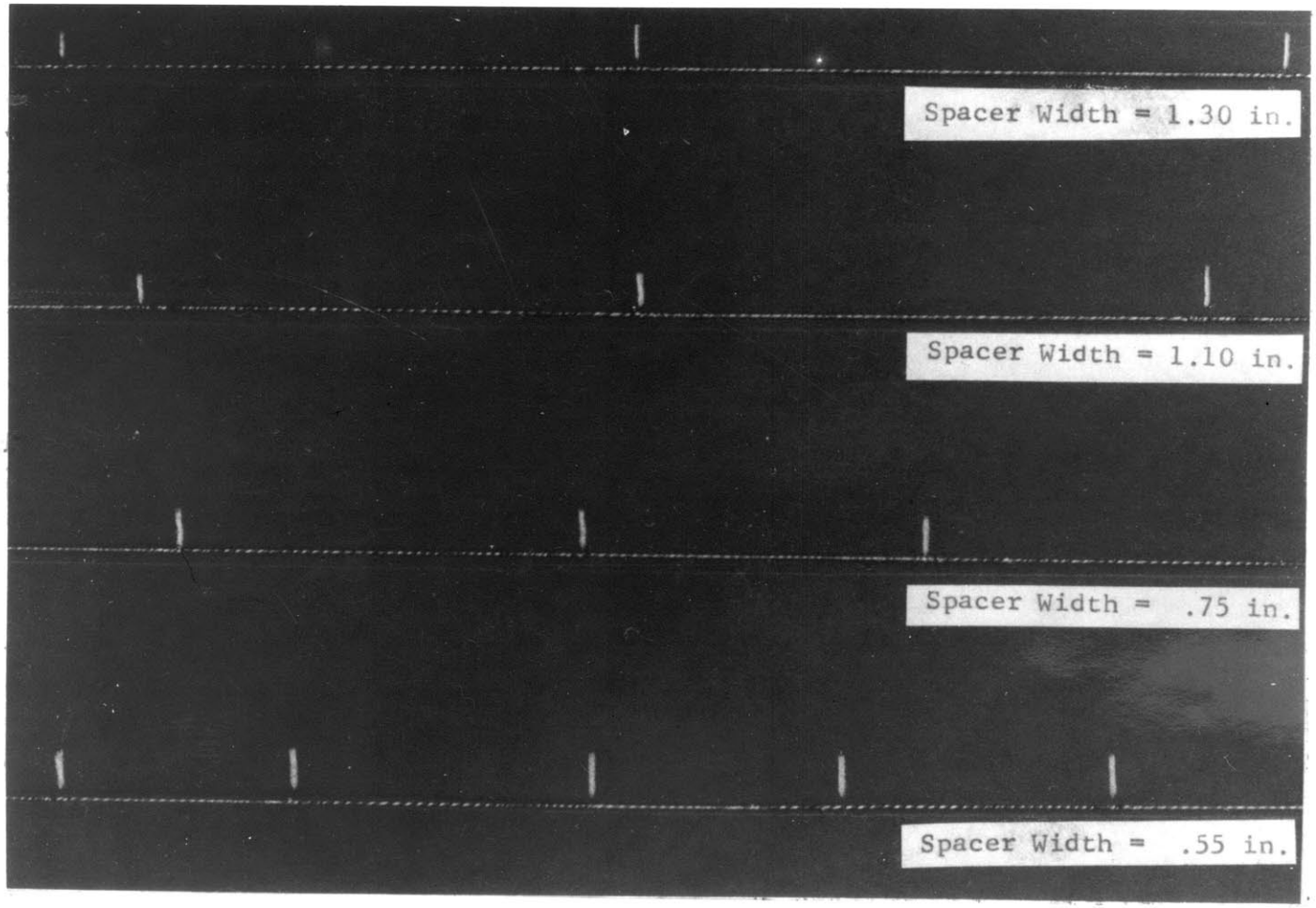

Fig. 3-31 Effect of Spacer Width on Fiber Migration

The width of the ribbon input was estimated to be equal to the sum of the diameters of the 7 components (in the untwisted configuration which is equal to .01") allowing the space between the fibers to be equal to three diameters.

Table 3.3

Effect of Twisting Tension on S_c/L for the No Spacer (Closed) Case

Material V.R. 75, t.p.i. = 12.1, γ = 5800 gms., α = 24°

W(in.)	L(in.)	T_y(gms.)	$\epsilon_s 10^{-3}$	S_c(in.)	S_c/L	C_v(%) of S_c
	.11	100	3.15	.12	1.09	17
0.10	.115	200	6.20	.13	1.20	10
	.12	300	9.16	.17	1.42	32

Table 3.4 represents the results obtained for S_c for three different twist levels (helix angles) and twisting tensions.

Table 3.4

Effect of Helix Angle and T_y (Twisting Tension) on S_c

Material V.R. 75, W = 0.70", γ = 5800 gms.

(°)	L(in.)	T_y(gms.)	$\epsilon_s \times 10^{-3}$	S_c(in.)	S_c/L	C_v(%)
	5.10	100	2.99	.72	.14	20
18	5.15	200	5.94	.96	.19	31
	5.2	300	8.90	1.40	.27	43
	4.50	100	3.15	.28	.06	42
24	4.60	200	6.20	.40	.09	33
	4.70	300	9.16	.63	.13	43
	4.30	100	3.44	.15	.035	31
35	4.40	200	6.70	.19	.043	36
	4.40	300	9.80	.25	.060	40

b. Determination of Singles Diameters. The values obtained for the singles diameter of the 75 denier

Table 3.5

Determination of Singles Diameter

Diameter* (in. x 10^{-3})	T_y (gms.)	t.p.i.
.0048	14.0	
.0039	28.0	8
.0037	43.0	
.0038	14.0	
.0036	28.0	12
.0034	43.0	
.0034	14.0	
.0032	28.0	20
.0030	43.0	

*Average of 5 readings

Material 75 denier viscose rayon.

c. Embedding of Twist Triangle. The cross-sections resulting from embedding the twist triangles when twisting 6 and 7 nylon monofilaments are shown in Figs. 3.23, 3.24, 3.32, 3.33 and 3.34.

6. Discussion

a. Determination of S_c

(1) On Ring Frame

(a) Effect of Twisting Tension. Fig. 3.35 shows a comparison of the predicted and measured values of S_c/L vs. ϵ_s. It is clear that both the theory and experimental results have the same trend (increasing S_c/L with increasing ϵ_s, i.e., twisting tension.) The experimental values (when using the average L for these tensions) agree reasonably well with the theoretical curve plotted for a 19° helix angle, and they are at a higher level compared to

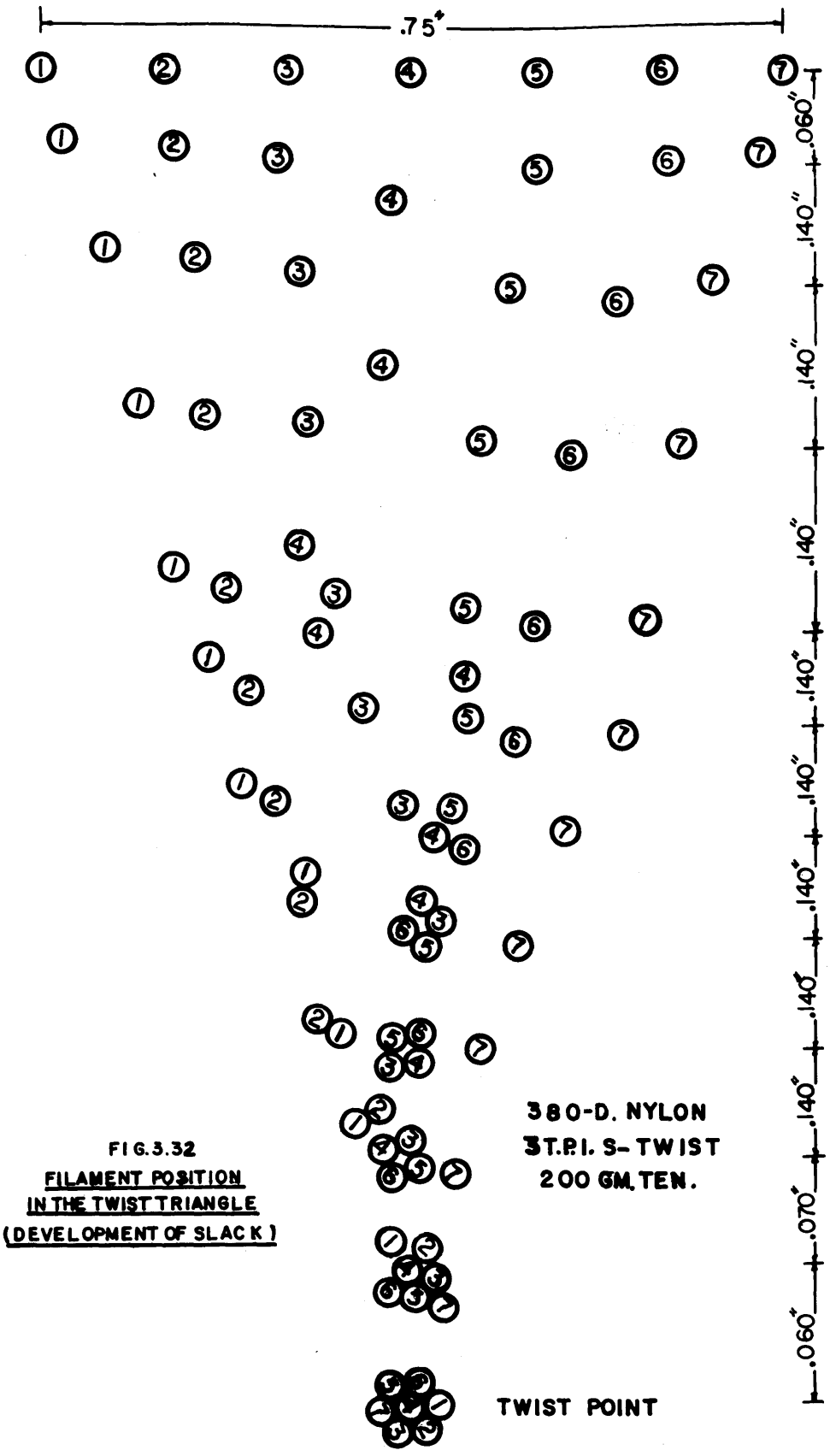

FIG. 3.32
FILAMENT POSITION
IN THE TWIST TRIANGLE
(DEVELOPMENT OF SLACK)

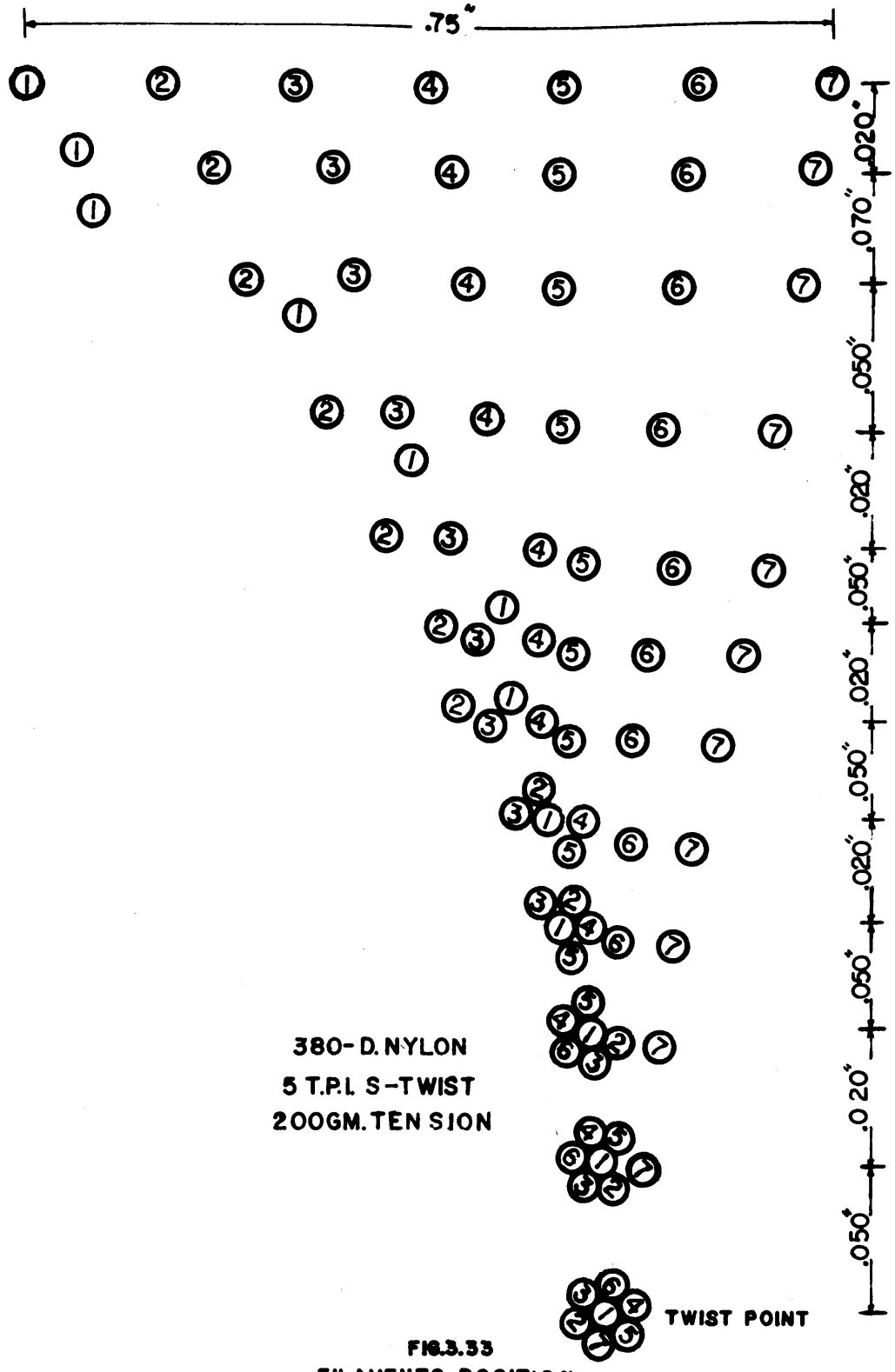

FIG.3.33
FILAMENTS POSITION
IN THE TWIST TRIANGLE
(DEVELOPMENT OF SLACK)

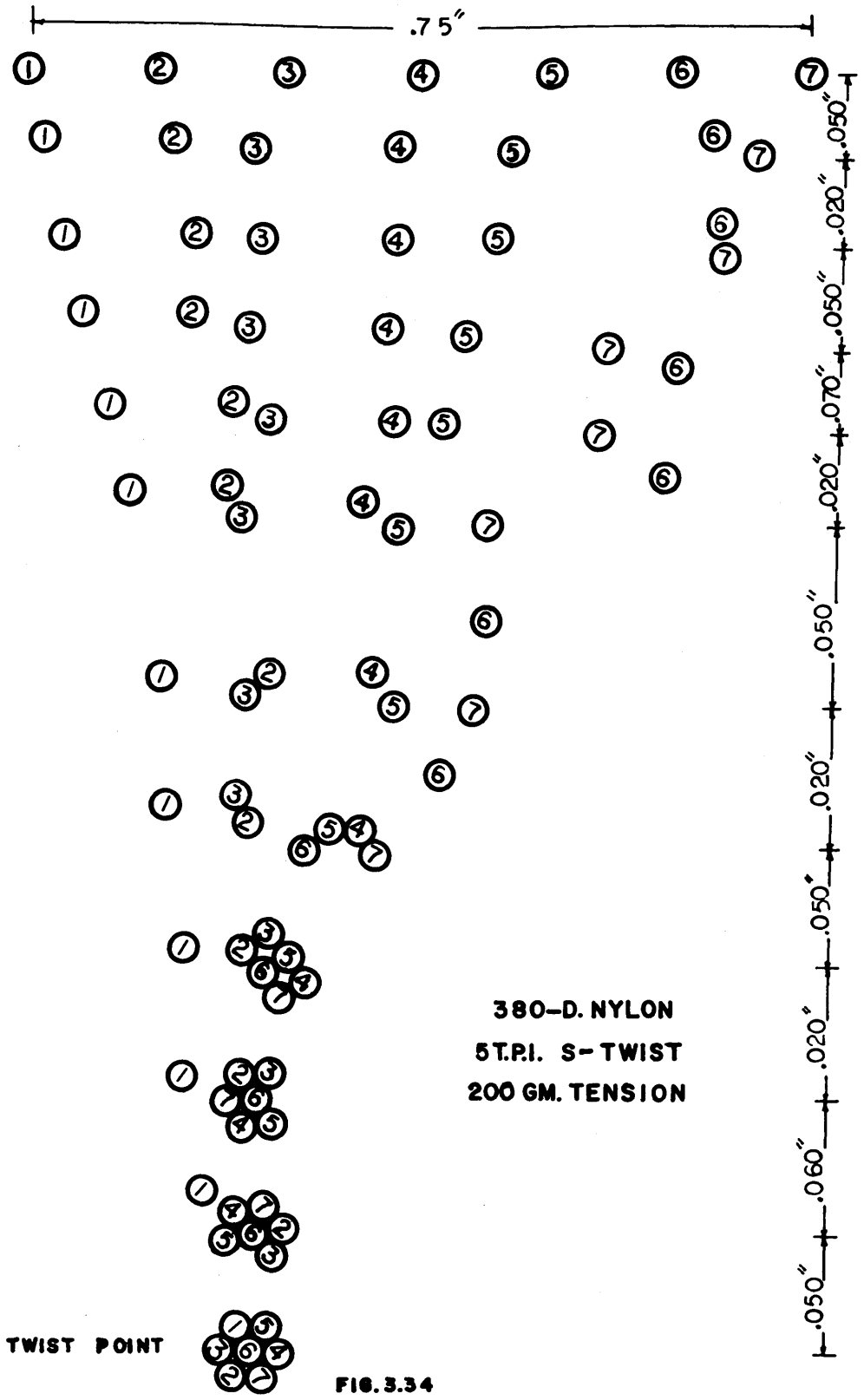

FIG. 3.34

FILAMENTS POSITION IN THE TWIST TRIANGLE (DEVELOPMENT OF SLACK)

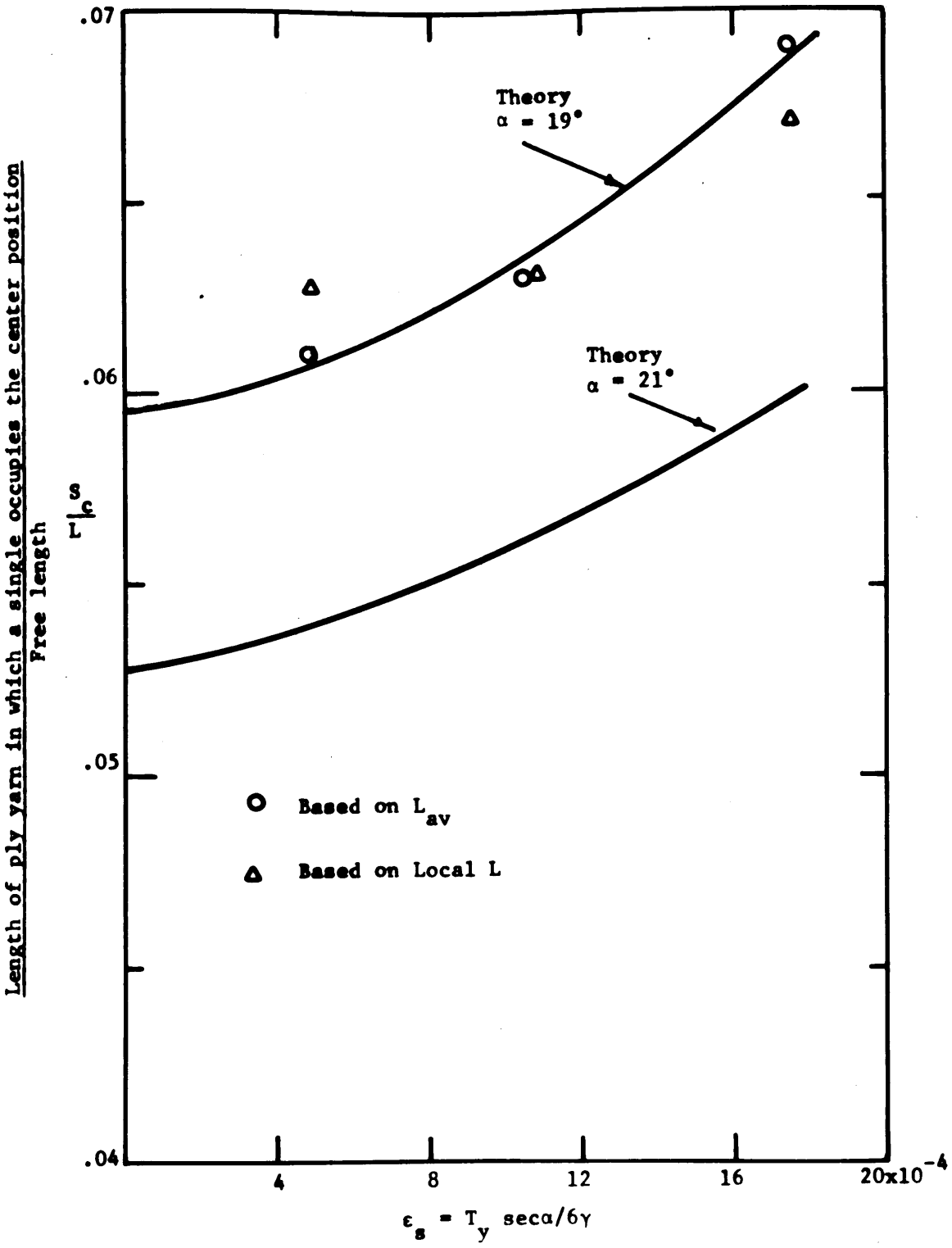

Fig. 3.35 Effect of Tension on Fiber Migration
Comparison between Theory and Experiments
(On Ring Frame)

the theory plotted for a 21° helix angle (the 21° helix angle corresponds to the final twist in the yarn on the bobbin.) This may be explained by the fact that the twist level at the front rollers (where migration is imposed) is lower than that on the bobbin, as will be explained in later chapters.

(2) On Model Twister

(a) Effect of Twisting Tension. Fig. 3.36, representing the relation between S_c/L and ϵ_s at three twist levels, indicates a reasonable agreement between the experimental and predicted values. The theoretical curves were obtained using Equation 3.17 with the amount of slack X (needed to initiate outward migration) computed from Equations 3.29, 3.32 and using Fig. 3.22. The plot shows that S_c/L increases as the twisting tension increases. This trend may be explained by considering that as the tension level increases, the length of ply yarn required to reduce the tension in the single in the center layer to a zero value, increases.

Fig. 3.37, showing the relation between the frequency of migration (as given by Equation 3.18) and ϵ_s for the same conditions used in Fig. 3.36, indicates that the rate of migration decreases with increasing tension.

b. Effect of Thread Spacer Width (i.e., Ribbon Width). Fig. 3.38 represents the variation of S_c/L with the average strain in the singles (ϵ_s) for both the cases of twisting with no spacer and with a spacer of .7" width. While the theoretical curve for the spacer case (open structure) is completely determined, we find that the curves for the no spacer case are not, because the critical strain needed to initiate buckling in the latter case is not known. In the no spacer case, the theoretical values were plotted using

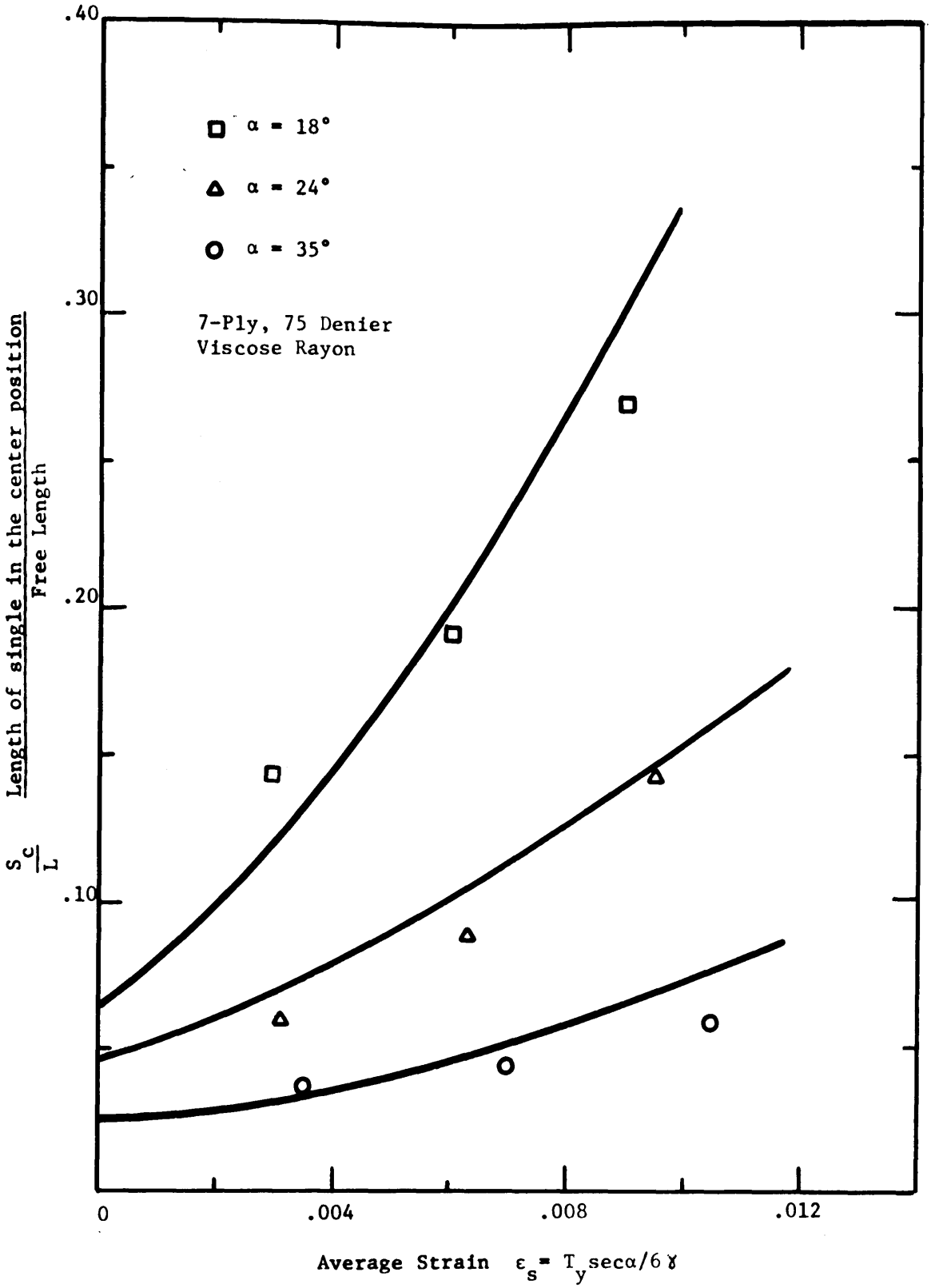

Fig. 3.36 Effect of Twisting Tension on Length of Fiber in Center Position. Comparison Between Theory and Experiments.

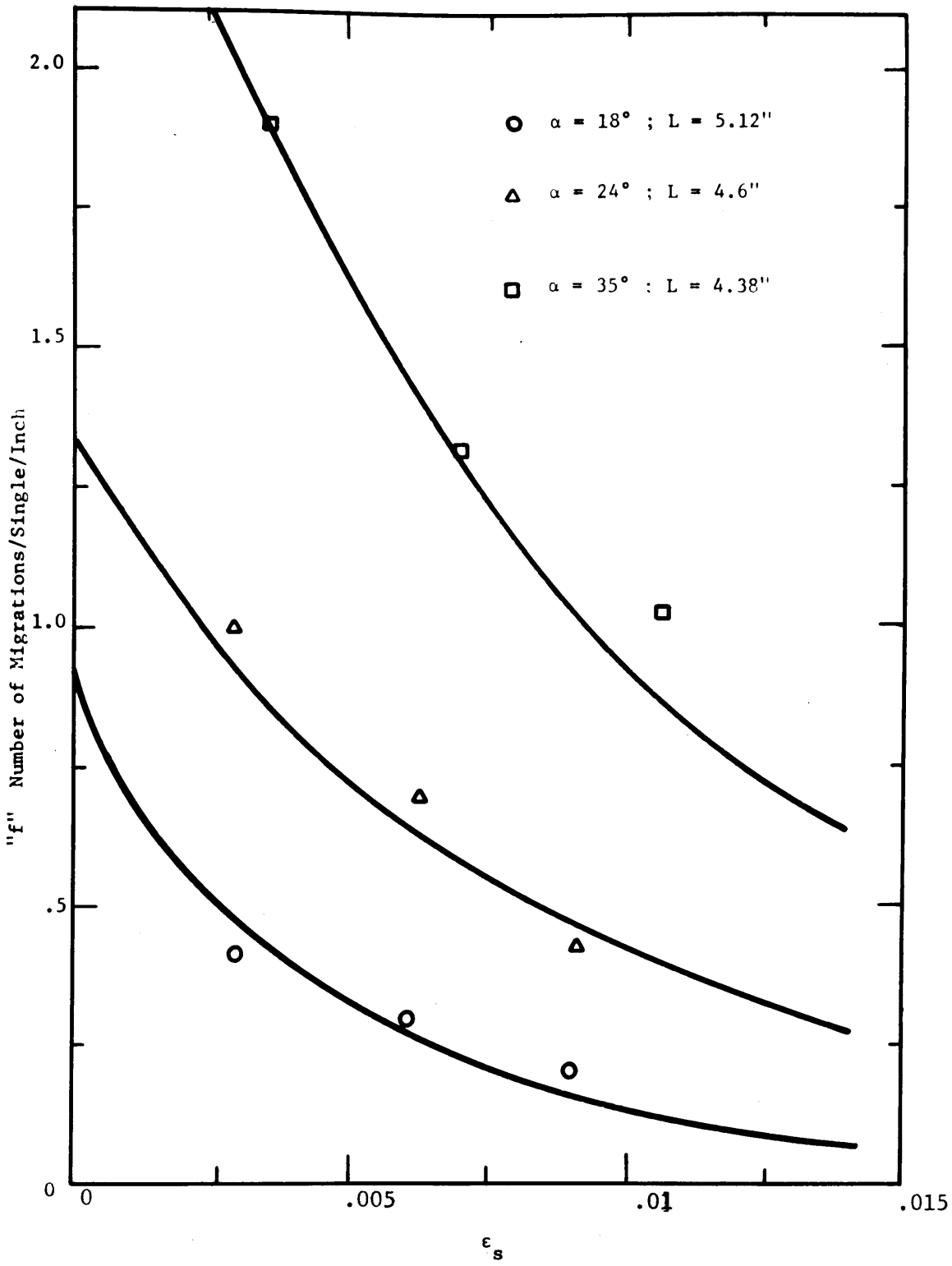

Fig. 3.37 Variation of Frequency of Migration With Twist and Yarn Tension

(Comparison between theory and experiments)

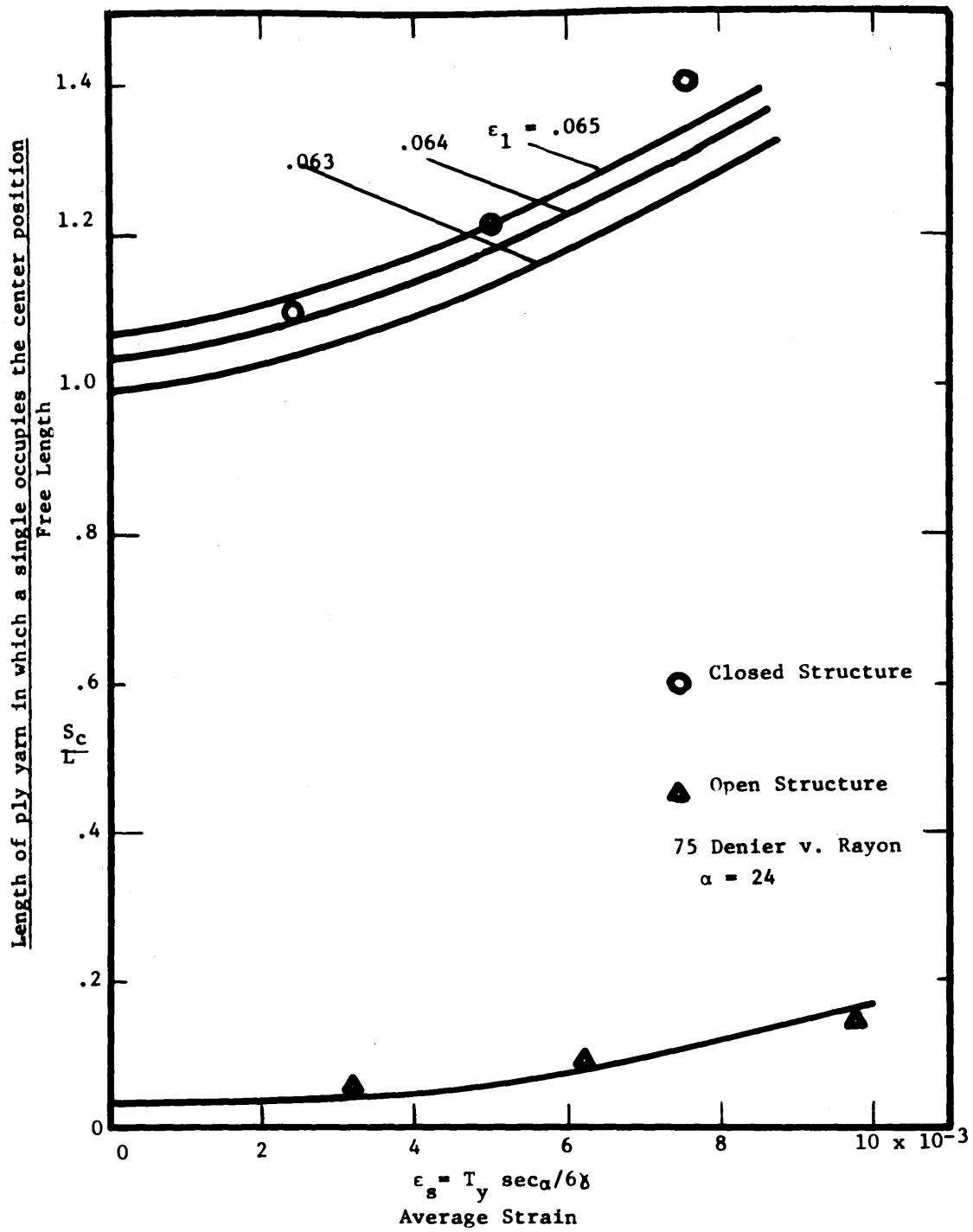

Fig. 3.38 Effect of Tension and Twist on Migration
Comparison between closed and opened structures
(Comparison between theory and experiments)

three different assumed levels of critical strain. It is apparent from the graph that the experimental results agree fairly well with the theory when the critical strain is .065.

It is also clear from the plot that values of S_c/L are much higher in the case of the no spacer case than that in the case of the spacer. Although the two plots correspond to two different migration mechanisms, it can be easily shown from the theory that as the spacer or ribbon width increases, the value of S_c/L decreases. On the other hand, it should be noticed that as the spacer width decreases, the frequency of migration will increase. This is easily shown in Fig. 3.39 where the amplitude of the wrapping pattern is plotted against the spacer width. The plot (Fig. 3.39) shows that as the width of the spacer increases, the amplitude increases, thus decreasing the frequency.

c. Effect of Twist Level. The effect of the twist level on S_c/L and the frequency of migration is shown in Figs. 3.38 and 3.37. It is clear that S_c/L (as measured under the same tension) increases as the helix angle decreases, while the frequency, f, increases with increasing helix angle.

d. Effect of Twisting Tension and α on Single Yarns Diameter. Fig. 3.40 shows the variation of the single yarn diameter with both twisting tension and helix angle. The plots indicate that the yarn diameter decreases with both increasing twisting tension (with constant twist) and increasing helix angle (for a constant tension provided that torsional buckling does not occur.) This is due to the increase in the packing factor of the yarn in both cases.

e. Interaction of Single Yarns in the Twist Triangle

(1) Twisted Form of a 6-Component Yarn. Figs. 3.23 and 3.24 show cross-sections of the six nylon mono-

filaments at different locations in the twist triangle. In Fig. 3.23 twist was inserted statically at constant length, while in Fig. 3.24 the twisting was carried at constant tension of 200 gms. The final form of the twisted structure (at the twist point) in both cases is the same with one component occupying the center position and the other five occupying the outer layer. This form is equivalent to the one obtained when twisting seven ends with the exception that in the former case there is an empty space corresponding to the missing monofilaments.

(2) Formation of Slack and Location of Twist point in a 7-Ply Structure. Figs. 3.32, 3.33 and 3.34 show cross-sections of the seven monofilaments at different locations in the twist triangle. In Fig. 3.32 S-twist of 3 t.p.i. was inserted at a constant tension of 200 gms. The twist triangle was embedded when slack was observed in monofilament number "4" as shown in the cross-sections taken progressively starting from the base of the twist triangle to the twist point. The pattern assumed by the slack monofilament may thus be observed. From the figure it is also seen that the twist point is located on the center line of the seven monofilaments (or ribbon.) This occurs because the center of gravity of the six monofilaments (on the outside) supporting the twisting tension, is located on the center line of the ribbon.

In Figs. 3.33 and 3.34 the seven monofilaments were S-twisted at 5 t.p.i. under a constant tension of 200 gms. In Fig. 3.33 the twist triangle was embedded when monofilament #1 was slack, while #6 was slack in Fig. 3.34. In both Figs. 3.33 and 3.34 the slack can be readily detected and the location of the twist point may be easily observed. In general, the twist point is located

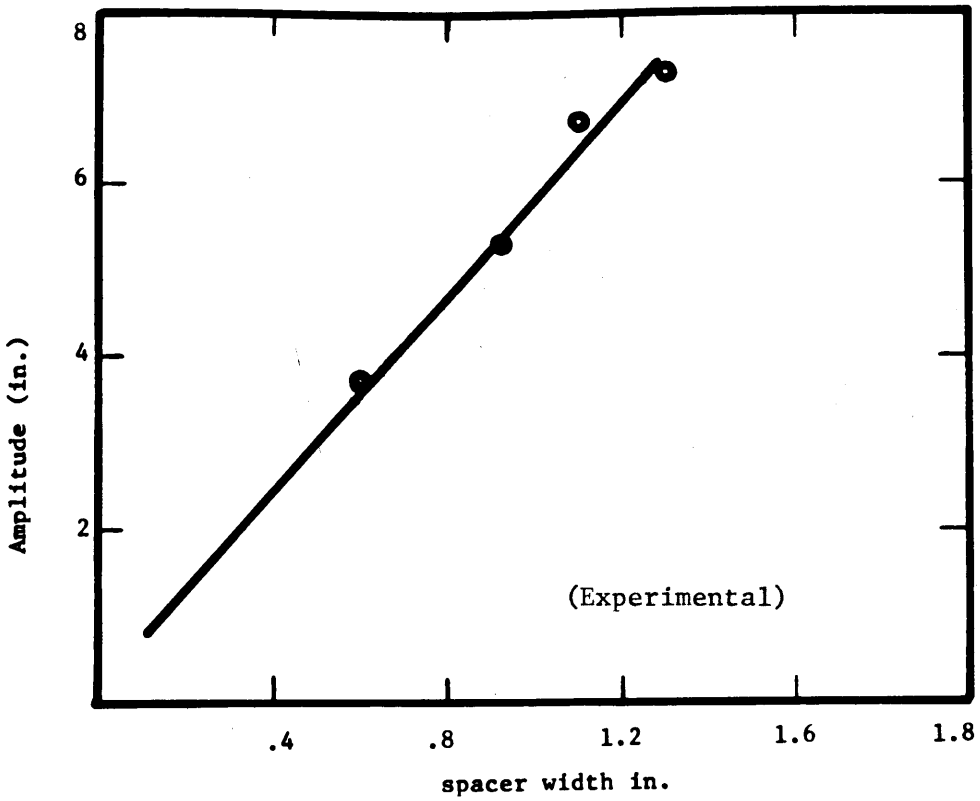

Fig. 3.39 Effect of Spacer Width on Migration Period

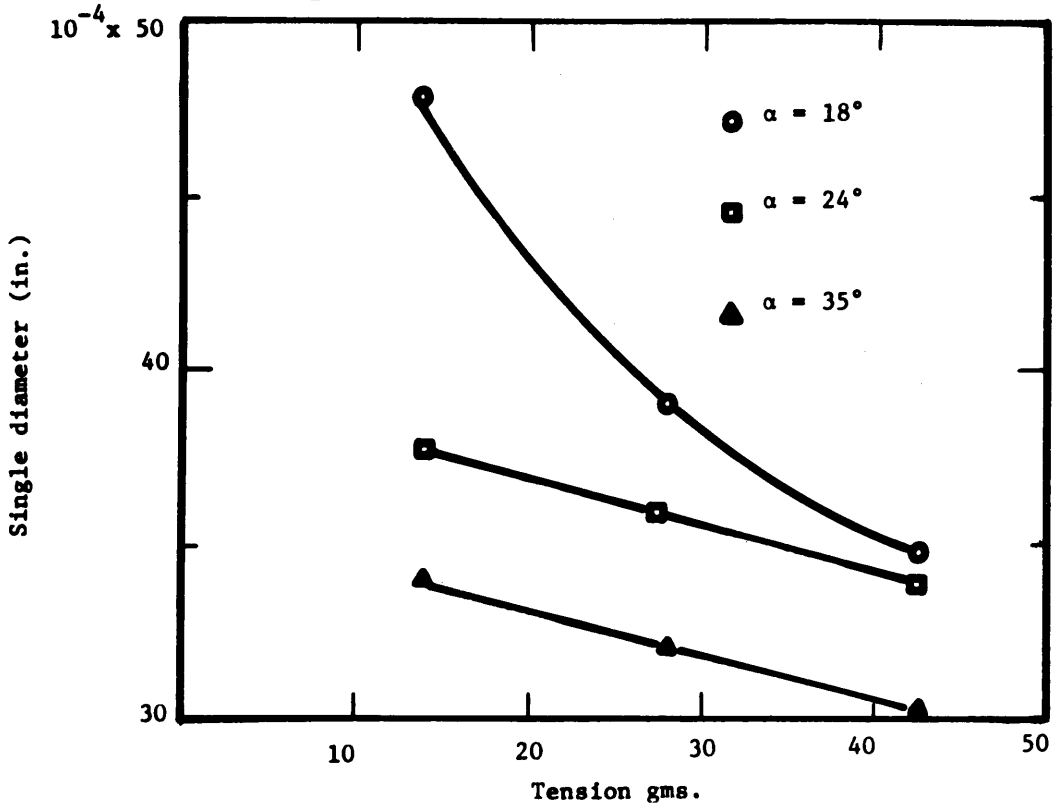

Fig. 3.40 Variation of Singles Diameter with Tension and Twist

(Experimental)

along the center of gravity of the six monofilaments supporting the twisting tension, that is, the twist point moves horizontally away from the single yarn occupying the center position.

7. Conclusions. The study of the 7-ply twisted structure shows that there is reasonable agreement between the experimental results and the theoretical predictions of the frequency of migration. It also establishes that the formation of slack is the mechanism of outward migration in an open structure and that the initiation of static buckling prevails in the case of closed structures or practical twisting. In particular, the following conclusions have been drawn:

(a) The rate of migration is dependent on: the twisting tension, the helix angle, the free length (the height of the twist triangle), the spacer width, the diameter of the single yarns and the tensile modulus of the material.

When twisting with no spacer (actual twisting conditions) the rate of migration depends on the above parameters (excluding spacer width) together with the critical compressive strain needed to initiate static buckling of the single yarn occupying the central layer of the ply structure.

In general, the frequency of migration varies with the above parameters as follows:

(1) It decreases with increasing tension, and free length

(2) It increases with increasing helix angle and ribbon or spacer width

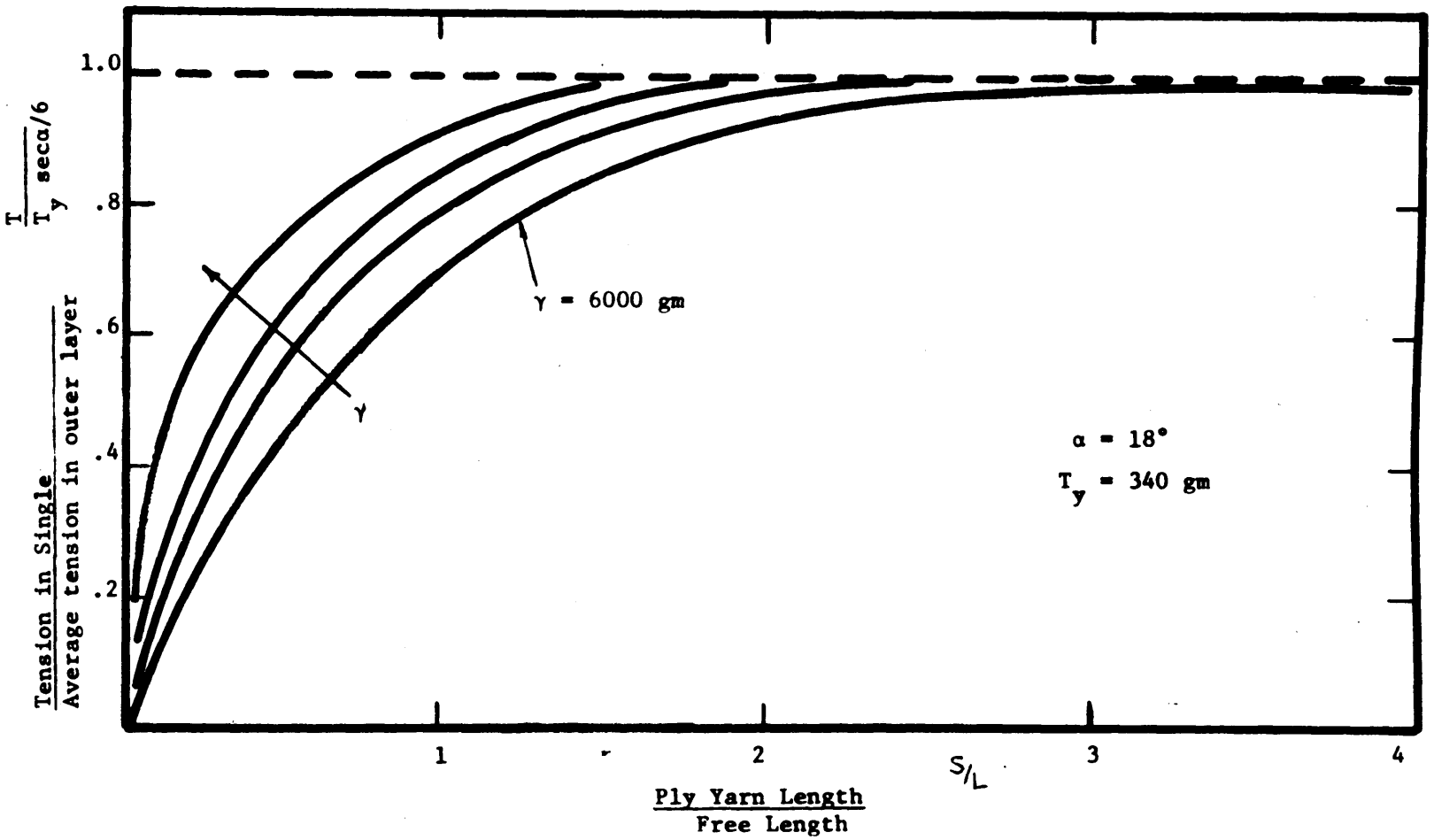

Fig. 3.41 Effect of Fractional Modulus on Tension Build Up in Outer Layer

(b) On the ring frame the frequency of migration does not correspond to the final twist level. This is due to the fact that the migration pattern is imposed in the yarn at the front roller (at the twist triangle) where both twist and tension levels are lower than those at the bobbin.

(c) In twisting fiber blends the tension in the outer layer increases at a faster rate in the high modulus yarns (as shown in Fig. 3.41) than in the low modulus ones. This will cause the former to migrate inward more than the latter. Also, it should be noted that the critical strain needed to initiate buckling will increase as the modulus increases, causing them to remain in the central layer for a longer period. This argument, however, is not completely true because high modulus yarns will loose their tension faster than the low ones, resulting in a smaller (S_o) for the former ones. But, in general, high modulus fibers will have a higher frequency of migration than low modulus ones, as indicated by Morton[19].

IV. THE TWISTING AND WINDING ZONE

A. Variation of Twist with Ring Rail Motion

1. Introduction. The problem of variability in yarn strength has been of great concern in the textile industry since it affects both the quality of the end product and the efficiency of the production. Variability in staple fiber yarn strength can be attributed to many factors, some of which are

Variability in linear density in the roving twisted due to factors such as drafting waves.
Variation in staple fiber length.
Degree of maturity of fibers in the case of cotton.
Variation of twist in the yarn due to both machine action and the presence of thin and thick places.

Variation of twist per unit length in a yarn (produced on a ring spinning frame) along the bobbin length was observed by both DeBarr et al[26] and Du Bois et al[27]. Both DeBarr and Du Bois agree that there is twist difference between the top and the bottom of the bobbin. However, they disagree on the location (on the bobbin) where the twist level is greater. While DeBarr showed experimentally that twist is higher at the bottom of the bobbin, Du Bois showed it to be least there. Both authors, however, agree that the variation of twist on the bobbin is due to the ring rail (chase) motion.

In this section theoretical expressions will be derived in an attempt to answer how this variation of twist depends on the motion of the chase and to point out the factors affecting it.

2. Theory

(a) Nomenclature

a = Ratio of local twist on bobbin to average twist in balloon

c = Ratio of yarn length in twisting zone to balloon height

d_b = Bobbin diameter

h = Balloon height at any time

h_o = Minimum balloon height

L = Yarn length in the twisting zone

N_s = Spindle speed (r.p.m.)

N_T = Traveller Speed at any time (r.p.m.)

N_w = Winding speed (r.p.m.)

n = Average twist/unit length in the twisting zone

n_o = Average twist/unit length

n_1 = Average twist/unit length on bobbin at balloon height h

n_2 = Average twist/unit length on bobbin at $h = h_o$

$\bar{n}$ = Nominal twist $= \dfrac{N_T}{V_3 + \dfrac{CV_2}{a}}$

t = Time

V_1 = Front Roller or delivery speed (linear)

V_2 = Ring rail speed (linear)

V_3 = Winding or take-up speed (linear)

(b) Assumptions. To simplify the analysis, let us assume that:

(1) The yarn length in the twisting zone is proportional to the balloon height, i.e., c = constant

(2) No twist contraction of yarn

(3) Constant ring rail speed, i.e., V_2=constant

(4) Change in balloon shape as h changes is negligible

(5) Ratio of twist on bobbin to average twist in balloon is constant, i.e., α = constant.

(c) Relation between Front Roller Speed, Ring Rail Speed and Winding Speed. Consider now the twisting zone to be a system of fixed identity; and in time period dt we have:

The material input to the system = $V_1\ dt$

The material output from the system = $V_3\ dt$

The material increase inside the system = $c\ dh$.

Continuity gives:

$$c\ dh + V_3\ dt = V_1\ dt \qquad 4.1$$

which can be written as:

$$V_3 = V_1 - c\frac{dh}{dt} \qquad 4.2$$

(d) Calculation of Traveller Speed. The traveller speed is given by the difference between the spindle speed and the winding speed, or

$$N_T = N_s - N_w \qquad 4.3$$

The winding speed in r.p.m. is given by

$$N_w = \frac{V_3}{\pi d_b} \qquad 4.4$$

From 4.2, 4.3 and 4.4 we have

$$N_T = N_s - \frac{1}{\pi d_b}(V_1 - c\frac{dh}{dt}) \qquad 4.5$$

(e) Calculation of Twist Variation in the System. Since twist is inserted in ring spinning frames by the rotation of the traveller, and for each traveller rotation one turn of twist is inserted and the average twist/unit length is given by

$$n = \frac{N_T}{V_1} \qquad 4.6$$

now consider the instant when the balloon height is h then we have:

Total number of turns in system (between twist point and traveller) at time t = c n h

Total number of turns in the system at time t + dt:

$$c(n + dn)(h + dh)$$

Number of turns removed from the system in time dt:

$$aV_3\ n\ dt = n_1 V_3\ dt$$

Total number of turns introduced into the system in time dt:

$$N_T\ dt$$

but since twist is conserved, it follows that:

$$N_T\ dt = c(h + dh)(n + dn) - cnh + aV_3\ n\ dt \qquad 4.7$$

Substituting for N_T from 4.5, we get

$$N_s - \frac{1}{\pi d_b}(V_1 - \frac{cdh}{dt})\ dt = cnh + ch\ dn + cn\ dh + c\ dh\ dn - cnh + an(V_1 - c\frac{dh}{dt})\ dt \qquad 4.8$$

and now neglecting second order terms we get:

$$N_s - \frac{V_3}{\pi d_b} = ch\frac{dn}{dt} + cn\frac{dh}{dt} + an(V_3) \qquad 4.9$$

or

$$N_s - \frac{1}{\pi d_b}(V_1 - d\frac{dh}{dt}) = ch\frac{dn}{dt} + cn\frac{dh}{dt} + an(V_1 - c\frac{dh}{dt}) \qquad 4.10$$

which leads to

$$N_s - \frac{1}{\pi d_b}(V_1 - c\frac{dh}{dt}) = ch\frac{dn}{dt} + cn\frac{dh}{dt}(1 - a) + aV_1 n$$

or

$$ch\frac{dn}{dt} + aV_1 n = \frac{dh}{dt}\left\{cn\ (1 - a) - \frac{c}{\pi d_b}\right\} - N_s + \frac{V_1}{\pi d_b} \qquad 4.11$$

The factor (1 - a) is small, in the order of 10% and may be neglected in order to simplify the equation and obtain a solution. Then equation 4.11 can be reduced to:

$$ch\frac{dn}{dt} + aV_1 n = \frac{1}{\pi d_b}(V_1 - c\frac{dh}{dt}) - N_s \qquad 4.12$$

and can be written as

$$\dot{n} + F_1(t)n = F_2(t) \qquad 4.13$$

where

$$\dot{n} = \frac{dn}{dt}, \quad F_1(t) = \frac{aV_1}{ch(t)}$$

and

$$F_2(t) = \frac{1}{ch}\left\{- N_s + \frac{1}{\pi d_b}(V_1 - c\frac{dh}{dt})\right\}$$

The general solution of equation 2.13 is given by

$$n(t) = e^{-\int F_1 dt}\int F_2 \cdot e^{\int F_1 dt} dt + b e^{-\int F_1 dt} \qquad 4.14$$

where b is a constant of integration and can be obtained from the boundary conditions of $n = n_o$ at $h = h_o$.

(f) Special Case (Constant Ring Rail Speed). This special case corresponds to the conditions of the single spindle spinning frame described in Section II, Fig. 2.1. If the ring rail speed (V_2) is assumed here to be constant, then V_2 will be equal to $\frac{dh}{dt}$ = constant, and we have

$$h = h_o + V_2 t \qquad 4.15$$

then

$$dt = \frac{dh}{V_2} \qquad 4.16$$

Then from 4.9 and 4.16 there follows

$$\frac{dn}{N_T - (aV_3 + CV_2)} = \frac{dh}{ch\ V_2} \qquad 4.17$$

which after integration with the boundary condition that

$$n = n_o \text{ at } h = h_o$$

will lead to

$$an = \frac{1}{V_3 + \frac{c}{a}V_2}\left\{N_T - \left[N_T - \left(V_3 + \frac{c}{a}V_2\right)\right]\left(\frac{h_o}{h}\right)^{\frac{aV_3}{cV_2}+1}\right\} \qquad 4.18$$

or with the notation that

$$n_1 = an \quad , \quad \bar{n} = \frac{N_T}{V_3 + cV_2/a} \quad \&$$

$$n_2 = an_o$$

gives

$$n_1 = \bar{n} - (\bar{n} - n_2)\left(\frac{h_o}{h}\right)^{\frac{aV_3}{cV_2}+1} \qquad 4.19$$

Substituting for V_3 from 4.2 and 4.1 then we get

$$n_1 = \bar{n} - \left[\bar{n}-n_2\right]\left(\frac{h_o}{h}\right)^{\left[\frac{aV_1}{cV_2} + (1-a)\right]} \qquad 4.20$$

which can be written in the form

$$\frac{n_1}{\bar{n}} = 1 - \left[1-\frac{n_2}{\bar{n}}\right]\left(\frac{h_o}{h}\right)^{\frac{aV_1}{cV_2} + (1-a)} \qquad 4.21$$

Fig. 4.1 represents equation 4.2 for different values of $\frac{n_2}{\bar{n}}$ with $\frac{aV_1}{cV_2} + (1-a) = 10$.

The figure shows that for $n_2/\bar{n}$ equal to unity the twist is constant along the bobbin. On the other hand, if $n_2/\bar{n}$ is greater than one, twist will decrease on the bobbin as the balloon height increases, and will increase for increasing balloon height if it becomes smaller than one. It is also clear that as the balloon height increases, the ratio $n_1/\bar{n}$ approaches 1.

To evaluate the theory obtained here, one should determine the ratio $n_2/\bar{n}$ (experimentally) by substituting in equation 4.21 the experimental values obtained at any known balloon height.

3. Experiments. The following set of experiments was designed to verify the expressions obtained.

(a) Twisting Machine and Testing Conditions: Yarns were twisted on the single spindle ring frame described in a

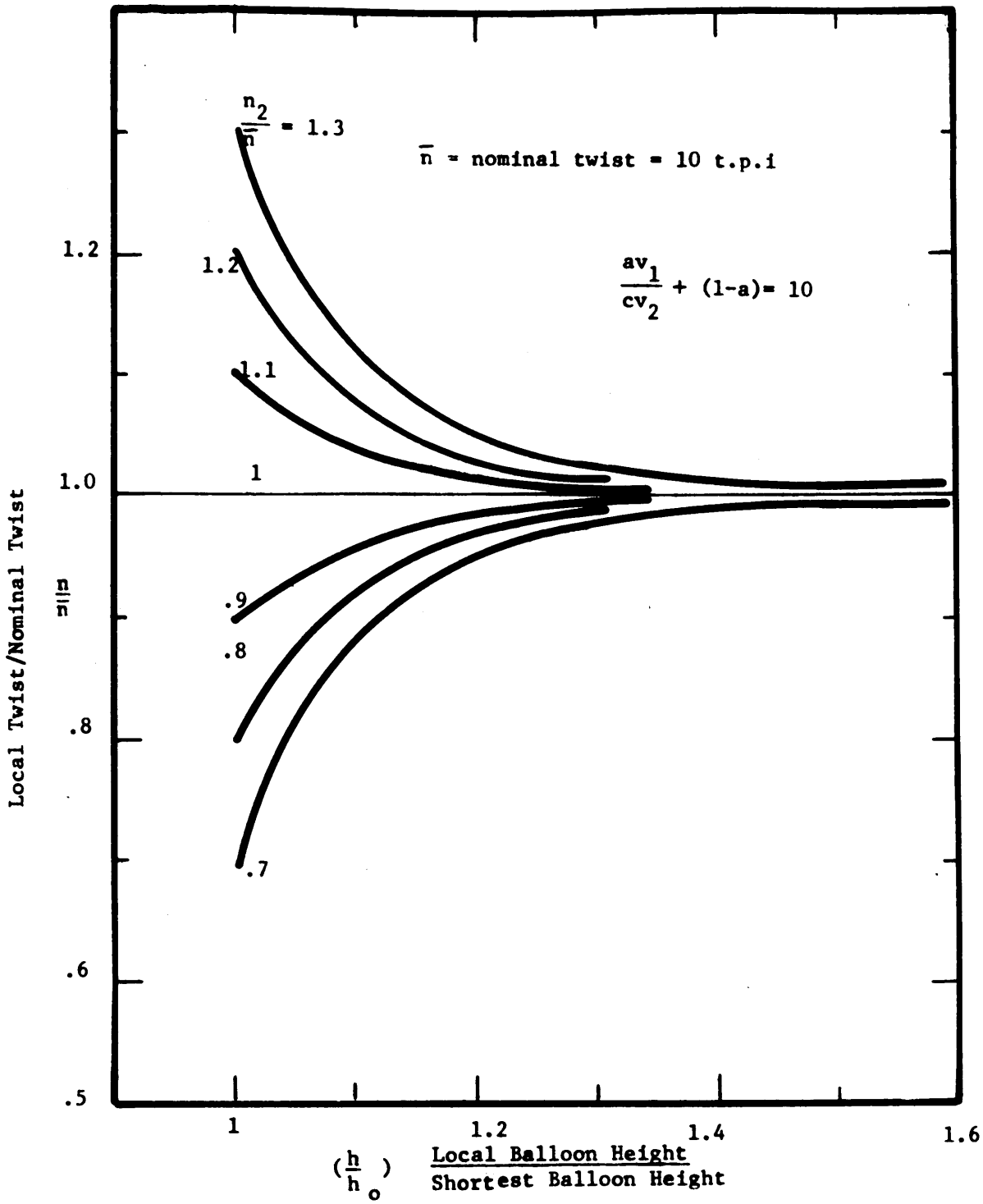

Fig. 4.1 Variation of Twist with Balloon Height

previous section under the following conditions:

spindle speed = 5820 rpm
traveller weight = 570 m.g.
ratio of front roller speed to ring rail speed = 10
nominal twist = 8.4 t.p.i.

(b) Material Used. Twist was inserted into a two-ply (one black and one grey) viscose rayon yarns 900 denier each. These yarns had 120 filaments and 3 T.P.I. "S" twist each.

(c) Test Procedure:

(1) The yarns were twisted on the ring frame in the conventional way (the bobbin produced was about 2" in diameter, 3.5" long).

(2) Lengths of yarn (about 10" long) were removed (by unwinding) from 3 different locations (1.5" apart) along the bobbin length.

(3) The total number of turns in each length removed was counted and the T.P.I. was determined for 10 samples at each location.

The twist was measured by counting the black or grey spots on the surface of the yarn, since each combination of one black and one grey represents a turn of twist.

4. Results. The results obtained are tabulated in table 4.1 and are plotted together with the predicted values in Fig. 4.2.

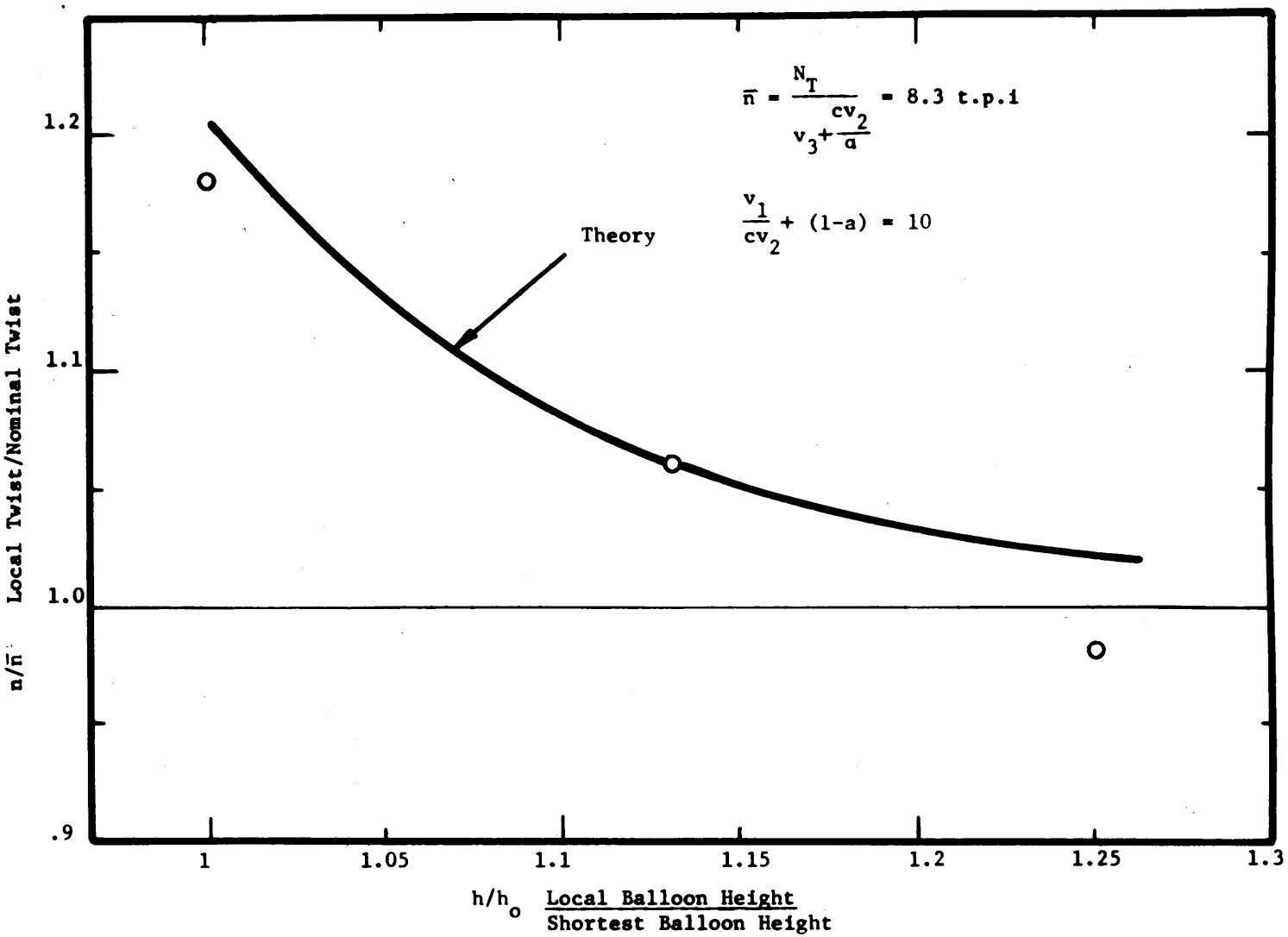

Fig. 4.2 Variation of Twist with Balloon Height
Comparison between Theory&Experiments

Table 4.1

Variation of Twist with

Balloon Height

h/h_o	t.p.i.*	C.V%
1	9.8	25
1.13	8.8	23
1.25	8.1-	20

*Average of 10 readings.

5. Discussion. Fig. 4.2 representing a comparison between predicted and experimental results shows a reasonable agreement between them. While the obtained theory shows that the ratio $n_1/\bar{n}$ approached unity, the experimental results are slightly lower. Figs. 4.1 and 4.2 show that the theory predicts that the change in twist takes place along a small portion of the bobbin height, but it is nearly constant in the remaining portion.

6. Conclusions. The study of twist variation along the bobbin length shows that there is a relation between the ring rail motion and the twist level on the bobbin at different balloon heights. From the theory which was experimentally verified, it may be concluded that the variation in twist along the bobbin is dependent on:

(a) The ring rail speed. As the speed increases, the twist level changes at a slower rate.

(b) The nominal twist.

(c) The ratio of twist in the balloon to the twist on the bobbin at any balloon height.

(d) The acceleration of the ring rail at both the end and the beginning of the stroke.

B. Twist Distribution in Yarns during Spinning on Ring Spinning Frame

1. Introduction. Twist is inserted on ring spinning frames by the rotation of the traveller on the ring. It is first inserted in the yarn balloon just above the traveller and propagates along the latter to the twist point. The level of twist propagating to the front roller nip (i.e., to the twist point) is of great importance in the spinning process. Its magnitude will determine the strength of the yarn at that point, which will influence the efficiency of the process. As less twist propagates to the twist point, the yarn will become weaker resulting in excessive end breakage which will affect both yarn quality and production efficiency. The quality of the produced yarn will be affected by the piecing up after breakage and by the fact that the pattern of migration, or migration frequency imposed in the yarn at the front roller, is different than that expected in the final twisted yarn, as discussed in Chapter III.

The distribution of twist in the spinning process has been subjected to extensive experimental study and a review of such work is given here. Baird[28] studied the speed of twist propagation in straight worsted yarns subjected to tension. The author reported that in such cases the speed of twist propagation along the yarns is from 20-200 m/sec., depending on both tension and twist levels. So, since the rate of delivery of material on spinning frames is far below the propagation rates given by Baird, then low twist levels at the twist point are due to factors other than slow propagation.

Misonow[29] showed experimentally (by suddenly gripping the yarn between pig tail and front roller) that twist levels

at the twist point are far below those on the bobbin. He explained this to be due to the frictional forces acting on the yarn at the pig tail and, with the use of a mechanically oscillating pig tail, he increased the twist level past the latter.

Wegner and Landwehrkamp[30], using high speed photography, found that twist is reduced by 15% at the balloon guide and by 18% across the pig tail. Later, Wegener and Wulfhorst[33] studied the effect of the angle (ψ) (Fig. 4.8) between the yarn and the axis of the bobbin at the pig tail on the twist level at the twist point. They also investigated the effect of pig tail diameter (wire diameter) on the twist level. Their results indicate that twist reduction increases as the angle increases and as the wire diameter decreases. The authors also studied the effect of the delivery angle (at front roller) on the distribution of twist between pig tail and front roller nip. Their report indicates the fact that twist is slightly higher at the pig tail than at the front roller and that there is no significant difference between the cases of different delivery angles.

The work of Gessner[31] on the causes of yarn breaks in worsted spinning is of great interest, and because of its close relation to the work described in this section, it will be reviewed in detail. Using high speed photography (while twisting black and white rovings) Gessner measured the twist between the front roller and pig tail and in the spinning balloon and finally he compared his results with the twist on the bobbin measured from the same length of yarn. This comparison was made possible by marking the yarn in the twisting zone (between front roller and pig tail) when taking the pictures, and comparing the twist in the pictures by that of the marked yarn on the bobbin. The author found that

the twist level between front roller and pig tail is about 50% to 90% of the corresponding twist on the bobbin depending on (provided the material is uniform):

Staple fiber length,

Twist level or twist multiple and yarn count,

Angle of deflection of yarn at pig tail.

The results obtained by Gessner can be summarized as follows:

(a) Effect of Staple Fiber Length. Fig. 4.3 shows the variation of the twist above the pig tail with the staple fiber length. Gessner explains this effect to be due to change in yarn rigidity (i.e., as fiber length increases, the rigidity increases), which will increase the twist propagation. At the same time, the author indicates that yarn rigidity has very little effect on twist propagation because the rate of propagation was found to be much higher than the rate of delivery on spinning frames. In his reasoning, the author did not give any reason for increasing yarn rigidity with staple fiber length.

According to the following analysis, the twist level above the pig tail depends to a great extent on the coefficient of friction between the yarn and the pig tail. From this, it seems that the change in friction between pig tail and yarn is the reason for the effect obtained by Gessner. This friction will change with changes in staple fiber due to the fact that yarn hairiness changes with staple length. As was discussed above in considering fiber migration, short staple fiber yarns have more ends on the surface than long staple fiber yarns, thus changing their surface characteristics.

(b) Effect of Twist Level and Yarn Count. Fig.

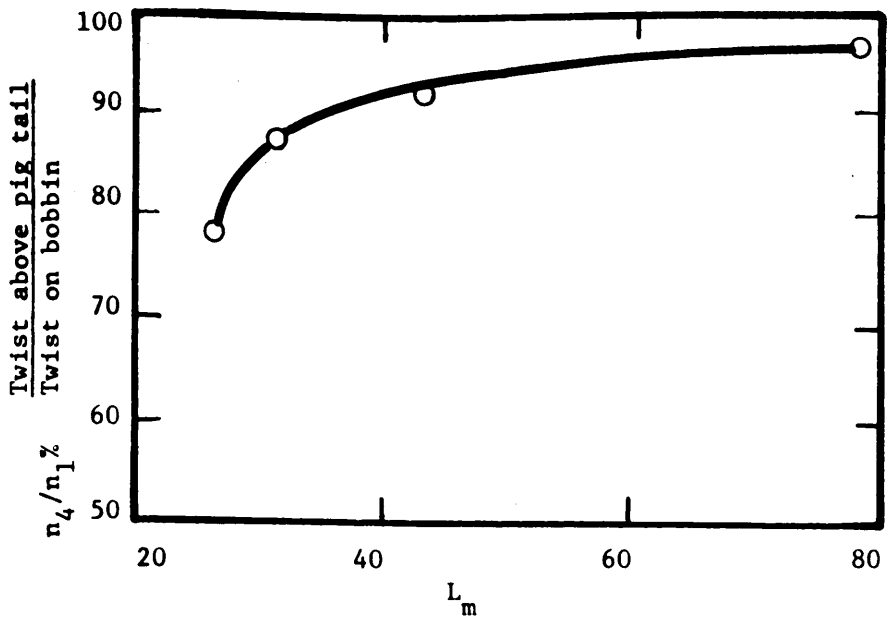

Fig. 4.3 Effect of Staple Length on Twist Level Above Pig tail (from Ref. 31)

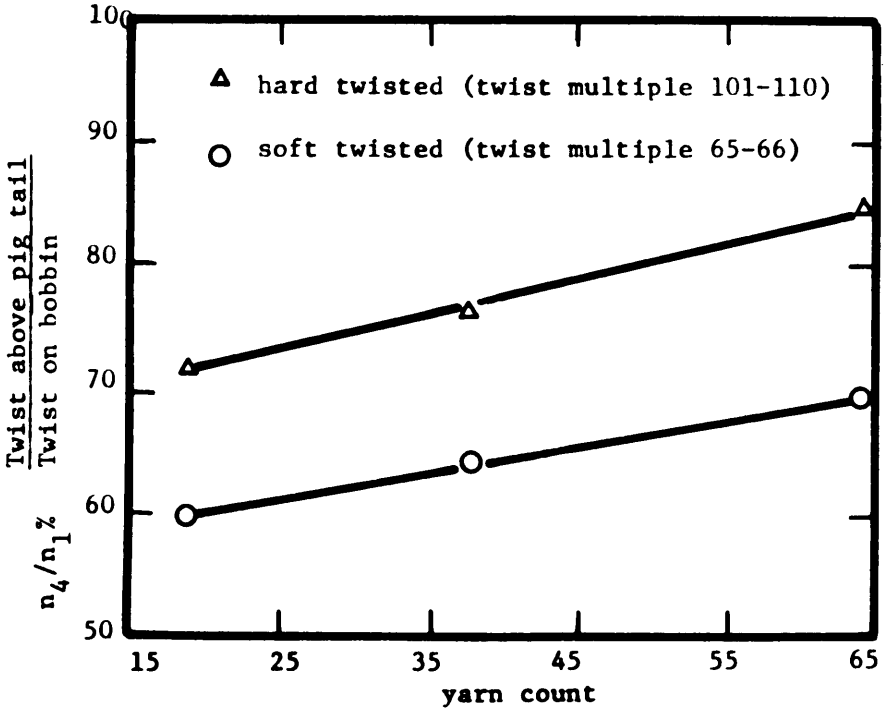

Fig. 4.4 Effect of Twist and Yarn Count on Twist Level Above Pig tail (From Ref. 31)

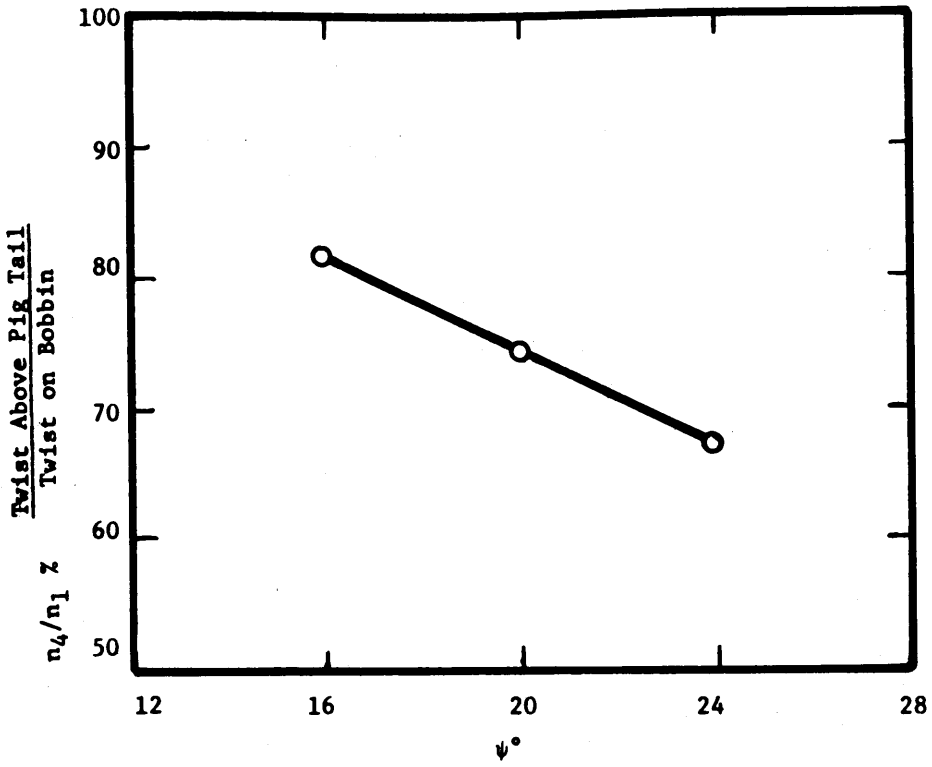

Fig. 4.5 Effect of Deflection Angle at Pig Tail on Twist Level at The Twist Point From Ref. 31

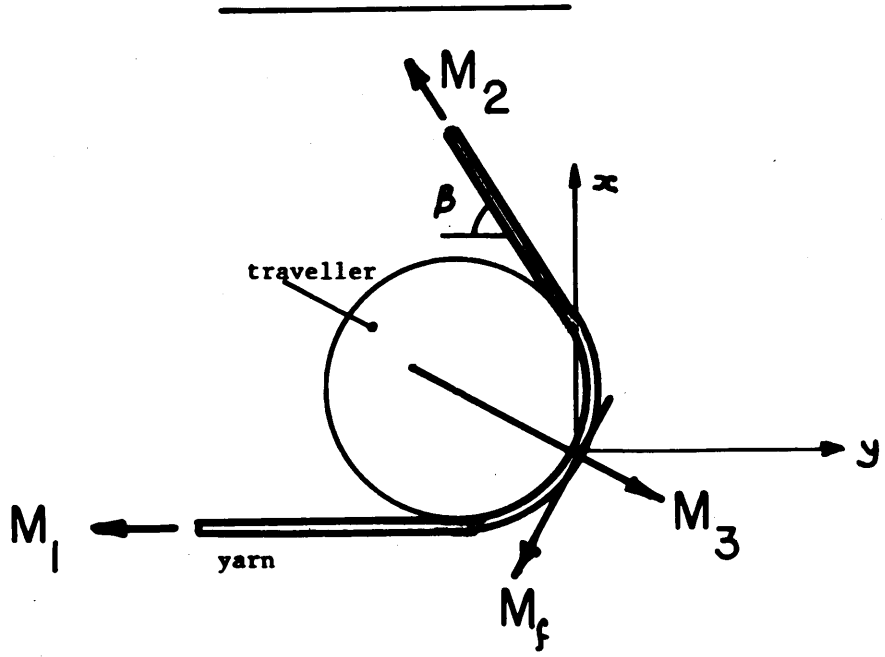

Fig. 4.6 Yarn Wrapping Around Traveller "Mathematical Model"

4.4 represents the variation of twist above the pig tail as a function of yarn count and twist level. The figure indicates that twist increases with yarn count for both soft and hard twisted yarns and that twist levels are higher in the latter case. Gessner explained this to be due to change in torsional rigidity of the yarn (as twist increases, rigidity increases, thus more twist will propagate faster.) Although the change in rigidity explains only the cases of different twist levels (i.e., hard twisted yarns versus soft twisted ones), the author did not give any reason for the increase of twist above the pig tail due to change in yarn count. This point will be discussed in greater detail in a following section.

(c) Effect of the Angle of Deflection at the Pig Tail. Fig. 4.5 indicates that twist level above the pig tail decreases as the angle of deflection (ψ) Fig. 4.8 increases. Gessner did not give any reason for these results and in a following section, this relation will be discussed in more detail.

In this section a theoretical treatment will be undertaken in order to find the twist distribution along the yarn in the twisting zone. Later the theory will be compared with experimental results so that to establish its validity.

2. Theory

(a) Nomenclature. The following nomenclature is used in the analysis of this section on the distribution of twist in the yarn in the twisting zone.

c = Proportionality constant = $\frac{\text{Length of balloon}}{\text{Height of balloon}}$

EI = Bending stiffness

GI_p = Torsional rigidity

H = Balloon height

L = Length of yarn in balloon

M_1 = Twisting torque in yarn between traveller and bobbin

M_2 = Twisting torque in yarn in balloon side

M_3 = Torque exerted by traveller to prevent the bent yarn from torsional buckling

M_f = Frictional torque between yarn and traveller

$M(x)$ = Local twisting moment (along yarn axis)

$M_b(x)$ = Local bending moment

M_t = An additional imag. torque at distance x

n_1 = Twist/unit length in yarn between traveller and bobbin

n_2 = Twist/unit length in yarn at the bottom of the balloon

n_3 = Twist/unit length in yarn at the top of the balloon

n_4 = Twist in turns/unit length between front roller and pig tail

$n(x)$ = Twist turns/unit length at any point in balloon

R = Ring rail radius

N = Total number of turns in the system (between traveller and front roller)

S = Length along yarn

U = Elastic energy

β = Angle of deflection of yarn at traveller

$\phi(x)$ = Local rotation in radians in the vertical direction, i.e., along the x axis

θ_1 = Local rotation in radians along yarn axis in balloon

$\tilde{\tau}$ = Frictional torque at pig tail

ω = $\frac{GI_p}{EI}$

L_o = Vertical distance between pig tail and front roller

ψ = Angle between yarn and vertical.

(b) Twist Drop across the Traveller

(1) Assumptions. In this analysis, it will be assumed that

Yarn-traveller contact is as shown in Fig. 4.6.

Yarn is a single monofilament.

Material to be twisted obeys Hook's law under any loading conditions (i.e., in bending, tension and torsion).

(2) Relation between Twist Levels across the Traveller. Consider the yarn to be wrapped around the traveller as shown in Fig. 4.6. The yarn is in a state of equilibrium under the following moments:

M_1 = twisting torque between traveller and bobbin

M_2 = twisting moment in yarn in the balloon side

M_f = frictional torque resulting from yarn-traveller friction

M_3 = torque exerted by traveller to prevent the bent yarn from buckling.

Now moment equilibrium in x-direction gives

$$M_2 \sin \beta = M_f \cos \beta/2 + M_3 \sin \beta/2 \qquad 4.22$$

and the y-direction leads to

$$M_1 + M_2 \cos \beta = M_3 \cos \beta/2 - M_f \sin \beta/2 \qquad 4.23$$

Solving equations 4.22 and 4.23 for M_3 gives

$$M_3 = 2 M_2 \cos \beta/2 - M_f \cot \beta/2 \qquad 4.24$$

Substituting 4.24 into 2.23 yields

$$M_1 = 2 M_2 \cos^2 \beta/2 - M_2 \cos \beta$$

$$-M_f \frac{\cos^2 \beta/2}{\sin \beta/2} - M_f \sin \beta/2$$

or

$$M_1 = M_2 (2 \cos^2 \beta/2 - \cos \beta)$$

$$- \frac{M_f}{\sin \beta/2}(\cos^2 \beta/2 + \sin^2 \beta/2) \qquad 4.25$$

but from simple trigonometry it can be shown that

$$\cos \beta = \cos^2 \beta/2 - \sin^2 \beta/2 \qquad 4.26$$

and

$$\cos^2 \beta/2 + \sin^2 \beta/2 = 1 \qquad 4.27$$

Substituting 4.26 and 4.27 into 4.25 and after reducing the results, one obtains

$$M_1 = M_2 - \frac{M_f}{\sin \beta/2} \qquad 4.28$$

But

$$M_1 = 2 \pi GI_p n_1 \text{ and } M_2 = 2 \pi GI_p n_2 \qquad 4.29$$

where n_1 and n_2 are the corresponding twist/unit length in the yarn and GI_p is the torsional rigidity of the yarn.
From 4.28 and 4.29

$$n_1 = n_2 - \frac{M_f}{2 \pi GI_p \sin \beta/2} \qquad 4.30$$

from which

$$\frac{n_2}{n_1} = 1 + \frac{M_f}{2 \pi GI_p n_1 \sin \beta/2} \qquad 4.31$$

Fig. 4.7 represents the variation of n_2/n_1 with the frictional torque for different deflection angles (β).

(c) Twist Distribution between Traveller and Front Roller. Consider the yarn length in the twisting zone (between the front roller nip and the traveller) to be stationary at any instant of time. Let the total number of turns in the system be equal to N. Now the twist distribution will be calculated as follows:

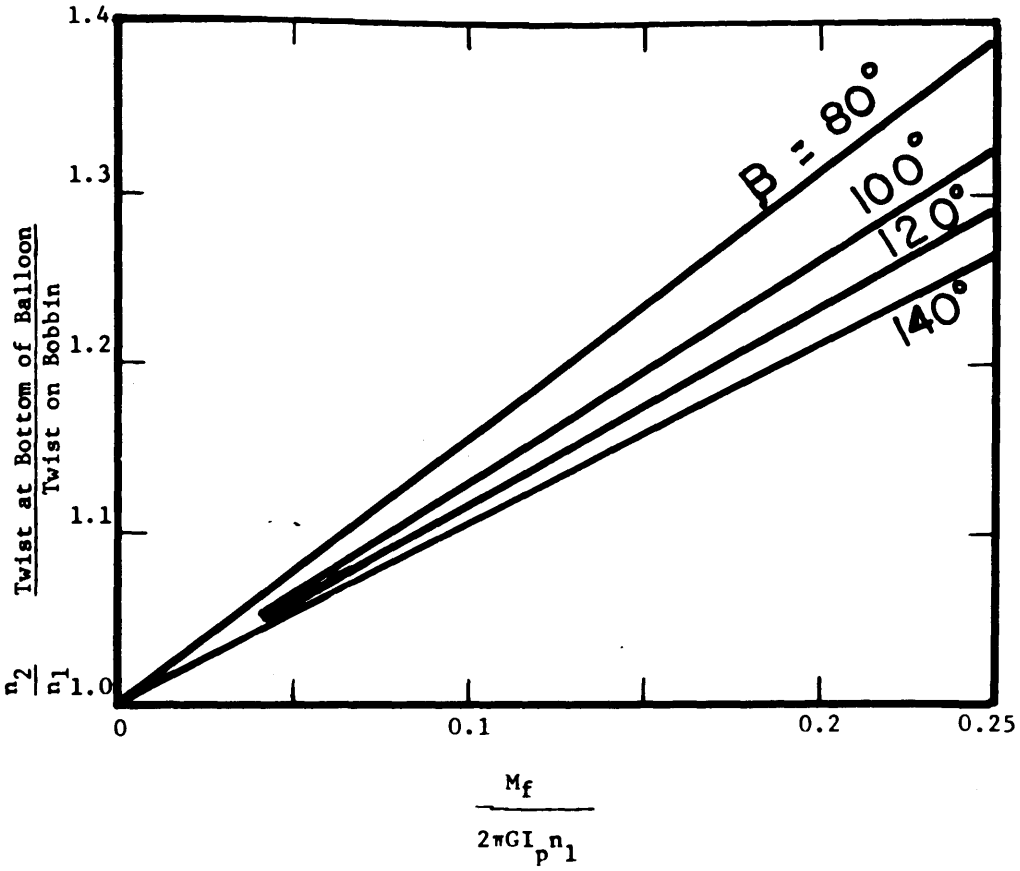

Fig. 4.7 Effect of Friction on Twist Ratio Across the Traveller

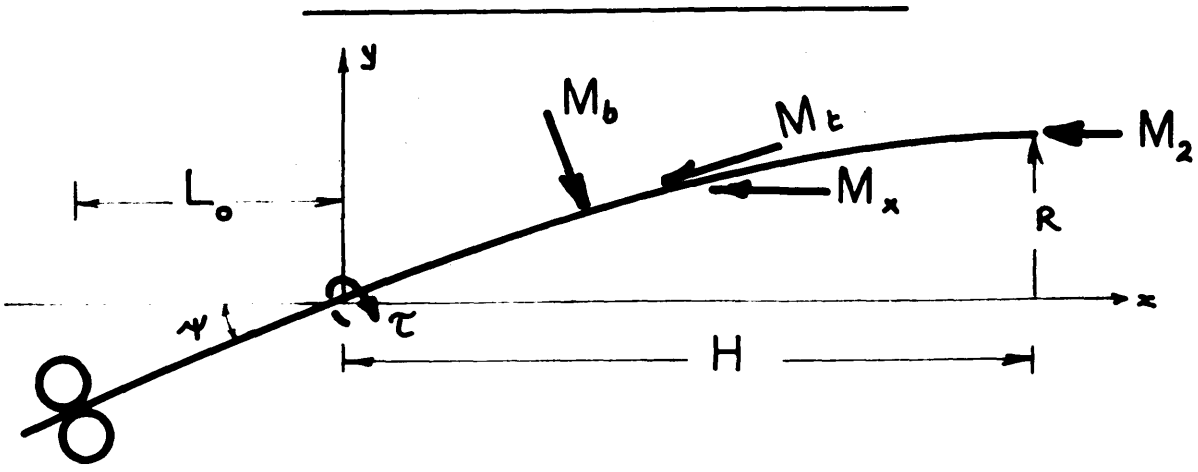

Fig. 4.8 Diagramatic Sketch of Yarn in Twisting Zone

(Mathematical Model)

(1) Assumption: Let us assume that

Portion of yarn between front roller and pig tail is a straight line.

Yarn balloon is a two-dimensional (i.e., neglect air drag) line curve with a zero tangent at the ring.

Yarn is completely elastic in both bending and torsion.(This assumption was justified experimentally and the results are discussed in a later section).

Yarn length in balloon is proportional to balloon height, or $c = \frac{L}{H}$.

That the yarn is a single continuous monofilament. No elastic energy in the yarn in the bent form before twisting.

(2) Geometry of System. Considering the origin of the axis to be at the pig tail, as shown in Fig. 4.8 , the yarn path is given by

$$y = \begin{cases} x \tan \psi & -L_o < x < o \\ R \sin \frac{x}{2H} & 0 < x < H \end{cases} \qquad 4.32$$

(3) Procedure for Calculation of Twist Distribution. The twist distribution will be calculated as follows:

(a) Assume an additional torque (M_t) to be acting (11$\frac{le}{}$ to x-axis) on the balloon at distance x from the pig tail.

(b) Calculate the local twisting and bending moments (M(x) and $M_b(x)$) acting on the yarn.

(c) Calculate the total elastic energy (U) in the system.

(d) Calculate the local defl$\frac{n}{}$ under M_t, or $\theta(x) = \frac{\partial U}{\partial M_t}$ at $M_t = o$ (and with the proper direction).

(e) Calculate the torque M_2 as a function of the total number of turns in the system N together with the

other variables of the system, or

$$\frac{\partial U}{\partial M_t}_{M_t = 0} = 2\pi N$$

(f) Calculate the local twist/unit length (n) in the balloon as

$$n = \frac{1}{2\pi} \frac{\partial \theta(x)}{\partial S}$$ (S is the length along the balloon).

(4) Calculation of Strain Energy. The moment distribution is given by (with the notation that $y' = dy/dx$)

(a) Twisting Moments

$$M(x) = \begin{cases} \dfrac{M_2 + M_t}{\sqrt{1 + y'^2}} & x=0 \text{ to } x=x \\ \dfrac{M_2}{\sqrt{1 + y'^2}} & x=x \text{ to } x=H \\ (M_2 + M_t)\cos\psi - \tau & x=0 \text{ to } x=L_0\cos\psi \end{cases} \quad 4.33$$

(b) Bending Moments

$$M_b(x) = \begin{cases} \dfrac{(M_2 + M_t)y'}{\sqrt{1 + y'^2}} & x=0 \text{ to } x=x \\ \dfrac{M_2 y'}{\sqrt{1 + y'^2}} & x=x \text{ to } x=H \\ (M_2 + M_t)\sin\psi & x=0 \text{ to } x=L_0\cos\psi \end{cases} \quad 4.34$$

The elastic energy U is now given by

$$\begin{aligned} U = \frac{1}{2GI_p} \Bigg\{ & \int_0^x \frac{c(M_t + M_2)^2}{1 + y'^2} dx + \int_x^L \frac{c M_2^2}{1 + y'^2} dx \\ & + \int_0^{L_0} \left[(M_2 + M_t)\cos\psi - \tau \right]^2 \frac{dx}{\cos\psi} \Bigg\} \\ & + \frac{1}{2EI} \Bigg\{ \int_0^x \frac{c(M_2 + M_t)^2 y'^2}{1 + y'^2} dx + \int_x^L \frac{c\, y'^2 M_2^2}{1 + y'^2} dx \\ & + \int_0^{L_0} \frac{(M_2 + M_t)^2 \sin^2\psi}{\cos\psi} dx \Bigg\} \end{aligned} \quad 4.35$$

(5) Calculation of the Torque M_2. If N is the total number of turns in the system, then N is given by

$$N = \frac{1}{2\pi}\frac{\partial U}{\partial M_2} \quad \text{with } M_t = 0$$

To integrate 4.35, let it be assumed that

$$\frac{\pi^2 R^2}{4H^2}\cos^2\frac{\pi x}{2H} < 1$$

i.e.

$$\frac{1}{1+y'^2} = \frac{1}{1+\frac{\pi^2R^2}{4H^2}\cos^2\frac{\pi x}{2H}} = 1-\frac{\pi^2R^2}{4H^2}\cos^2\frac{\pi x}{2H} \qquad 4.36$$

and

$$\frac{y'^2}{1+y'^2} = \frac{\pi^2R^2}{4H^2}\cos^2\frac{\pi x}{2H} \qquad 4.37$$

Integrating, then differentiating, we get

$$2\pi N = \frac{M_2}{GI_p}\left\{\left[CH\left(1-\frac{\pi^2R^2}{8H^2}\right)+L_o\cos\psi\right]\right\}-\frac{\tau L_o}{GI_p} + \frac{M_2}{EI}\left\{\frac{C\pi^2R^2}{8H}+L_o\frac{\sin^2\psi}{\cos\psi}\right\}$$

or

$$2\pi N+\frac{\tau L_o}{GI_p} = M_2\left\{\frac{C}{GI_p}\left(H-\frac{\pi^2R^2}{8H}+\frac{L_o\cos\psi}{C}\right) + \frac{C}{EI}\left(\frac{\pi^2R^2}{8H^2}+\frac{L_o\sin^2\psi}{C\cos\psi}\right)\right\} \qquad 4.38$$

from which we have

$$M_2 = \frac{2\pi N GI_p + L_o\tau}{CH\left[1+\frac{\pi^2R^2}{8H^2}(\omega-1)+\frac{L_o}{CH}\cos\psi(1-\tan^2\psi)\right]} \qquad 4.39$$

(6) Calculation of the Twist Distribution along the Balloon. The local deflection in radians at any point along the balloon is given by

$$\Phi(x) = \frac{\partial U}{\partial M_t} \qquad \text{with } M_t = 0$$

or

$$\Phi(x) = \frac{1}{GI_p}\left\{\int_0^x \frac{c M_2}{1+y'^2}\,dx + \int_0^{L_o} \frac{M_2\cos\psi - \tilde{C}}{\cos\psi}\,dx\right\}$$

$$+\frac{1}{EI}\left\{\int_0^x \frac{c M_2 y'^2}{1+y'^2}\,dx + \int_0^{L_o} \frac{M_2 \sin^2\psi}{\cos\psi}\,dx\right\} \qquad 4.40$$

where $\phi(x)$ is the deflection in radians in the direction of the x-axis and the rotation in the direction of the axis of the yarn is given by

$$\theta(x) = \phi(x)\,\frac{dS}{dx} = \phi(x)\,.\,\sqrt{1+y'^2} \qquad 4.41$$

Using the simplifications 4.36 and 4.37 used before, the equation can be written as follows:

$$\Phi(x) = \frac{1}{GI_p}\left\{M_2\left[cx\left(1-\frac{\bar{\pi}^2R^2}{8H^2}\right) - \frac{c\bar{\pi}R^2}{8H}\sin\frac{\bar{\pi}x}{H} + L_o\right] - \frac{\tau L_o}{\cos\psi}\right\} + \frac{M_2}{EI}\left\{\frac{c\bar{\pi}^2R^2}{8H^2}x + \frac{c\bar{\pi}R^2}{8H}\sin\frac{\bar{\pi}x}{H} + L_o\frac{\sin^2\psi}{\cos\psi}\right\} \qquad 4.42$$

The twist/unit length (n_2) in the balloon is then given by

$$n = \frac{1}{2\pi} \cdot \frac{\partial \theta(x)}{\partial S} = \frac{1}{2\pi} \frac{\partial \theta}{\partial x} \cdot \frac{\partial x}{\partial S}$$

or

$$n = \frac{1}{2\pi\sqrt{1+y'^2}} \cdot \frac{\partial}{\partial x} \phi(x)\sqrt{1+y'^2}$$

$$= \frac{1}{2\pi} \frac{\partial \phi(x)}{\partial x} + \frac{1}{2\pi} \frac{\phi(x)}{\sqrt{1+y'^2}} \cdot \frac{\partial \sqrt{1+y'^2}}{\partial x} \qquad 4.43$$

which, after differentiation, will lead to

$$n = \frac{M_2}{2\pi G I_p} \left\{ C + \frac{c\pi^2 R^2}{8H^2}\left(1+\cos\frac{\pi x}{H}\right)(\omega-1) \right.$$

$$+\left[cx + L_0 + \frac{c\pi^2 R^2}{8H}(\omega-1)\left(\frac{x}{H} + \frac{1}{\pi}\sin\frac{\pi x}{H}\right) + \right.$$

$$\left.\left. \omega L_0 \frac{\sin^2\psi}{\cos\psi} \right] \frac{y' \cdot y''}{1+y'^2} \right\} - \frac{\tau L_0}{2\pi G I_p \cos\psi} \cdot \frac{y'y''}{1+y'^2} \qquad 4.44$$

where

$$y'' = \frac{\partial^2 y}{\partial x^2}$$

Substituting for M_2 from equation 4.39, we get

$$n(x) = \frac{2\pi N G I_p + L_0 \tau}{2\pi G I_p H c\left[1 + \frac{\pi^2 R^2}{8H^2}(\omega-1) + \frac{L_0 \cos\psi}{cH}(1-\tan^2\psi\right]} \left\{ C \right.$$

$$+ \frac{c\pi^2 R^2}{8H^2}\left(1+\cos\frac{\pi x}{H}\right)(1-\omega) + \left[c\frac{x}{H} + \frac{L_0}{H} + \frac{L_0\omega}{H}\frac{\sin^2\psi}{\cos\psi} \right.$$

$$\left. \left. + \frac{c\pi^2 R^2}{8H^2}(\omega-1)\left(\frac{x}{H} + \frac{1}{\pi}\sin\frac{\pi x}{H}\right) \right] \frac{H y' y''}{1+y'^2} \right\}$$

$$- \frac{L_0 \tau}{2\pi G I_p \cos\psi} \cdot \frac{y' x''}{1+y'^2} \qquad 4.45$$

The ratio n_3/n_2, where n_2 is the twist/unit length in balloon at traveller at x = H, and n_3 = twist/unit length in balloon at pig tail at x = o, is given by

$$\frac{n_3}{n_2} = 1 - (1 - \omega) \frac{\pi^2 R^2}{4 H^2} \qquad 4.46$$

Fig. 4.9 shows the relation between the ratio n_3/n_2 and $(\frac{R}{H})^2$ as given by equation 4.46 for different values of .

From equation 4.45 it is seen that the local twist in the balloon zone depends on the torsional rigidity (GI_p), the bending stiffness (EI), the balloon height (H), the number of turns of twist in the system (N), the frictional torque at the pig tail (τ), the vertical position of the pig tail under the front roller (L_o), and the deflection angle of the yarn at the pig tail (ψ).

(7) Calculation of the Twist Distribution in the Straight Section (between front roller and pig tail). The torque acting on the yarn above the pig tail is constant and is given by

$$M = M_2 \cos\psi - \tau \qquad 4.47$$

and

$$\theta_1(x) = \frac{M x}{GI_p \cos\psi} = \frac{M_2 \cos\psi - \tau}{GI_p \cos\psi} x$$

The number of turns/unit length n_4 is given by

$$n_4 = \frac{1}{2\pi} \cdot \frac{\partial \theta_1}{\partial S} = \frac{1}{2\pi} \cdot \frac{\partial \theta}{\partial x} \cdot \frac{\partial x}{\partial S} = \frac{1}{2\pi} \frac{M_2 \cos\psi - \tau}{GI_p} \qquad 4.48$$

with M_2 as given by equation 4.39, we get

$$n_4 = \frac{1}{2\pi GI_p} \left\{ \frac{(2\pi N GI_p + \tau L_o)\cos\psi}{CH\left[1 + \frac{\pi^2 R^2}{8H^2}(\omega - 1) + \frac{L_o \cos\psi}{CH}(1 - \tan^2\psi)\right]} - \tau \right\} \qquad 4.49$$

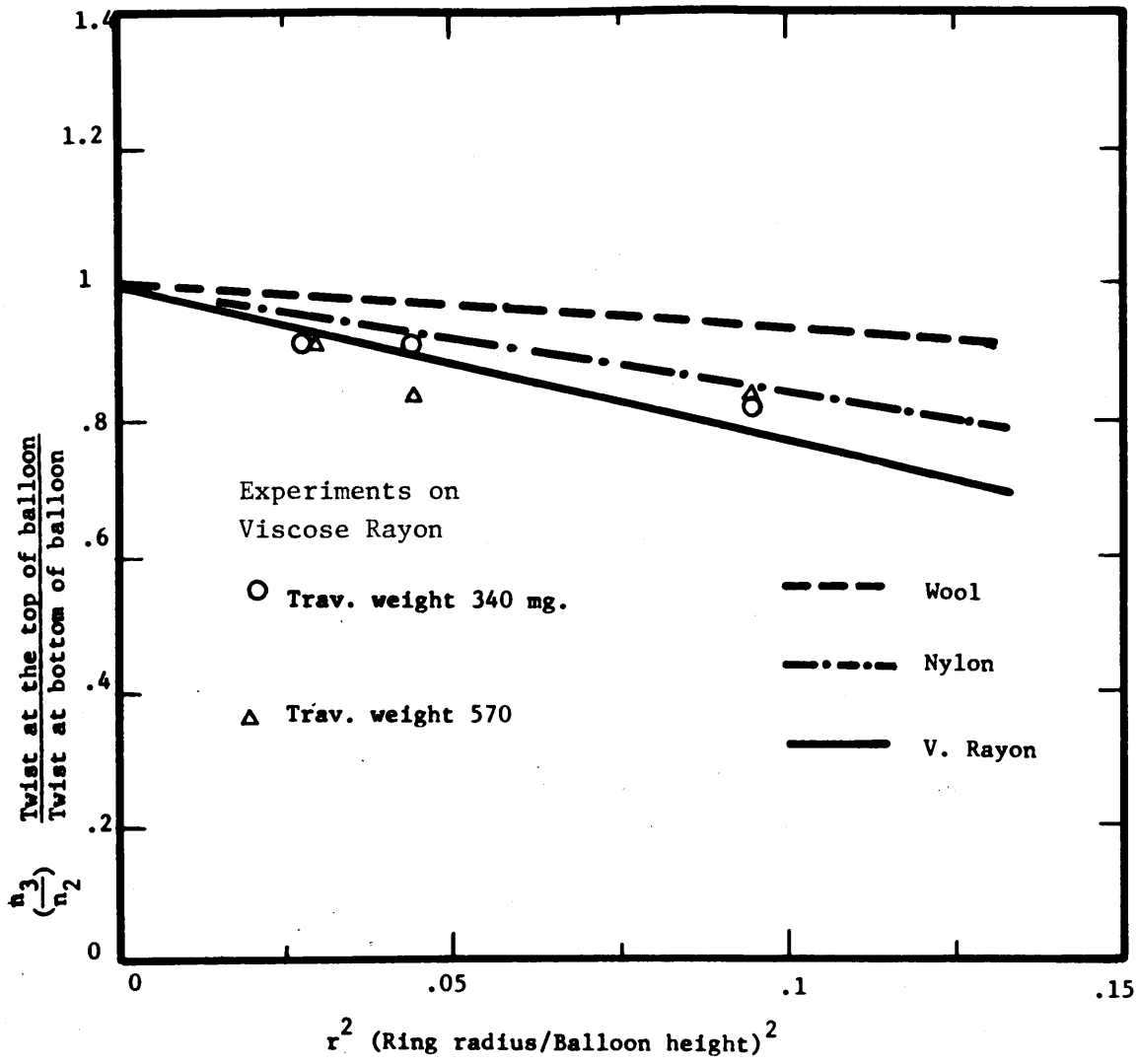

Fig. 4.9 Effect of Balloon Height on Twist Drop Along the Balloon

(Comparison between theory and experiments)

The ratio n_4/n_3, or ratio between twist levels across the pig tail, is given with the use of equations 4.25 and 4.40 by

$$\frac{n_4}{n_3} = 1 - \frac{\tau}{2\pi G I_p n_3} \cdot \frac{c}{\cos\psi} \cdot \left\{ 1 - \frac{\pi^2 R^2}{4H^2}(1 - \omega) \right\} \qquad 4.50$$

but from equation 4.46

$$\frac{n_3}{n_2} = 1 - \frac{\pi^2 R^2}{4H^2}(1 - \omega)$$

then

$$\frac{n_4}{n_2} = \left\{ 1 - \frac{\pi^2 R^2}{4H^2}(1 - \omega) \right\} \left\{ 1 - \frac{c\tau}{2\pi G I_p n_2 \cos\psi} \right\} \qquad 4.51$$

and since n_2 is given by

$$\frac{n_2}{n_1} = 1 + \frac{M_f}{2 G I_p n_1 \sin \beta/2}$$

then we have

$$\frac{n_4}{n_1} = \left[1 + \frac{M_f}{2\pi G I_p n_1 \sin \beta/2} \right] \left[1 - \frac{\pi^2 R^2}{4H^2}(1-\omega) \right] \cdot \left[1 - \frac{c\tau}{2\pi G I_p n_1 \cos\psi + \frac{M_f \cos\psi}{\sin \beta/2}} \right] \qquad 4.52$$

Equation 4.52 can be written as

$$\frac{n_4}{n_1} = \frac{n_2}{n_1} \cdot \frac{n_3}{n_2} \left[1 - \frac{c\tau/2\pi G I_p n_1}{\frac{n_2}{n_1}\cos\psi} \right] \qquad 4.53$$

Now it can be easily shown that t (the frictional torque at the pig tail) as shown in Appendix C is proportional to yarn tension times x sin ψ or $\tau = A T_0 \sin\psi$ where A is a constant of proportionality and is dependent on coefficient of friction at pig tail, the yarn radius and the slope of the yarn in balloon at the pig tail.

Then equation 4.53 can be written as

$$\frac{n_4}{n_1} = \frac{n_2}{n_1}\cdot\frac{n_3}{n_2}\left\{1 - \frac{CAT_0/2\pi GI_p n_1 \tan\psi}{n_2/n_1}\right\}$$

which can be written as

$$\frac{n_4}{n_1} = \frac{n_2}{n_1}\cdot\frac{n_3}{n_2}\left\{1 - \frac{B\tan\psi}{n_2/n_1}\right\} \qquad 4.54$$

Fig. 4.10 shows equation 4.54 plotted (assuming that $n_2/n_1 = 1.15$ and $n_3/n_2 = .8$) for n_4/n_1 as a function of for different values of $B = \frac{CAT_0}{2\pi GI_p n_1}$ of 0.35, 0.45 and 0.55. It is clear from this plot that the theory agrees with the result obtained by Gessner[31], Fig. 4.5 .

Equation 4.52 represents the ratio n_4/n_1 of twist in the yarn above the pig tail to the twist level in the yarn on the bobbin. It is clear that this ratio (n_4/n_1) is dependent on:

the torsional rigidity of the yarn (GI_p),
the ratio of bending to torsional rigidities (ω),
the twist level on the bobbin,
the frictional torque between yarn and traveller (M_f),
the frictional torque (τ) between yarn and pig tail,
the balloon height,
the ring radius,
the deflection of yarn at pig tail (ψ) and
deflection of yarn at traveller (β).

3. Experiment. The following experimental work was designed to evaluate the validity of the proposed theory. In particular it was of interest to measure and observe:

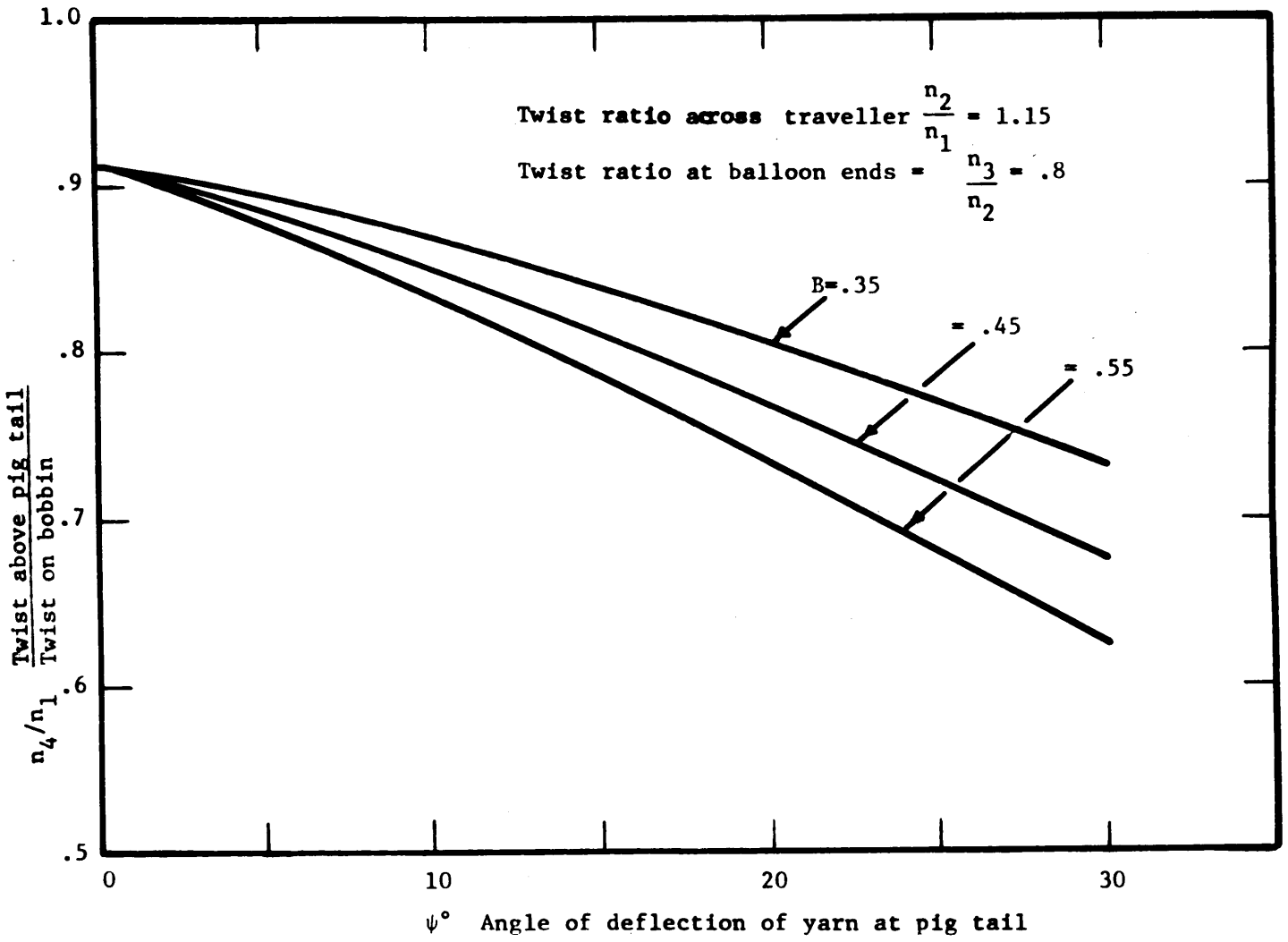

Fig. 4.10 Theoretical Effect of Deflection Angle at Pig Tail on Twist Level at Twist Point. (Equation 4.54)

the twist distribution between front roller and bobbin, on the ring spinning frame,

the torsional rigidity (GI_p) of the material used,

the bending stiffness (EI) for the twisted yarn.

(a) Material Used. The experiments discussed here were conducted using continuous filaments viscose rayon yarns. Twist was inserted into two of these yarns (one black and one grey), having the following specifications:

Number of filaments/yarn = 120 filaments

Producer twist is (S) twist = 3 T.P.I.

Yarn count = 900 denier.

Fig. 4.11 shows the load elongation curve for these yarns which was obtained on the Instron tensile testing machine under the following conditions:

Strain rate = 10%/min.

Gauge length = 10".

(b) Procedure. The twist distribution between the bobbin and the front roller was measured using high speed photography using a technique similar to that used by Gessner[31]. High speed pictures were taken for the twisting zone while twisting the black and grey viscose rayon yarns. The pictures were taken on high speed negatives (1250 ASA), using a high speed micro flash with a duration time of 2 μ sec. They were taken with the room kept in darkness and the shutter on the camera fully opened. The lighting equipment is described in greater detail in Chapter II. The triggering device for the flash was a photo cell. The photo cell was placed beside the ring and gave the triggering signal as the traveller (which was painted with a white paint) passed in front of it. Two pictures were taken on each negative, with the traveller at two different positions 90° apart, to correct for the effect of air drag on yarn length. These two pictures were taken

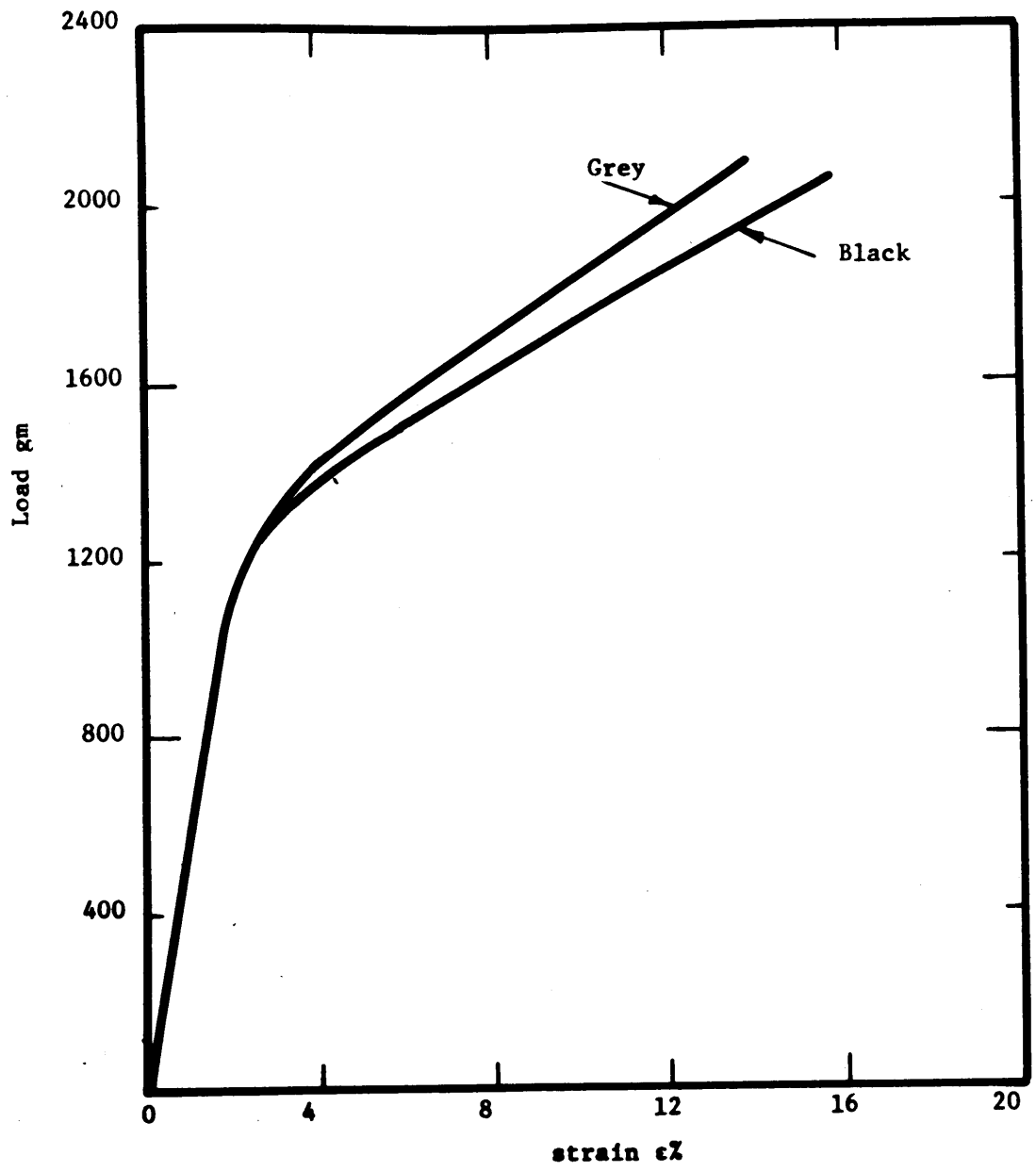

Fig. 4.11 Load-elongation Curve of 900 Denier Viscose Rayon

using the flash delay unit (2), Fig. 2.8, discussed in Chapter II.

The negatives were then developed and printed and the twist was then measured by computing the length of yarn for each 4 turns of twist. The twist was measured in 4 locations, namely:

between the pig tail and the front roller (n_4)

at the top of the balloon (n_3)

at the bottom of the balloon (n_2)

between the traveller and the bobbin (n_1).

Figs. 12-A and 12-B show typical pictures of the yarn in the twisting zone.

(c) Twisting Conditions. The following conditions were used:

Balloon heights:	15, 12 and 8 inches
Traveller weights:	570 and 340 mgs.
Spindle speed:	2620 r.p.m.
Nominal twist levels:	8 and 11 t.p.i.

(d) Measurements of Torsional Rigidity

(1) Apparatus. The torsional rigidity of the two-ply viscose rayon yarn used in this investigation was measured on the torque measuring device (Fig. 2.6) described in Chapter II.

(2) Procedure. The specimen (1) to be twisted is first clamped in the two jaws (2 and 3) of the apparatus, as shown in Fig. 2.6, and twist was then inserted by rotating the jaw (2) which can slide to allow for specimen contraction under constant tension.

The torque turns curves are then obtained using the Instron recording system. The torsional rigidity was then calculated using the following formula

$$GI_p = \frac{M_t L}{2\pi N}$$

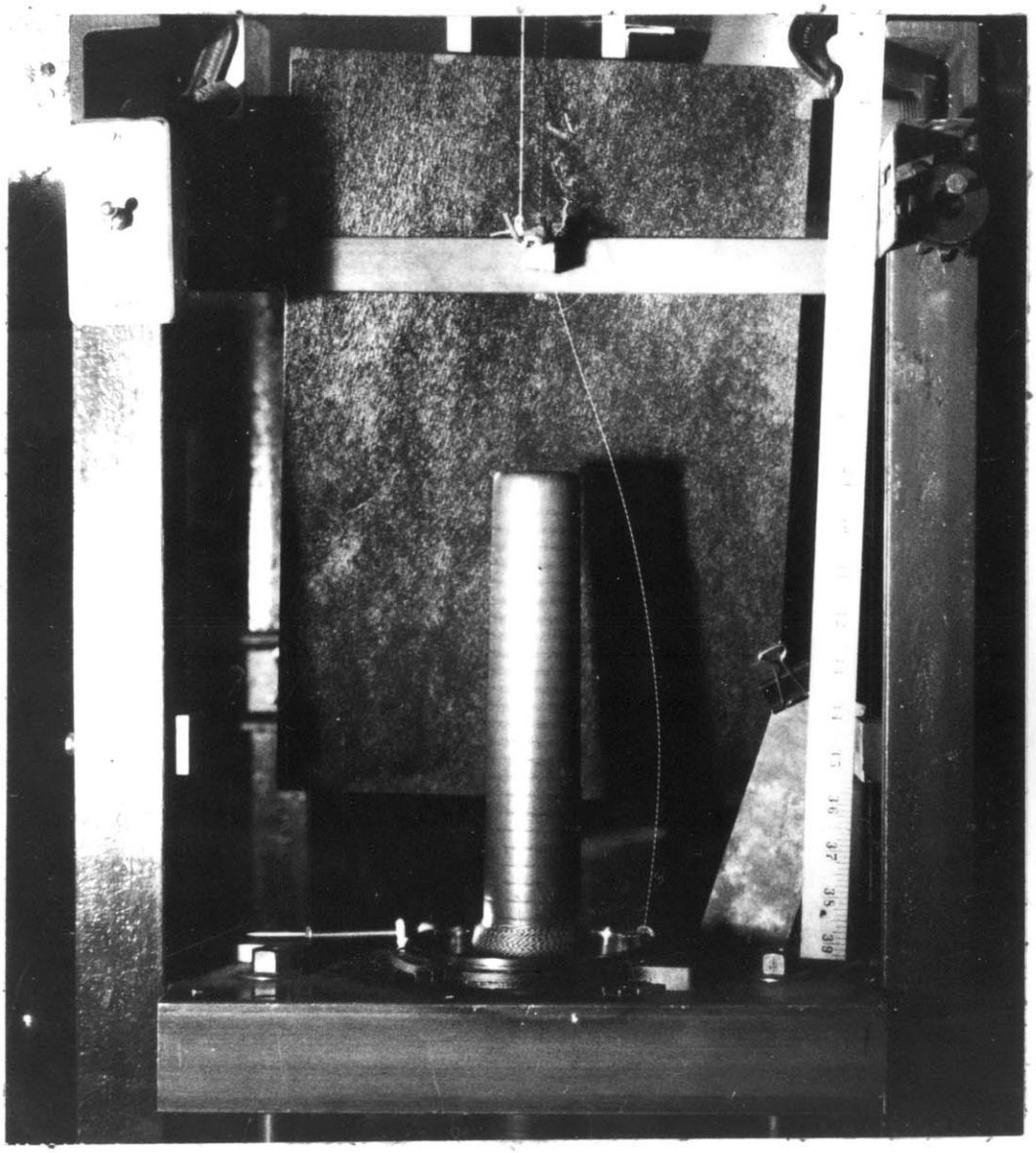

Fig. 4.12A Twist Distribution in The Twisting Zone

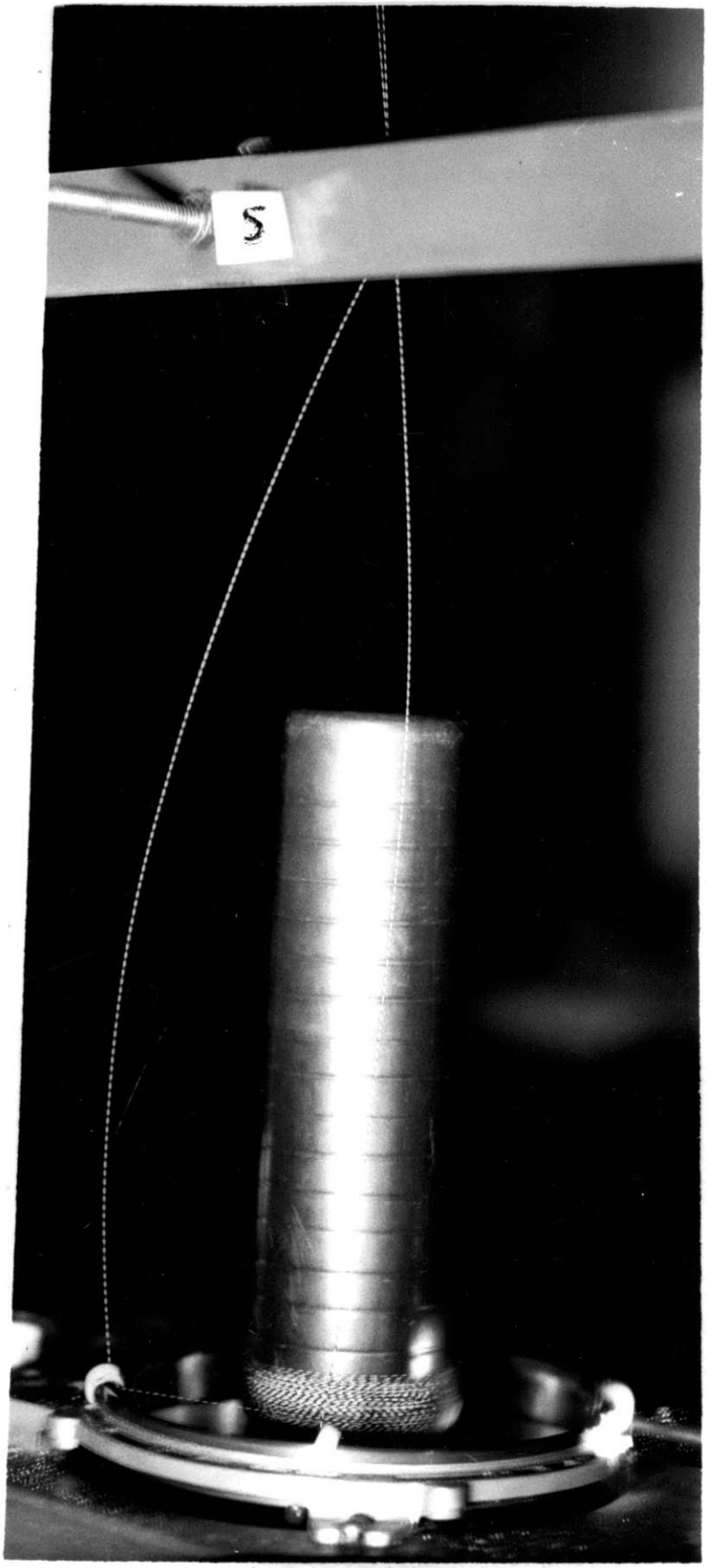

Fig. 4.12B

where

M_t = torque in yarn

L = length of sample

N = number of turns in the yarn.

(e) Bending Stiffness (EI) Measurements

(1) Procedure. The bending stiffness measurements were made as follows:

(a) Samples were twisted on the model twister to different twist levels.

(b) The diameter of each specimen was measured under the microscope (2 readings were taken for each sample)

(c) Load-elongation curves were obtained on the Instron tensile testing machine.

(d) From the load-elongation curves the value EI was calculated using the initial slopes of the curves and the cross-sectional area to be that of the total area of the filaments in the yarn.

(2) Experimental Conditions.

Twist levels: 2.59, 4.93, 9.26 and 12.36 tpi

Twisting tension = 75 gms.

Strain rate = 10%/min.

Sample length = 10".

4. Results

(a) Twist Distribution in the Twisting and Winding Zone. Table (4.2) shows the experimental results obtained for the twist distribution between the bobbin and the traveller for different twist levels, balloon heights and traveller weights.

Table 4.2

Twist Levels in the Twisting Zone

Balloon Height inch.	Nominal Twist t.p.i.	n_1 T.P.I. 340 mg.	n_1 T.P.I. 570 mg	n_2 T.P.I. 340 mg	n_2 T.P.I. 570 mg	n_3 T.P.I. 340 mg	n_3 T.P.I. 570 mg	n_4 T.P.I. 340 mg	n_4 T.P.I. 570 mg
8	8	9	8	11.7	8.6	9.7	7.3	8	6.2
	11	11.3	11.5	12.2	13	10.3	10.8	9.6	9.5
12	8	7.1	8.2	8.6	10.7	7.9	8.6	6.4	7.2
	11	11.4	12.4	13.4	13	11.1	12.2	9.8	10.2
15	8	8.5	7.1	10.6	8.75	9.2	7.7	6.7	6.4
	11	11.4	11.9	12.2	13.1	10.9	11.1	9.8	10.3

(b) Torsional Rigidity. Fig. 4.13 represents the typical torque-twist curves for different twisting tensions, while Table 4.3 shows the results of GI_p obtained from these curves.

Table 4.3

Effect of Tension on Torsional Rigidity

Twisting Tension (gms.)	GI_p* (lb. in^2)
100	2.2×10^{-6}
226	4.6×10^{-6}
326	5.5×10^{-6}

*Average of 4 readings.

Fig. 4.15 represents the variation of the torsional rigidity with twisting tension.

(c) Bending Stiffness. Fig. 4.14 shows the typical load elongation curves for the two-ply yarn obtained at different twist levels. The calculated data obtained for EI,

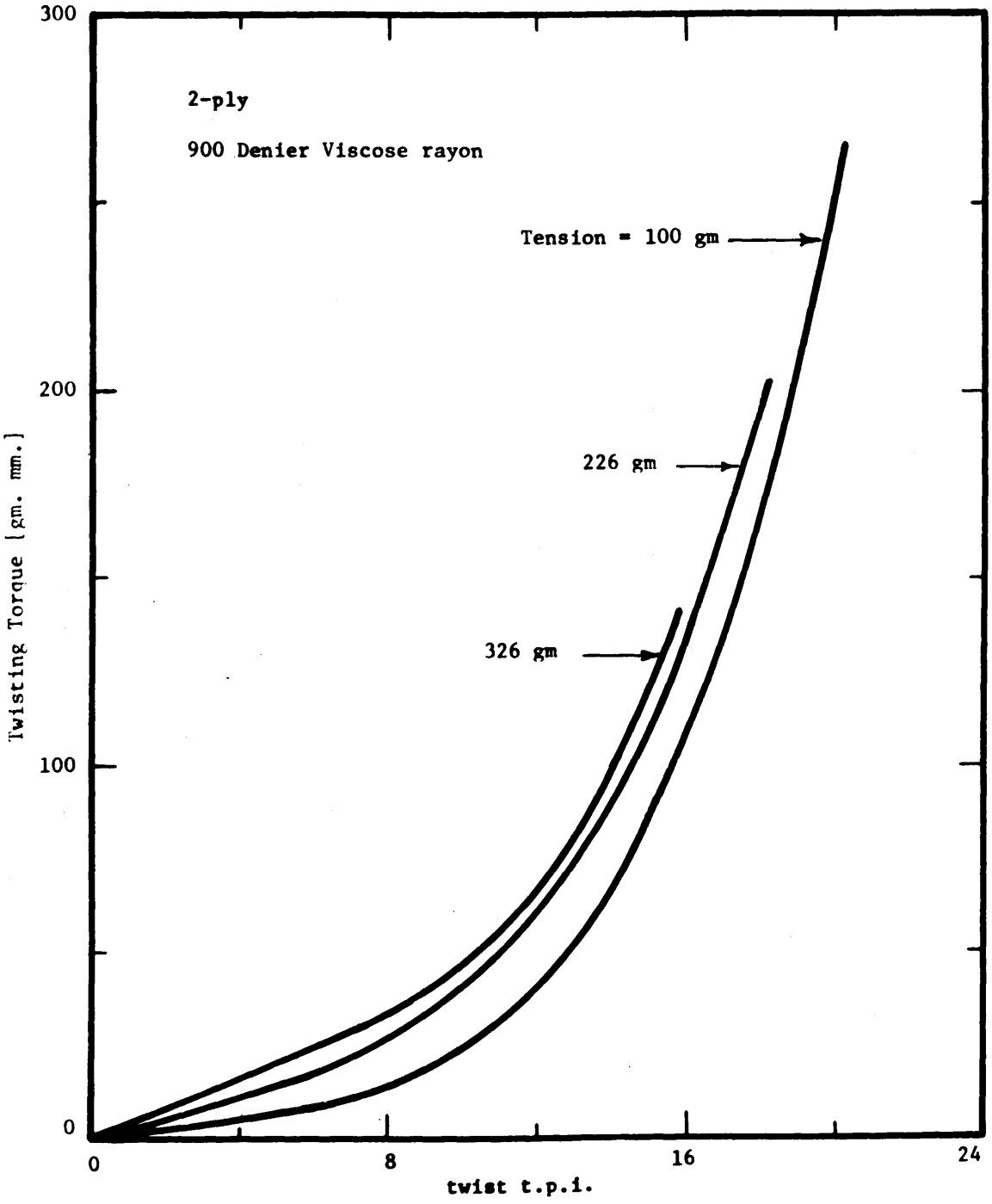

Fig. 4.13 Torque-Twist Curves

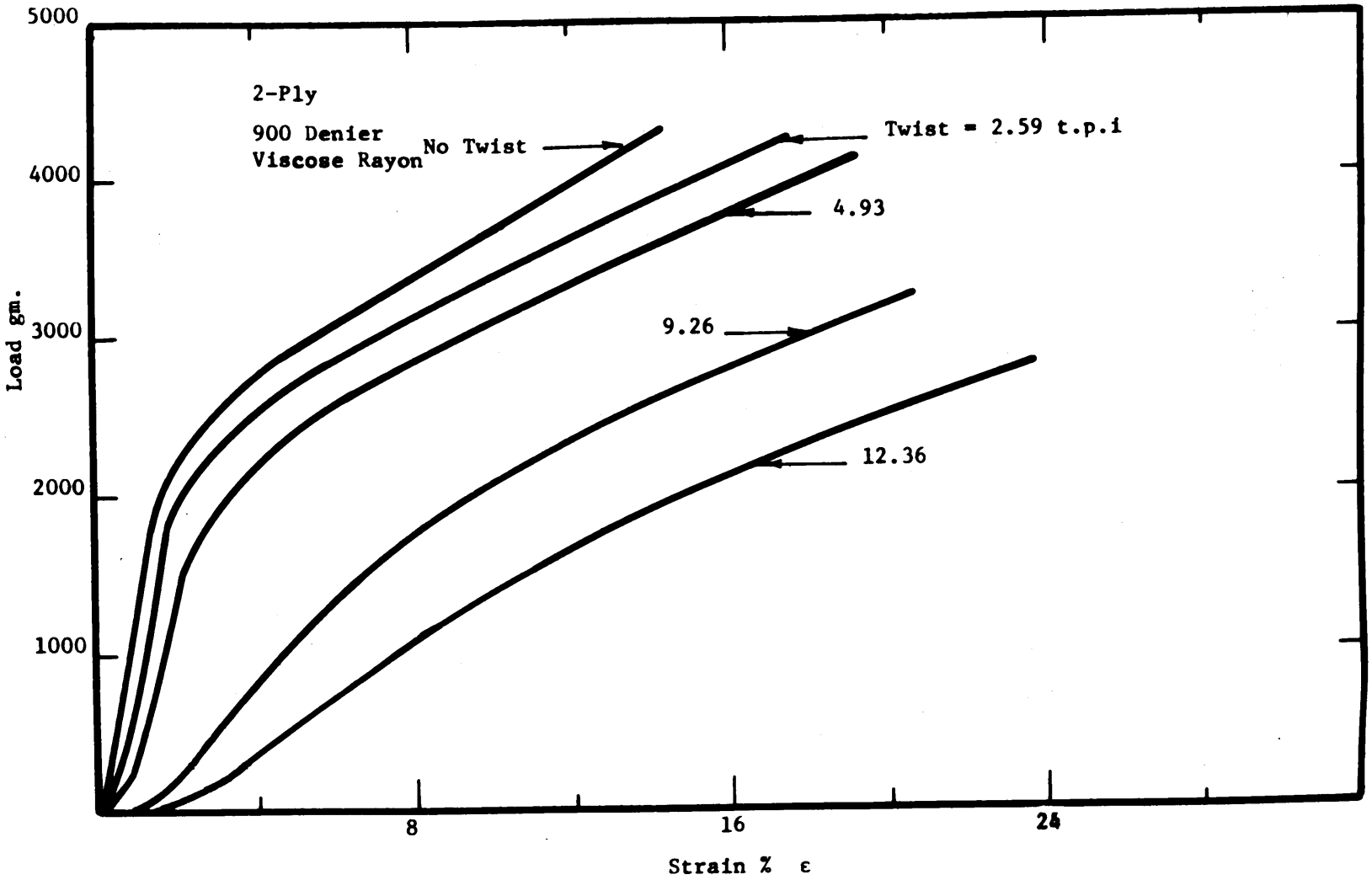

Fig. 4.14 Load-Elongation Curves

the measured yarn diameter, together with the data obtained from the load elongation curves, are shown in Table 4.4.

The values for the bending stiffness given in Table 4.4 are based on the sum of the moments of inertia of the filaments in the yarn cross-section with the single filament diameter being .0013".

Table 4.4

Effect of Twist on Mechanical Properties of a 2-Ply Viscose Rayon Yarn (900 Denier)

Twist	Diameter "	Breaking Load °	Breaking Strain	EA Initial Slope	EI*° (lb.in.^{2})
T.P.I.		Lbs.		lbs.	
2.59	.025*	91.4	17.2	239.5	239.5 x 10^{-7}
4.93	.0244	91.3	19.7	156.2	156.2 x 10^{-7}
9.26	.0237	71.6	20.6	64.7	64.7 x 10^{-7}
12.36	.0233	62.8	23.6	39.3	39.3 x 10^{-7}

*Average of 4 readings.

Fig. 4.16 shows the variation of the bending stiffness with the twist level.

5. Discussion

(a) Change of Twist Across the Traveller. Fig. 4.17 represents the variation in the ratio of twist levels across the traveller as a function of the deflection angle of the balloon at the traveller for two traveller weights. As the angle of deflection increases, the twist ratio decreases both theoretically and experimentally. This is due to the reduction in the angle of wrap around the traveller which will reduce the

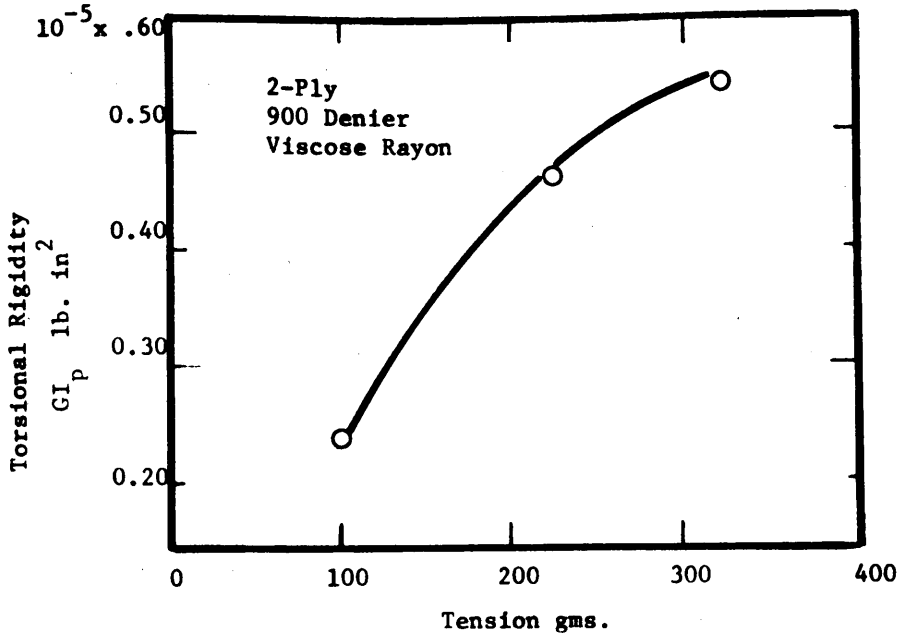

Fig. 4.15 Effect of Twisting Tension on Torsional Rigidity

(Experimental)

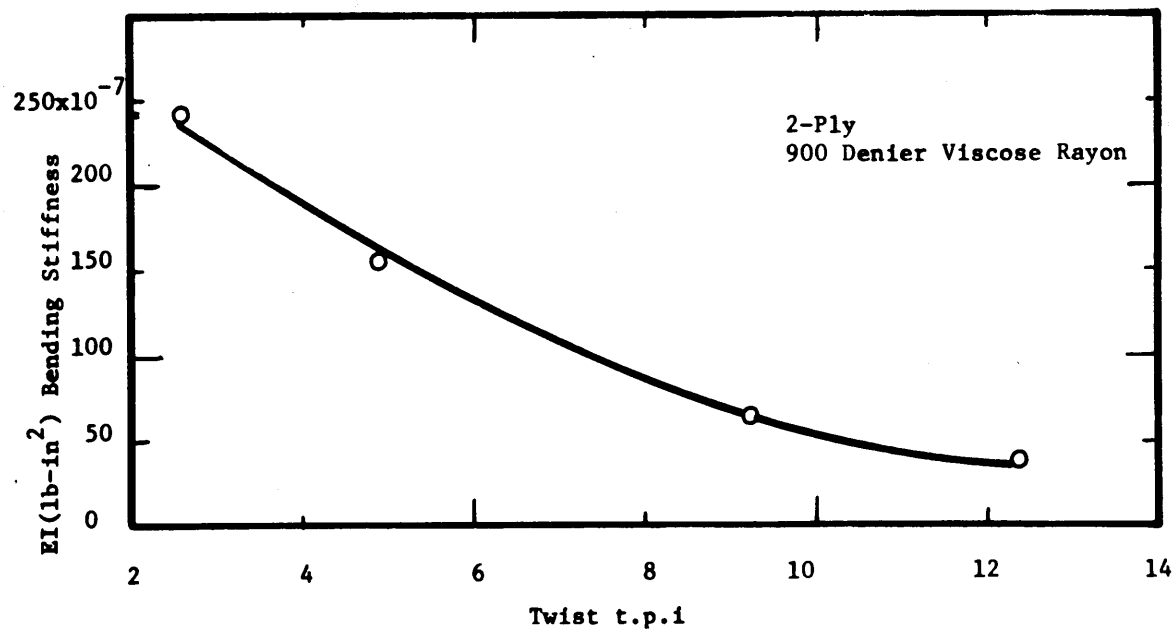

Fig. 4.16 Variation of Bending Stiffness with Twist

(Experimental)

friction, thereby causing more twist to pass across the traveller. The plot shows a fairly good agreement between the predicted equation (4.31) and the experimental results.

(b) Twist Drop along the Balloon. Fig. 4.9 shows a plot of the ratio of the twist levels at the balloon ends (top over bottom) (n_3/n_2) vs. the square of the ratio of the ring rail radius to balloon height (r^2). The ratio n_3/n_2 was plotted vs. r^2 rather than vs. the balloon height (H) in order to obtain linear relation which is unobtainable when using the balloon height as an independent variable. The theoretical relation is plotted for three different materials (V. Rayon, Nylon and Wool) with the value of the ratio of the torsional rigidity to the bending stiffness at the yarn, taken as given by Platt[32]. These values for the ratio of the torsional rigidity to the bending stiffness (ω) were measured by Platt dynamically on single fibers.

The experimental values obtained for viscose rayon show a reasonable agreement with the predicted curve for two different traveller weights. Both theory and experiment show a reduction in the twist level ratio (n_3/n_2) as the ratio r^2 increases (i.e., as the balloon height decreases.) The reduction in the twist ratio (n_3/n_2) with decreasing balloon height is due to the fact that the balloon curvature increases (thereby decreasing the twisting component of the torque at the top of the balloon.)

(c) Twist drop across the Pig Tail. Fig. 4.18 represents the variation of the ratio of the twist levels across the pig tail as a function of the balloon height. The predicted theory shows a small reduction in the twist ratio across the pig tail as the height increases. The experimental results show a reasonable agreement with the theory.

(d) Torsional Rigidity of the Yarn. Fig. 4.13 shows a representative twisting torque vs. turns of twist curve at different twisting tension levels for the two-ply viscose rayon yarn. It is apparent that whereas the curves show a reasonable linearity in the initial region, the rigidity of the material increases as the twist level increases (as indicated by the higher slope) which may be explained by a jamming of the structure at high twist levels.

Fig. 4.15 shows a plot of the torsional rigidity as a function of the twisting tension. It is clear from Figs. (4.13 and 4.15) that the torsional rigidity increases as the twisting tension increases.

(e) Bending Stiffness of the Yarn. Fig. 4.14 shows a representative load-elongation curve for the 2-ply viscose rayon plotted for different twist levels. From the curve, it is apparent that both the elastic modulus (obtained from the initial slope) and the breaking load decrease with increasing twist, while the breaking extension increases with increasing twist. Fig. 4.16 shows the variation of the bending stiffness EI with twist. Under the assumption that there is no friction between the fibers in the yarn, which has been shown to be a reasonable one, the bending stiffness of yarn is approximately equal to the sum of the bending rigidities of the individual fibers, times a factor to correct for the inclination of the fibers. The corrected fiber modulus used in this analysis includes this correction factor. This was done by dividing the value of EA, given in Table 4.4, by the sum of the fiber areas. The resulting modulus is the corrected one for the fibers in bending, since the correction for the helix angles is the same for tension and bending deformations.

In summary, the values of EI in Table 4.4 are obtained using the following relation:

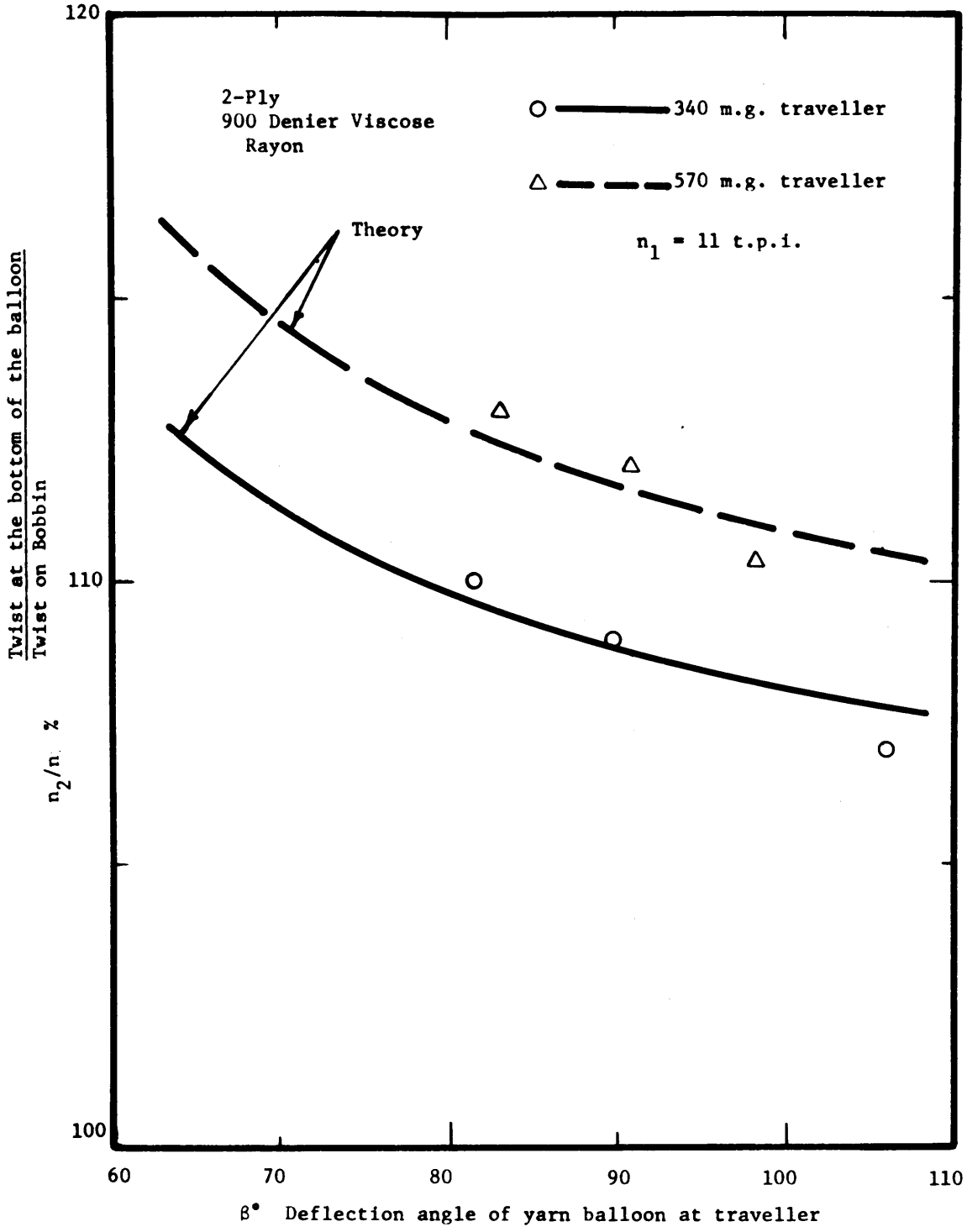

Fig. 4.17 Variation of Twist Across the Traveller
Comparison Between Theory and Experiments

$$EI = \frac{EA}{\text{total area of fibers}} \times \text{sum of moment of inertia of fibers in the yarn.}$$

6. Conclusions. The study of the twist distribution in the twisting and winding zone with the assumptions that the yarn behaves elastically on both torsion and bending shows a reasonable agreement between the theoretical predictions and the experimental results.

Both the theory and the experiments show that there is a drop of twist across both the traveller and the pig tail and between the bottom and the top portions of the balloon. The experimental results so far published in the surveyed literature have indicated a constant level of twist in the balloon zone. This appears not to be true according to both the theory and the experimental results. The values of (.11) given by Platt for the fibers agreed fairly well with those (.14) obtained from the measurements on the 2-ply structure. The assumption that the yarn behaves elastically both in torsion and in bending was proved to be a reasonable one by the linearity of the torque-turns curve (Fig. 4.13) and the load-elongation curves (Fig. 4.14) in the initial region--in particular, the following conclusions may be drawn:

(a) The twist drop across the traveller is dependent on:

(1) The deflection angle β of the balloon at the traveller. As β increases, (i.e., reduction of wrap around the traveller) the twist ratio (n_2/n_1) decreases (i.e., more twist will pass across the traveller.)

(2) The frictional torque between yarn and traveller. Depending on coefficient of friction and yarn tension--as frictional torque increases, the twist ratio (n_2/n_1)

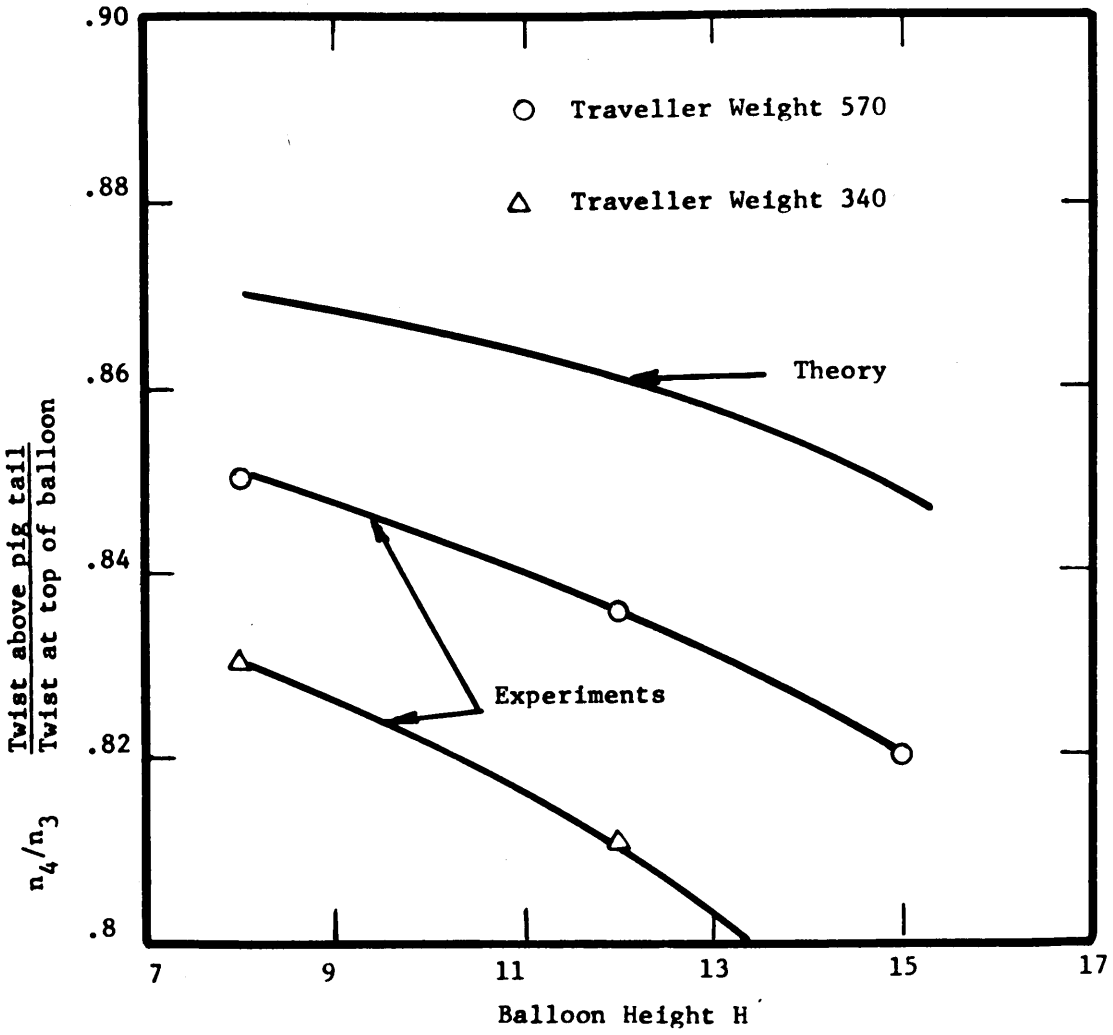

Fig. 4.18 Effect of Balloon Height
On Twist Drop Across Pig Tail

increases. Then less twist passes across the traveller.

(3) The torsional rigidity. As the rigidity increases, the twist ratio decreases.

(4) The twist level on the Bobbin (n_1). Specifically, as the final twist on the bobbin increases, the twist ratio (n_2/n_1) increases.

(b) The twist drop (n_3/n_2) along the balloon depends on:

(1) The ratio of torsional rigidity to bending stiffness; particularly as ω increases, the twist ratio increases. i.e., Twist drop along the balloon decreases.

(2) The balloon height. As the height increases, the twist ratio n_3/n_2 increases.

(c) The twist drop (n_4/n_3) across the pig tail depends on

(1) The torsional rigidity. As the rigidity increases, the twist drop decreases.

(2) The ratio of torsional rigidity to bending stiffness. As this ratio increases, the twist ratio (n_4/n_3) decreases.

(3) The frictional torque between pig tail and yarn, which depends on both the coefficient of friction and the yarn tension at the pig tail. As the torque increases, the twist ratio (n_4/n_3) decreases.

(4) The twist level (n_3) at the top of the balloon. As the twist (n_3) increases, the twist ratio (n_4/n_3) increases.

(5) The balloon height. As the height increases,

the twist ratio decreases. The variation here is a slight, almost insignificant, decrease.

(6) The deflection angle at the pig tail (ψ). As the deflection angle increases, the twist ratio decreases.

V. APPLICATION OF RESEARCH TO STAPLE FIBER SPINNING

A. Effect of Yarn Wrap around Front Roller on Draft in the Twisting Zone.

1. Introduction. During the twisting process, yarns are subjected to twisting tensions depending on different factors such as traveller weights, spindle speed, friction between yarn and machine elements, the geometry of the process and the density of the yarn to be twisted. The yarn then will be under tensile strain levels corresponding to the different tension values and resulting in a permanent elongation, or draft, of these yarns due to the slippage of the fibers in the yarns. The majority of this drafting will take place between the pig tail and the front roller nip because of the low twist levels in that area as discussed before.

The increase of the height of the twist triangle is one of the most important factors causing the increase of the draft level in the twisting zone (especially in the case of short fiber yarns). The increase of the twist triangle height is caused primarily by the increase of the angle of wrap of the roving around the bottom delivery roller.

In this section an experimental investigation will be carried out to clarify the effect of the angle of wrap around the front roller on the drafting levels taking place in the twisting zone.

2. Experiments. The following set of experiments were designed to investigate the effect of the angle of wrap (η) Fig. 5.1, of a yarn around the bottom delivery roller on drafting in the twisting zone of a ring spinning frame.

(a) Material Used. The experimental work discussed here was conducted using a worsted roving whose staple fiber distribution is given in Fig. 5.2.

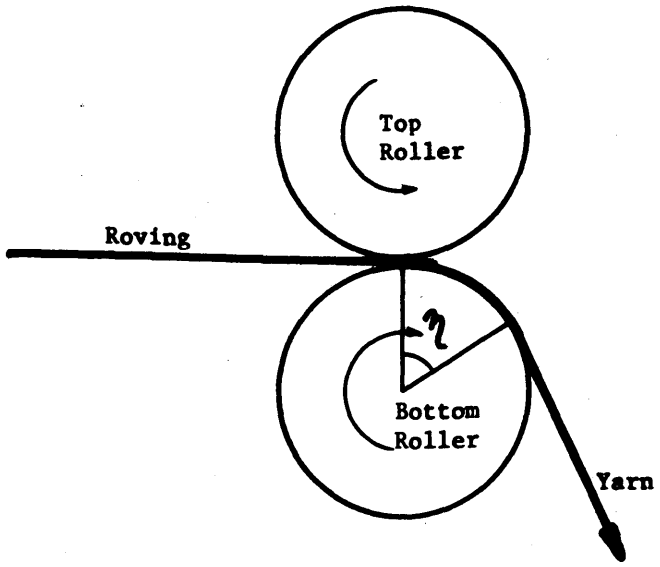

Fig. 5.1 Wrapping of Roving on Bottom Delivery Roller

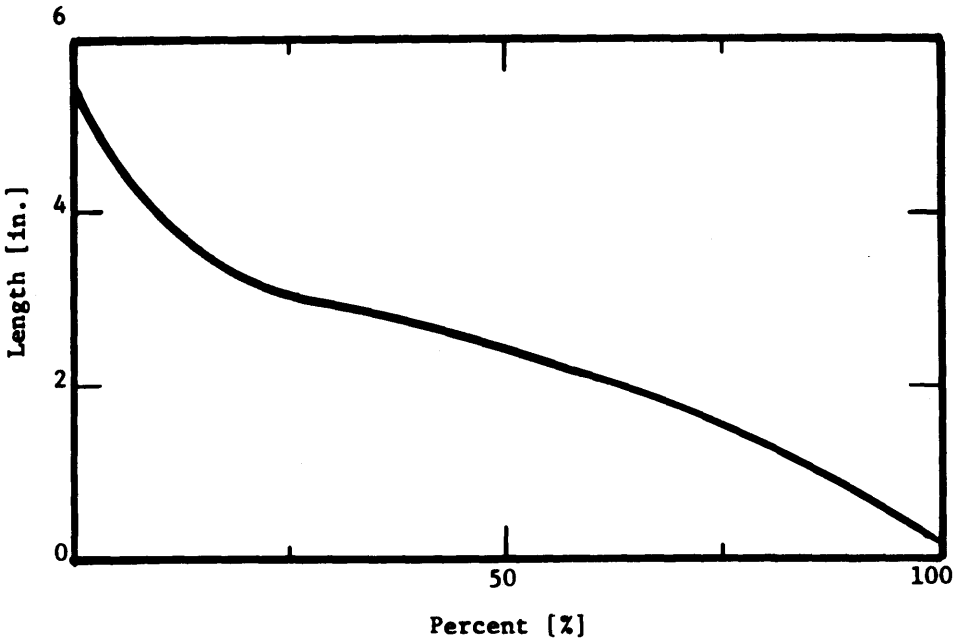

Fig. 5.2 Staple Fiber Diagram

(b) Procedure. To measure the draft taking place in the twisting zone, the following procedure was used:

(1) The roving was marked using a black marking pen at different locations equally spaced, 10" apart.

(2) The material was then twisted on the frame with no drafting taking place in the drafting zone. i.e., Between back and front roller.

(3) The twisted material was then untwisted carefully by hand so that no drafting would be introduced and the distance between each two successive marks was recorded.

(4) The ratio of the recorded measurements to the initial length (i.e., 10") was considered to be the draft taking place in the twisting zone.

(5) Ten measurements were made in each case.

c. Twisting Conditions. The conditions for the experiments were:

Balloon height	15"
Spindle Speed	2620 r.p.m.
Nominal Twist	6.4 t.p.i.
Angles of Wrap	15, 70 and 100°
(Obtained by tilting the drafting unit)	
Traveller Weights	159, 570 and 910 mgs.

3. Results. Table 5.1 shows the experimental results obtained for the draft in the twisting zone where the draft is defined by the formula

$$\text{Draft} = \frac{\text{Final untwisted length}}{\text{Original length before twisting}}$$

Table 5.1

Change in Draft in the Twisting Zone with Traveller Weight and Angle of Wrap at Bottom Delivery Roller

Angle of Wrap °	Traveller Weight m.g.	Draft
	159	1.004
10	570	1.014
	910	1.025
	159	1.018
70	570	1.03
	910	1.046
	159	1.039
100	570	1.051
	910	1.061

4. Discussion. Figs. 5.3 and 5.4 represent the variation of draft with both traveller weight (tension) and angle of wrap around the bottom delivery rollers. From the plot it is apparent that the draft increases with both increasing wrapping angle and twisting tension (traveller weight).

(a) Effect of Twisting Tension. Two effects cause an increase of draft as the twisting tension increases, i.e.

(1) The effect due to high tension, i.e. as the tension increases, the strain (or fiber slippage) will increase.

(2) The effect of twist level between the pig tail and the front roller. Twist level will decrease as tension increases.

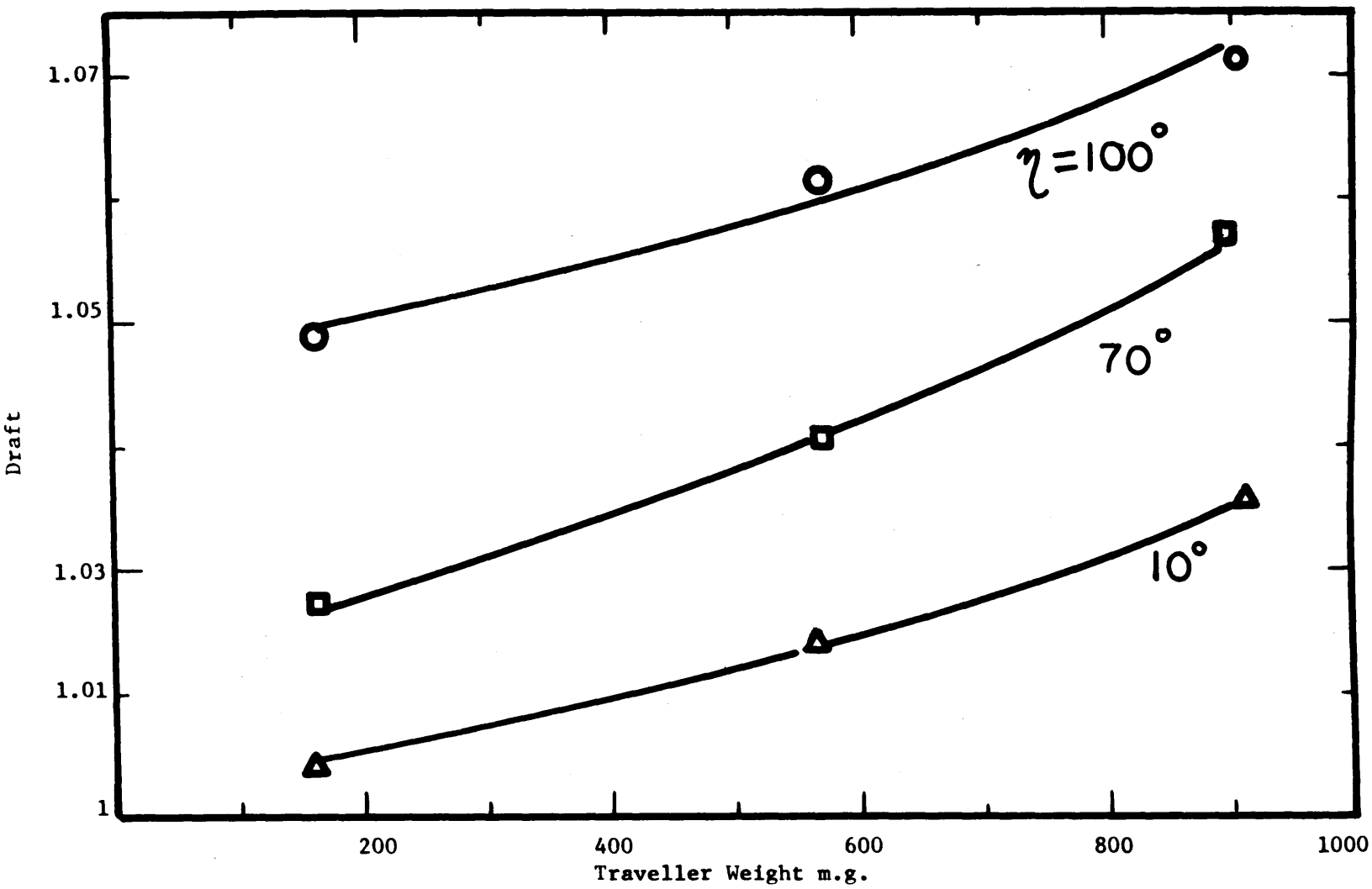

Fig. 5.3 Effect of Traveller Weight on Drafting in the Twisting Zone

(Experimental)

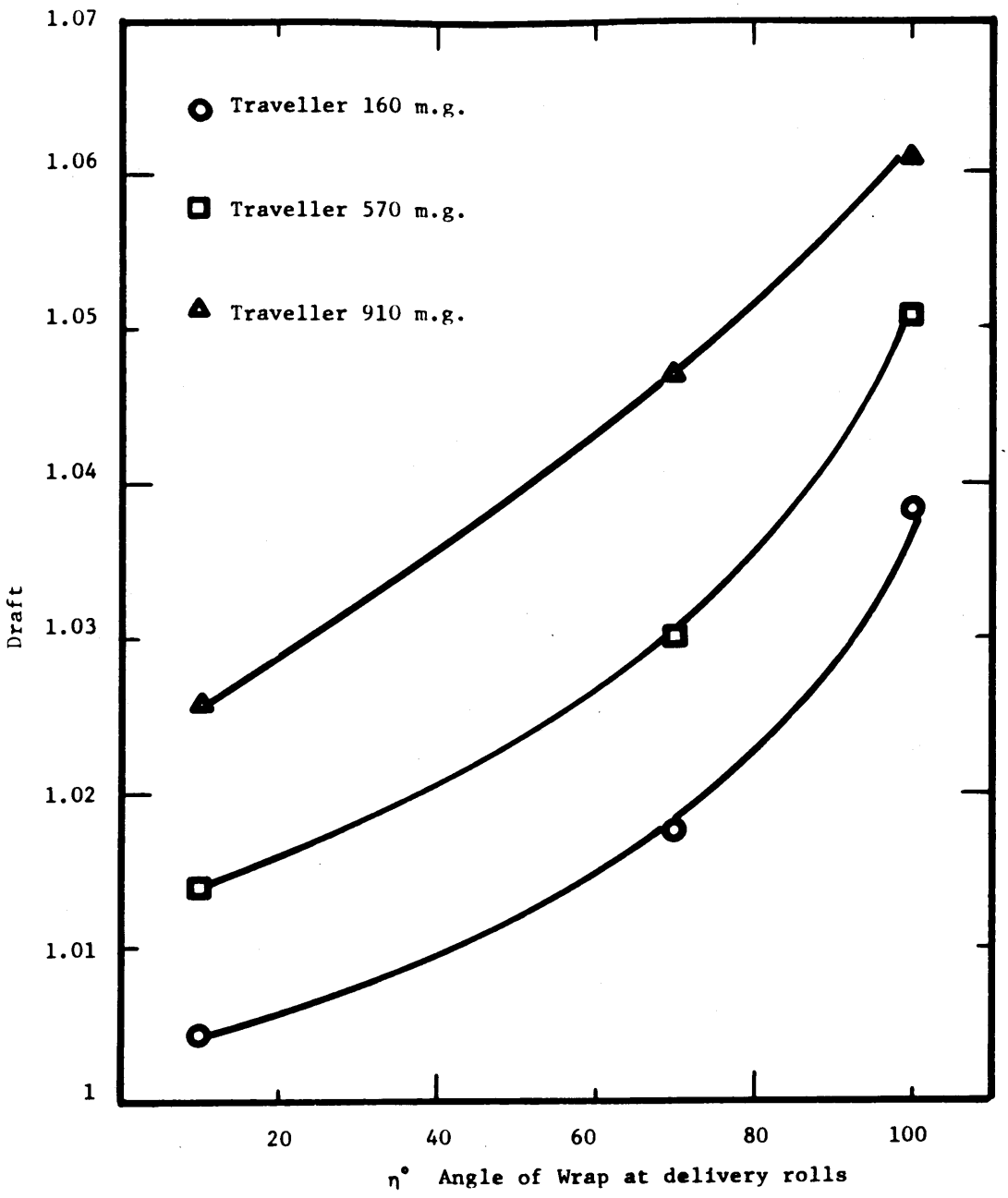

Fig. 5.4 Effect of Angle of Wrap on Draft in Twisting Zone

(Experimental)

The increase in tension will cause less twist to propagate past the pig tail to the front roller, thereby reducing the strength of the yarn in that zone and increasing the height of the twist triangle. The decrease of yarn strength and the increase in the twist triangle height will result in increasing extensions at high tension levels, thereby increasing the amount of draft.

(b) The Effect of Angle of Wrap in Draft. The increase of draft with increasing angle of wrap as shown in Fig. 5.4 follows from the fact that the twist triangle height will increase due to the friction between the bottom roller and the roving. The increase of the twist triangle which corresponds to an increase of the untwisted length of the roving, will cause an increase of the draft taking place in this zone.

5. Conclusions. The study of the draft level taking place in the twisting zone shows that there is a definite relation between angle of wrap, twisting tension and draft. In general, it may be concluded that the factors governing the draft level taking place in the twisting zone are:

(a) Angle of Wrap. As the angle of wrap increases the draft level will increase.

(b) Twisting Tension. The increase in twisting tension will result in increasing draft in the twisting zone.

(c) Twist Level. As the twist increases, the cohesive forces between the fibers in the twisted yarn will increase, causing a reduction of the draft levels taking place in the twisting zone.

From the above, the following general conclusions may be drawn:

Soft spun yarns will be drafted more than hard

twisted yarns, which will lead to an increase in yarn count (cotton system) from the originally estimated ones.

In spinning short staple fiber yarns with high angle of wraps, high draft levels will occur. Even with low wrap angles, draft will be higher in the case of short staple fiber yarns than in the case of long staple fiber yarns. This is due to the fact that less twist will flow from the balloon past the traveller in the case of short staple yarns.

B. Twist Distribution in the Twisting Zone as a Cause of End-Breakage.

1. Introduction. End-breakages rates in ring spinning frames are of great importance in the textile industry and it is necessary to minimize end-breakage to increase both the quality of yarn produced and the efficiency of the process. The problem of end-breakage is known to all spinners, most of whom are aware of the different factors affecting its rate.

Most of the research done on end-breakage was based on statistical analysis considering the irregularity in the yarn, rather than a mechanical analysis. It is understood that a break will occur when the tension applied to the yarn exceeds its strength. It is also known that the twisting tension levels in ring spinning frames are far below the strength of the yarn produced, hence end-breakages would take place in the region where the yarn is weakest during spinning. The yarn in the spinning zone is weakest between the pig tail and the front roller because of its low twist level in that region.

Misono[29] considered the region between the pig tail and the front roller to be the critical area where end-breakage will occur. By the use of a mechanically oscillating pig tail, he increased the twist level above the pig tail, hence decreasing the end-breakage rate.

Gessner[31] experimentally studied the twist distribution in the twisting zone and considered the reduction in twist level above the pig tail to be the main cause of end-breakages.

In this section the use of the results ob tained on the twist distribution in Chapter IV will be correlated with both the theory for yarn tension derived by DeBarr, and the variation of yarn strength with twist, in order to establish a sound understanding of where end-breakages occur and the factors affecting them.

2. Balloon Theory

(a) Nomenclature

A	= Maximum radius of balloon
C	= Centrifugal force of traveller
d	= Yarn diameter
H	= Balloon height
m	= Linear density of yarn
R	= Ring radius
T_a	= Tension at balloon apex including air drag effect
T_{a_1}	= Tension at balloon apex excluding air drag effect
T_b	= Tension in balloon at the traveller excluding air drag effect
T_{wA}	= Effect of air drag on winding tension
T	= Total winding tension
T_{w_1}	= Winding tension excluding air drag effect
α and γ	= as defined in Fig. 5.5
ϕ	= Angle of wrap of yarn around pig tail
η	= Angle of wrap of yarn around traveller
Ω	= Angular velocity of traveller
μ	= Coefficient of friction between ring and traveller
μ_1	= Coefficient of friction between traveller and yarn
μ_2	= Coefficient of friction between yarn and pig tail.

The balloon theory obtained by DeBarr[11] is considered to be of great practical value because of its simple equations, to obtain the yarn tension in the twisting zone. This theory had been evaluated experimentally by the writer[6] and there was a

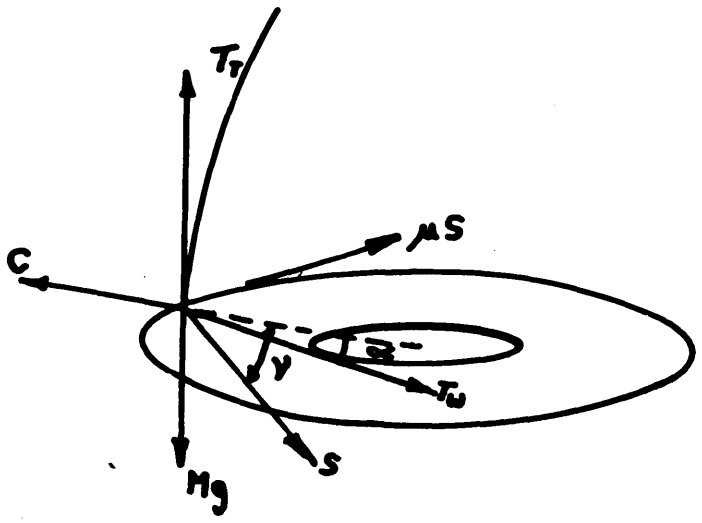

Fig. 5.5 Forces Acting On Traveller
From Ref. 11.

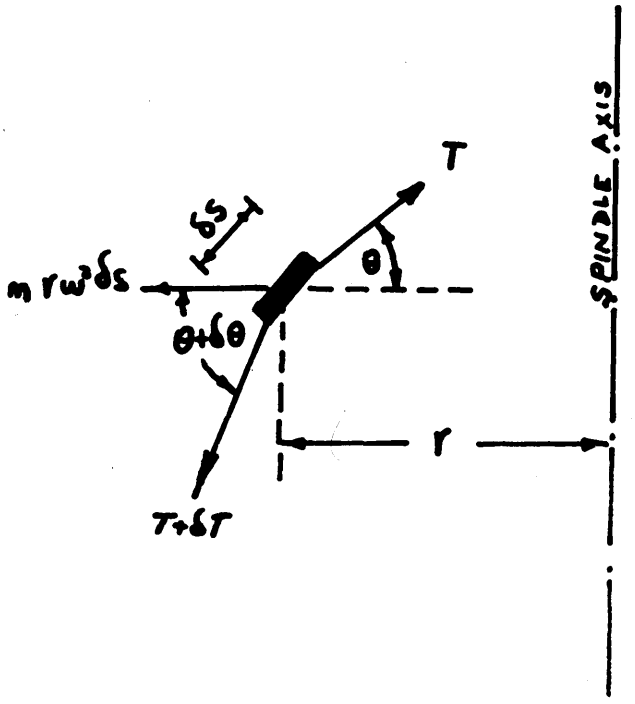

Fig. 5.6 Forces Acting on an Element
Of Yarn in the Balloon
From Ref. 11

reasonable agreement between it and the experimental results obtained.

(b) Calculation of Yarn Tension. The forces acting on both the traveller and an element of the yarn in the balloon are shown in Figs. 5.5 and 5.6. DeBarr showed that the winding tension between the bobbin and the traveller (neglecting air drag) is given by:

$$T_{w_1} = \frac{\mu C}{\sin\alpha\cos\gamma + \mu\cos\alpha} \qquad 5.1$$

and the tension T_b in the balloon at the traveller is then given by

$$T_b = T_{w_1}\, a \qquad 5.2$$

where

$$a = e^{-\mu_1 \eta} \qquad 5.3$$

and

$$\sin\gamma = \frac{a\mu}{\sin\alpha} \qquad 5.4$$

Substituting 5.1 into 5.2 yields that

$$T_b = \frac{a\mu C}{\sin\alpha\cos\gamma + \mu\cos\alpha} \qquad 5.5$$

The author showed that the tension T_{a_1} at the balloon apex is given by

$$T_{a_1} = T_b + 1/2\ m\,\Omega^2\,R^2 \qquad 5.6$$

and using Equations 5.5 and 5.6 gets

$$T_{a_1} = \frac{a\mu C}{\sin\alpha\cos\gamma + u\cos\alpha} + 1/2\ m\,\Omega^2\,R^2 \qquad 5.7$$

Considering air drag, DeBarr found that the increase in twisting tension due to air drag is given by

$$T_{w_A} = c_1 \rho_a d A^3 \Omega^2 H / 4R\sin\alpha \qquad 5.8$$

Combining Equations 5.1 and 5.8, then, the total winding tension T_w is given by

$$T_w = \frac{\mu C}{\sin\alpha\cos\gamma + \mu\cos\alpha} + \frac{c_1 \rho_a d A^3 \Omega^2 H}{4R\sin\alpha} \qquad 5.9$$

from which, together with Equations 5.2 and 5.6, the tension at balloon apex is given by

$$T_a = a\left\{\frac{\mu C}{\sin\alpha\cos\gamma + \mu\cos\alpha} + \frac{C_1 \rho_a d A^3 \Omega^2 H}{4R\sin\alpha}\right\} + \frac{1}{2} m \Omega^2 R^2 \qquad 5.10$$

and then the tension in the yarn between the pig tail and the front roller is given by

$$T_o = b\left\{a\left[\frac{\mu C}{\sin\alpha\cos\gamma + \mu\cos\alpha} + \frac{C_1 \rho_a d A^3 \Omega^2 H}{4R\sin\alpha}\right] + \frac{1}{2} m \Omega^2 R^2\right\} \qquad 5.11$$

where

$$b = e^{-\mu_2 \phi} \qquad 5.12$$

The contribution of air drag to yarn tension was found by DeBarr to be in the order of 12% in practical spinning. The author also found that the effect of centrifugal force in the balloon on yarn tension to be negligible (in the order of 1-3%).

Fig. 5.7 represents a typical plot of yarn tension in the twisting zone for the following conditions:

Spindle speed = 8,000 r.p.m.
Traveller weight = 570 mg.
Balloon height = 12"
Ring diameter = 5"
Bobbin diameter = 1.75"

Using the balloon theory by DeBarr and the expressions for twist distribution derived in the preceding chapter, one can obtain the theoretical distributions of both twist and tension in the yarn in the twisting zone. If the strength twist curve for a yarn to be twisted is known, then the strength distribution along the yarn in the twisting zone

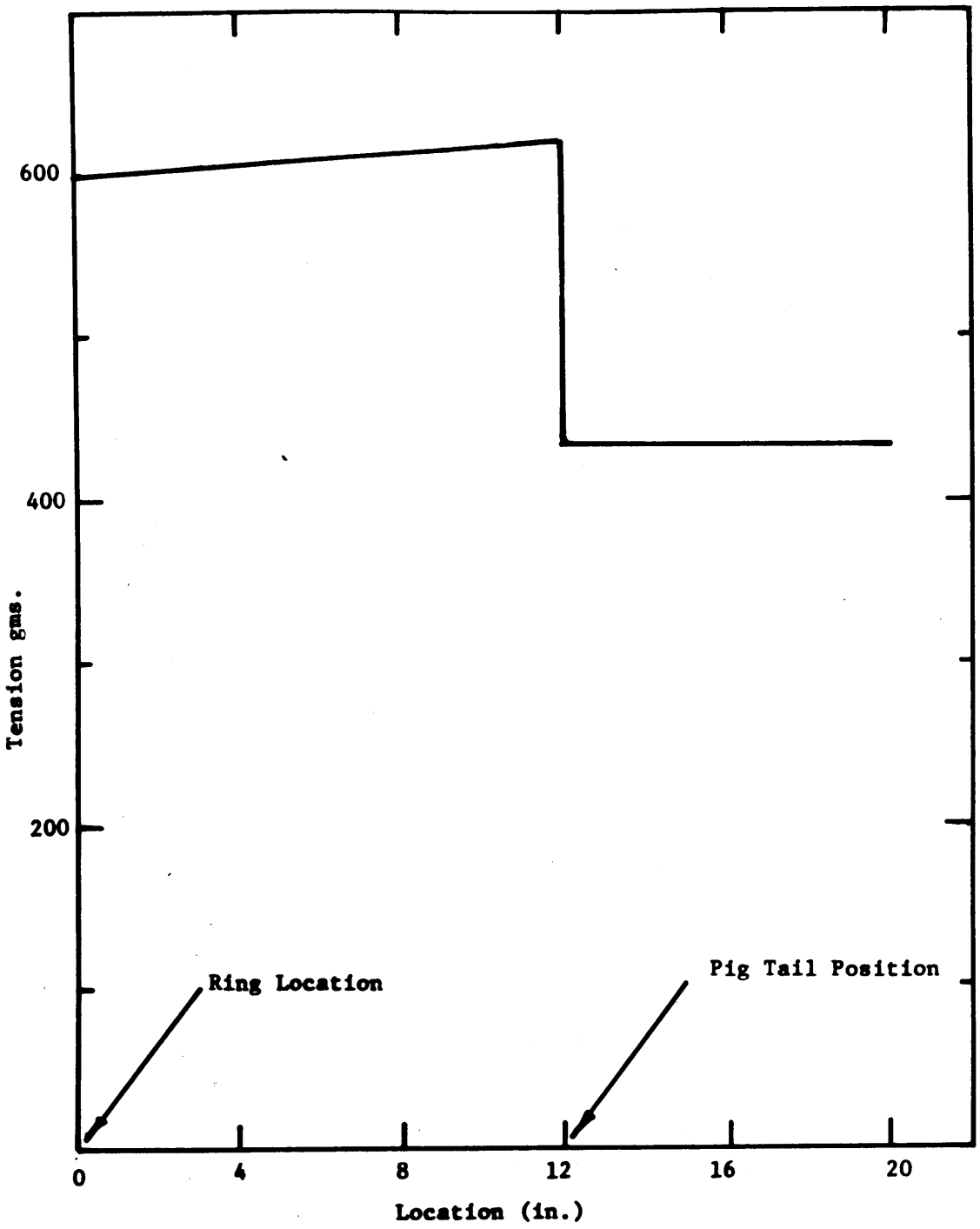

Fig. 5.7 Tension Distribution in Twisting Zone (Theory)

can be obtained by the use of both the twist distribution and the twist-strength curve.

The ratio of strength to tension at any point is the safety factor for the yarn in the twisting zone. If this factor is always greater than unity (when twisting uneven yarns) end breakage will not occur and if it becomes less than one (i.e., the yarn strength is lower than the tension) at any point, end breakages will take place at that point. So, it is clear that the greater this factor is above one, the safer the yarn will be.

In the following experimental work to be discussed, the strength-twist curves for someyarns will be measured and the strength distribution curves will be obtained from it, and a comparison between tension and strength will be made to find the critical region where end breakage may occur.

3. Experiments.

(a) Material Used. During the course of this investigation two different rovings were used. The rovings will be identified in this work by #1 and #2, with #1 being a worsted (280 Tex) roving and #2 a woolen (180 Tex) roving. Fig. 5.8 represents the staple fiber distribution for both rovings #1 and #2.

(b) Procedure. Both roving #1 and #2 were twisted to different twist levels--namely, 1.87, 2.7, 3.75, 5.08, 7.61, 9.24 and 13 t.p.i. on the ring spinning frame under the following conditions with the draft in the frame set equal to unity

Spindle speed 8,000 r.p.m.

Traveller weights 100, 159, 340, 570 and 910 mgs.

Roving #1 was twisted with the heavier travellers, since it is much higher in density and stronger than roving #2.

The load-elongation curves were obtained for 10 specimens (10" long) at each twist level and the breaking load was recorded on the Instron tensile testing machine at a strain rate of 10%/min.

4. Results. Table 5.2 shows the experimental results obtained for the breaking load and the diameter for both rovings (#1 and #2) as a function of twist. Fig. 5.9 represents the variation of yarn strength with twist for both rovings #1 and #2. Fig. 5.10 represents the twist distribution as obtained from Equations 4.45 and 4.49, Chapter IV, along the yarn in the twisting zone for roving #1. The plot shows that twist drop along the balloon is 20% and across the pig tail is 20%. The tension and the strength distributions in the twisting zone are also shown in Fig. 5.10. The tension distribution is obtained from the balloon theory

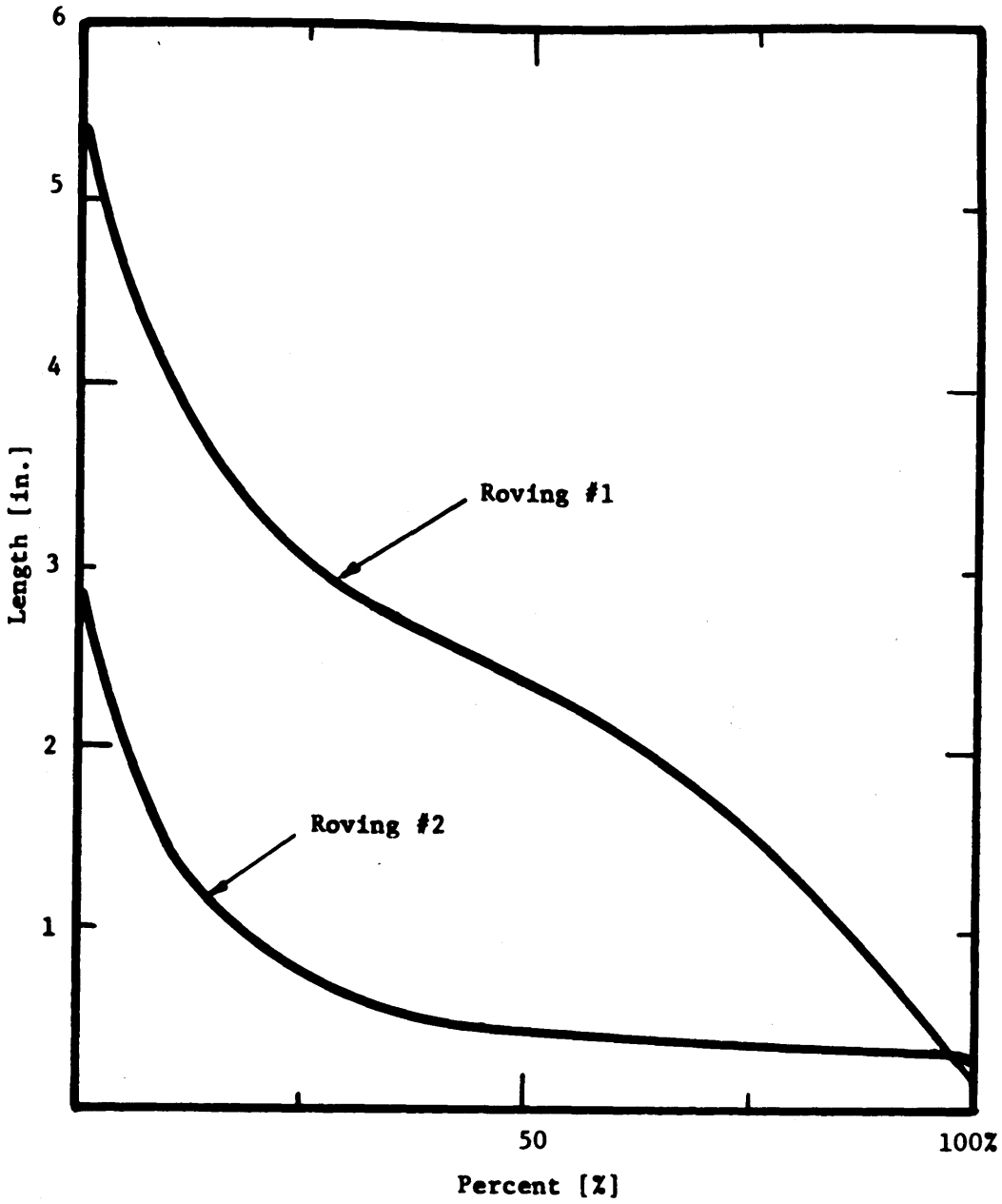

Fig. 5.8 Staple Fiber Distribution

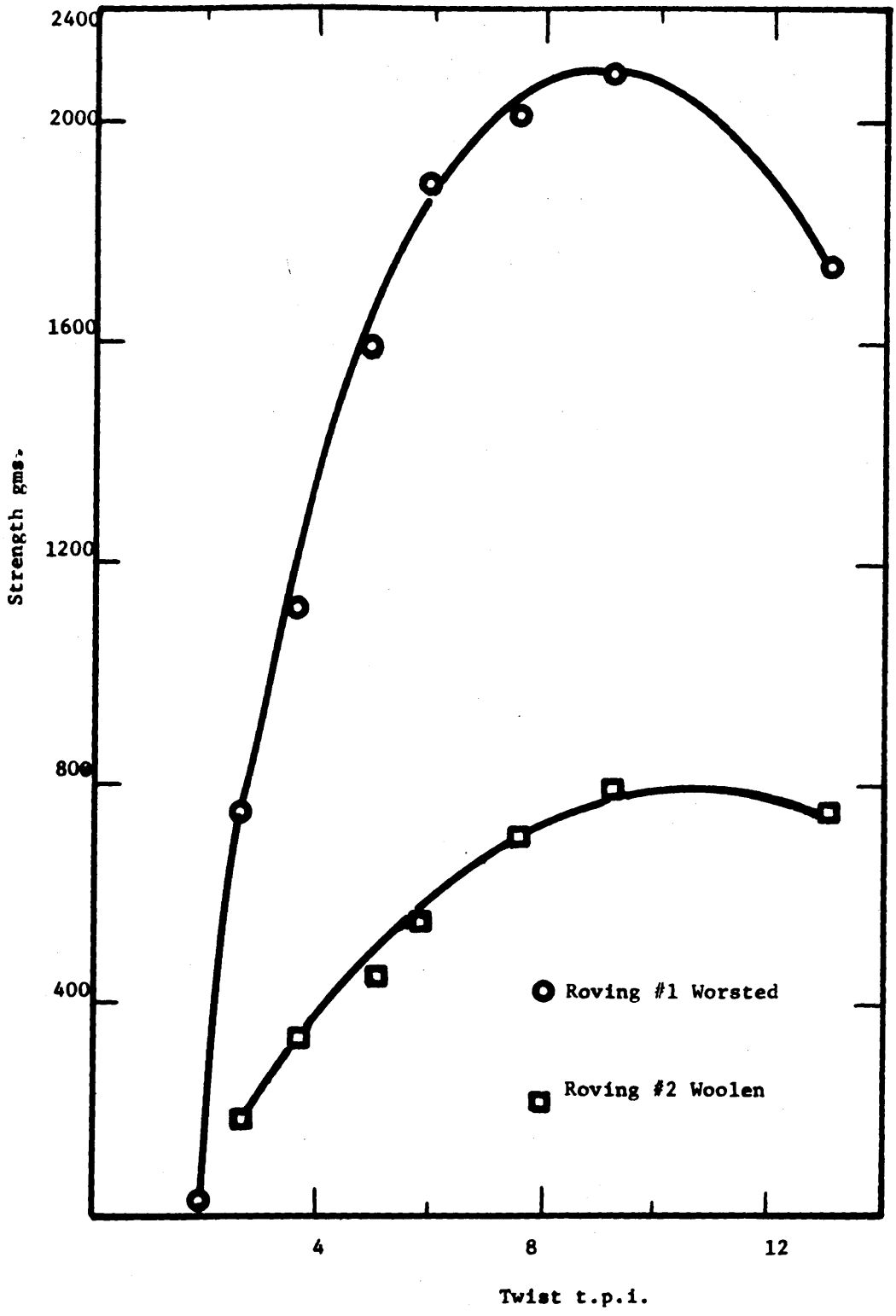

Fig. 5.9 Variation of Strength With Twist

(Experimental)

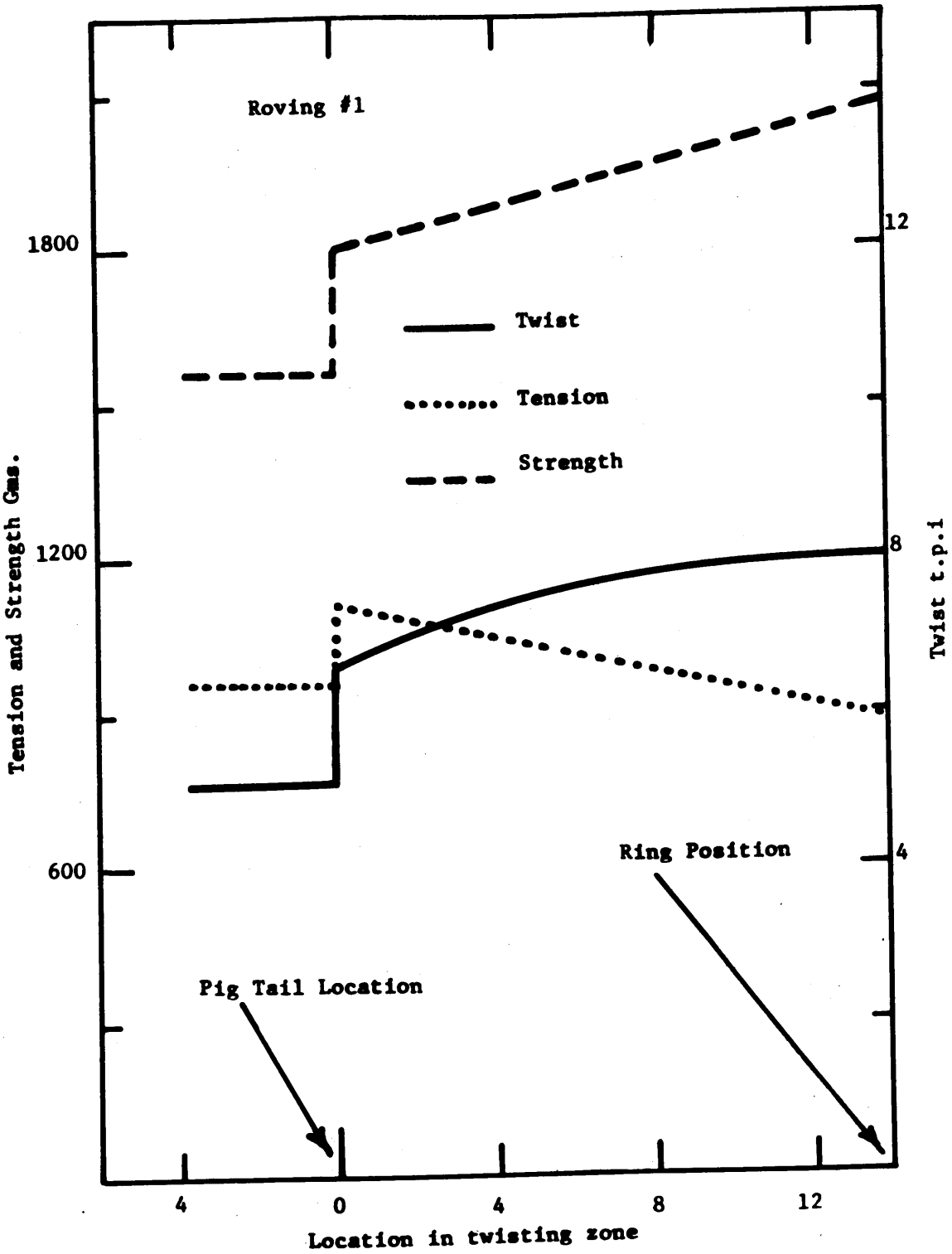

Fig. 5.10 Distribution of Twist, Tension and Strength in the Twisting Zone

by DeBarr, i.e., Equation 5.11. The strength distributions are obtained from the twist distribution and the strength-twist curves, Fig. 5.9, by simply recording the yarn strength corresponding to any twist level in the twisting zone.

Fig. 5.11 represents the same results for roving #2. The drop along the balloon in this case is as in roving #1 (i.e., 20%) while the drop across the pig tail is 25%.

Table 5.2

Variation of Breaking Strength and Diameter with Twist for Woolen and Worsted Rovings

Twist	Yarn Diameter		Breaking Load Gms.	
t.p.i.	Roving #1	Roving #2	Roving #1	Roving #2
1.87	.039		140	
2.7	.037	.04	800	190
3.75	.029	.032	1000	330
5.08	.03	.031	1600	470
5.86	.026	.031	1900	570
7.61	.026	.027	2000	700
9.24	.024	.024	2100	850
13	.023	.022	1750	780

5. Discussion. Fig. 5.9, representing the variation of spun yarn strength with twist, shows that for both rovings #1 and #2, the strength rises with twist until it reaches a maximum and then falls off. The rise of strength is due to the build-up of lateral yarn pressure, hence of cohesive forces between the fibers with increasing twist. The reduction in strength at higher twists is due to the excessive strains (both in torsion and in tension) which occur in the highly twisted state.

Figs. 5.10 and 5.11 represent the twist-tension and strength distributions in the twisting zone for both the

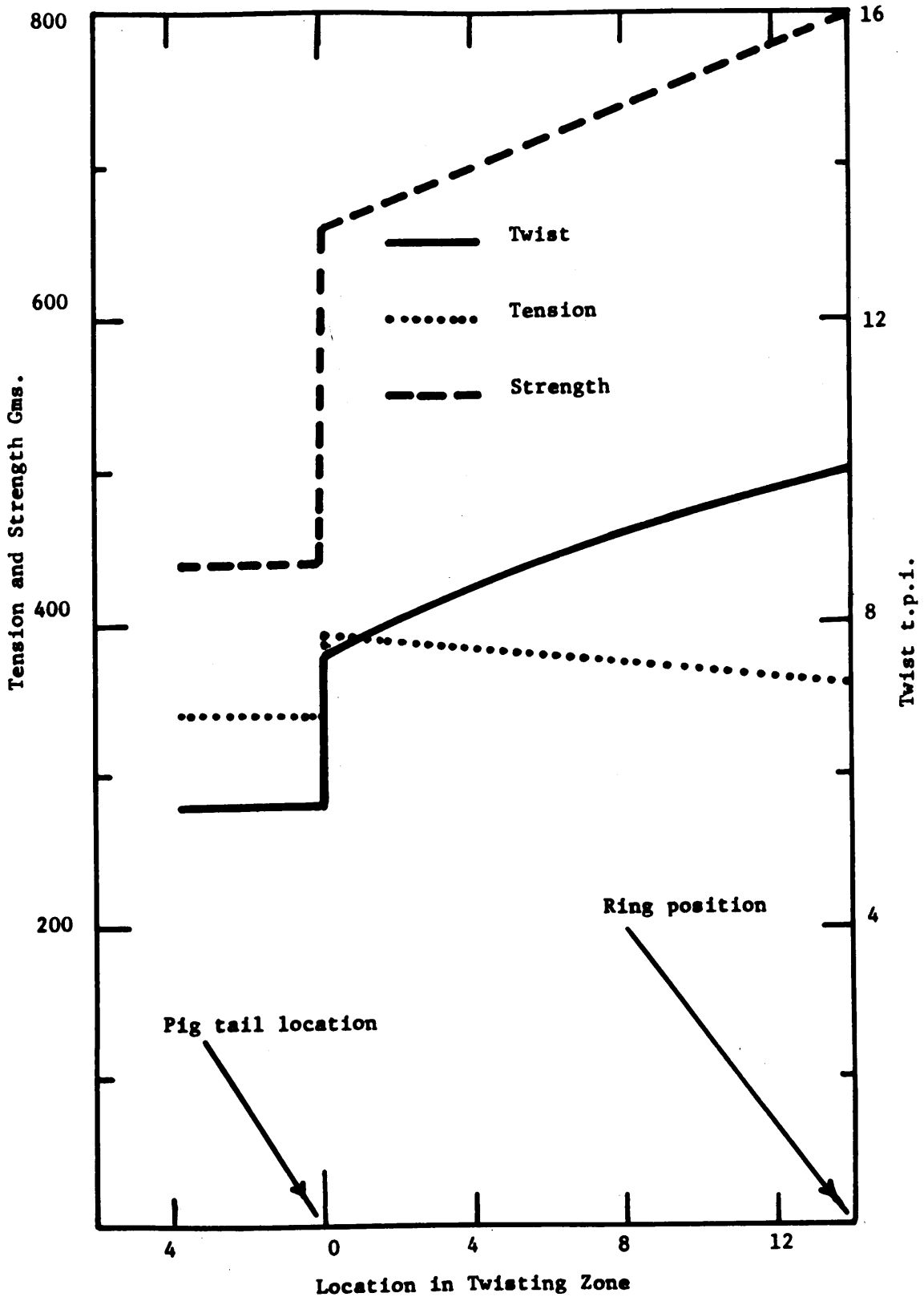

Fig. 5.11 Distribution of Twist, Tension and Strength in the Twisting Zone

worsted (#1) and the woolen (#2) rovings. The twist drop across the pig tail is higher for the woolen than for the worsted roving because of the high friction between the former and the pig tail due to the fact that it is more hairy. From the comparison between strength and tension it is evident that the critical tensile region for both rovings is located between the pig tail and the front roller. The ratio of strength to tension in that region is 1.3 for the woolen and 1.65 for the worsted roving. As discussed before, as this ratio approaches the value of one, the rate of end breakages will increase.

If the roving under consideration is uniform, the ratio of strength to twist will change only due to changes in the process variables as discussed in Chapter IV, with the main change being due to balloon height. Recall that the drop in twist along the balloon will increase as the balloon height decreases. However, since in practical spinning rovings have a certain degree of irregularity, the ratio of strength to tension will change with time as the roving being twisted varies in linear density. Furthermore, there will be a tendency towards twist concentration in the thin spots because of their lower torsional rigidity.

Rovings in general have both long and short term irregularity. These irregularities will affect the distribution of twist level leading to low twist in thick spots in the rovings. As a result end breakages will occur at these thick spots more readily than at the thin spots.

6. Conclusions. The study of twist distribution in the twisting zone as a cause of end breakage provides a sound understanding on the mechanisms of end breakage. The use of both twist distribution and balloon theories, together with the strength-twist curve to obtain the ratio of strength to

tension of the yarn in the critical region (between pig tail and traveller) may be used as a tool to predict end breakage. In particular, the following conclusions may be drawn:

(a) End breakage will occur between the pig tail and the front roller where the twist level is low.

(b) End breakages will occur more in short balloons rather than in tall ones.

(c) Rovings with long term variations will have more end breakage rates than one with short term variations.

(d) End breakage rates are higher when twisting short staple fiber yarns than when twisting long staple yarns.

(e) The increase in deflection of yarn at the pig tail will reduce the twist level above the pig tail, therefore reducing yarn strength and increasing end breakage rates.

VI. SUMMARY, CONCLUSIONS AND RECOMMENDATIONS

A. Summary and Conclusions. This investigation was basically concerned with the understanding of the mechanics of twist insertion on ring frames and the factors influencing it. The action taking place in the twisting zone between the front roller nip and the wind-up point on the bobbin may be summarized as follows:

As the fibrous ribbon is delivered by the front rolls it forms a twist triangle. In this triangle the interchange of fiber position takes place, i.e., fiber migration.

As twist is inserted by the traveller, the twist level will vary along the balloon and will drop substantially across both the traveller and pig tail. While winding takes place, twist will vary between the top and bottom portions of the bobbin due to the ring rail motion.

These actions were investigated both theoretically and experimentally and the following general conclusions may be drawn:

(1) Geometry of the Twist Triangle.

(a) The height of the twist triangle is dependent on twist, tension, the mechanical and physical properties of the fibers, and the ribbon width. Specifically, it was found that the twist triangle height increases with decreasing twist and fractional modulus (at constant twisting tension) and it increases with increasing tension.

(b) Fiber migration will cause the twist point to oscillate sideways about the line passing through the center of gravity of the cross-section of the ribbon.

(c) The apex angle of the twist triangle measured

at maximum triangle height is equal to twice the helix angle measured on the twisted yarn.

2. Fiber Migration. The study of the migratory behavior of a 7-ply structure shows that:

(a) The frequency of migration for an open structure increases with decreasing twisting tension, increasing twist and decreasing ribbon width.

(b) For a closed structure the frequency of migration depends to a great extent on the spring constant of the matrix of fibers surrounding the filament occupying the center of the ply structure and (as for the case of open structures) the frequency of migration increases with decreasing tension, increasing twist level and decreasing spring constant.

(c) Using this model, it was experimentally verified that the mechanisms proposed by the theory of migration (development of slack for an open structure and initiation of static buckling for a closed structure) are indeed valid.

3. Twist Variation in the Yarn on the Bobbin. The investigation of twist variation on the bobbin showed that the twist level is higher at the top of the bobbin than at the bottom depending on (1) the ring rail speed, (2) the nominal twist, (3) the ratio of twist in the balloon to twist in the bobbin and the acceleration of the ring rail at both the end and the beginning of the stroke.

4. Twist Distribution in the Yarn in the Twisting and Winding Zone. The twist level in the yarn was found to vary across the traveller, along the balloon and across the pig tail as follows:

(a) Ratio of Twist Levels $\left(\frac{\text{balloon side}}{\text{bobbin side}}\right)$ Across the Traveller. This ratio decreases as the deflection angle

of the balloon increases, as the twisting tension decreases, as the torsional rigidity increases and as the coefficient of friction between the yarn and the traveller decreases.

(b) Ratio of Twist Levels $\left(\frac{\text{At top of balloon}}{\text{At bottom of balloon}}\right)$ at the Balloon Ends. The ratio increases as both the ratio of the torsional rigidity to the bending stiffness of the yarn and the balloon length increase.

(c) Ratio of Twist Levels $\left(\frac{\text{Front roller side}}{\text{Top of the balloon}}\right)$ Across the Pig Tail. The ratio increases with a decrease in torsional rigidity of the yarn, the ratio of torsional rigidity to bending stiffness, the coefficient of friction between yarn and pig tail, the twisting tension, the deflection angle of yarn at the pig tail and the yarn diameter.

B. Recommendations for Future Work

In order to complete the improvement and the understanding of the mechanics of twist insertion in practical spinning, additional work should be undertaken in the following areas:

(1) Fiber Migration

(a) Predict theoretically and verify experimentally the frequency of migration of the components of a 7-ply blended structure.

(b) Study the migratory behavior of a 19-component twisted structure as a step toward a better understanding of multicomponent yarns.

(c) Complete the theoretical work started in this thesis on the mechanism of migration in closed structures, the factors affecting the spring constant of a fiber assembly should be studied both theoretically and experimentally.

(d) Find the effect of dynamic buckling (or snapback) on the migration behavior of spun yarns, the snapback of a filament supported by an elastic foundation should be the subject of further investigation.

(2) Twist Distribution in the Twisting and Winding Zone.

(a) In order to improve the theory obtained for the twist distribution in the twisting zone, the analysis should be carried out taking into account viscoelastic behavior of yarns as they are being spun.

(b) The theory for the twist distribution in the twisting zone obtained in this thesis should be used as a tool to predict end breakage rates in practical spinning conditions. Statistical considerations relating to weak spot occurrence

should be included.

(c) The effect of both long and short term roving variations on the twist distribution in the twisting zone should be investigated.

VII. APPENDICES

Appendix A. Variation of Twist Triangle Height in Static Twisting.

Nomenclature

E = Filament elastic modulus

h = Vertical location of the twist point (height of twist triangle)

n = Number of filaments

r = Radius of filament

R = Radius of yarn

T = Tension in yarn

w = Width of the ribbon to be twisted.

In considering the twisting of a uniformly distributed bundle of filaments at constant length, it is assumed that:

(1) The filaments are completely elastic

(2) The filaments in the region $-x < R < x$ are not strained. (The x-axis is chosen as shown in Fig. 7.1)

(3) The strain of any filaments at a distance x is given by

$$\epsilon_x = \frac{\sqrt{h^2 + (x - R)^2} - h}{h^2} \qquad 7.1$$

Consider now a length dx at distance x along the base of the twist triangle, then:

The number of filaments in the element is given by

$$dn = \frac{n}{w}\, dx \qquad 7.2$$

Area of filaments in the element dx is

$$dA = \frac{\pi r^2 n}{w}\, dx \qquad 7.3$$

Stress in filaments in dx is

$$\sigma_x = E\, \epsilon_x \qquad 7.4$$

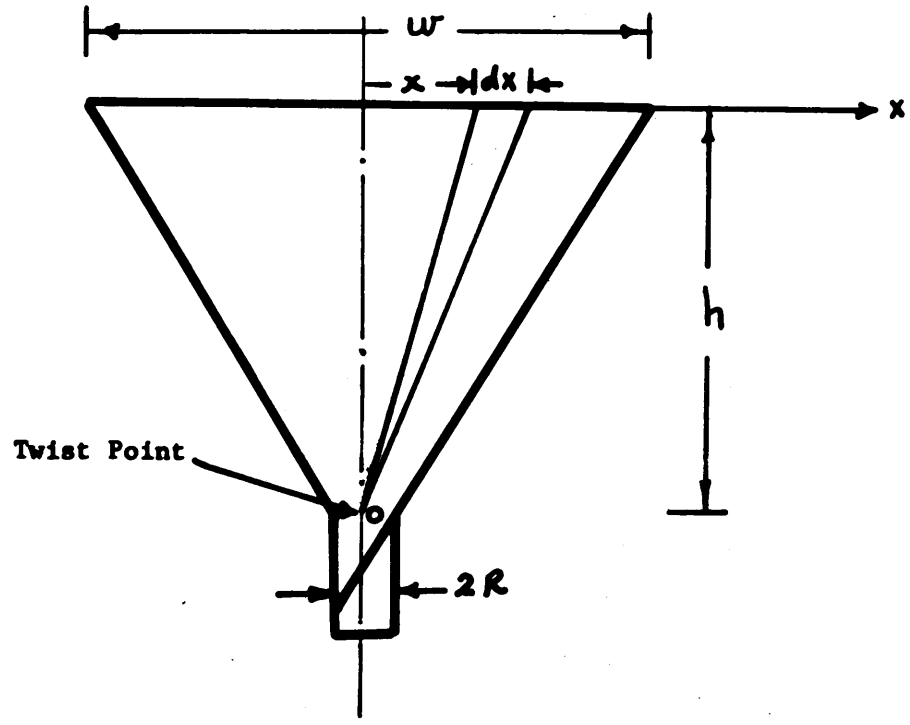

Fig. 7.1 Mathematical Model for the Twisting of Uniformly Distributed Monofilaments at Constant Length

The force (dF) carried by the filaments in dx is

$$dF = {}_x dA = \frac{E\,\epsilon_x\,\pi r^2 n\,dx}{w} \qquad 7.5$$

Contribution of the force in the filaments (dF_v) to yarn tension is then

$$dF_v = \pi \frac{E\,\epsilon_x\,r^2\,n\,dx}{w} \cdot \frac{h}{\sqrt{h^2 + (x - R)^2}} \qquad 7.6$$

The total yarn tension T is given from "7.6" by

$$T = 2\int_0^{W/2} \pi E r^2 \epsilon_x \frac{n}{w} \cdot \frac{h}{\sqrt{h^2+(x-R)^2}} \qquad 7.7$$

by using Equation 1 and integrating we get

$$\frac{T}{\pi E r^2 n} = 1 - \frac{2h}{W} \ln \frac{\sqrt{(\frac{2h}{w})^2 - 4R/w + 1} - 2R/w + 1}{\frac{2h}{w} + 2R/w} \qquad 7.8$$

Equation 7.8 has been checked experimentally by twisting nylon monofilaments at constant length on the Instron tensile testing machine and as twist is being inserted, tension is built up in the strand, of parallel filaments.

The experimental results are plotted together with the theory (Equation 7.8) in Fig. 7.2. The experimental results agree fairly well with the theoretical curve at high $\frac{2h}{w}$ (i.e., at low filaments strains). However, the discrepancy between predicted and experimental values at low $\frac{2h}{w}$ can be explained by the fact that the Young's modulus of nylon decreases with increasing strain. If local (strain related) values of E are used on the basis of the stress-strain curve, the agreement should improve as shown in Fig. 7.3.

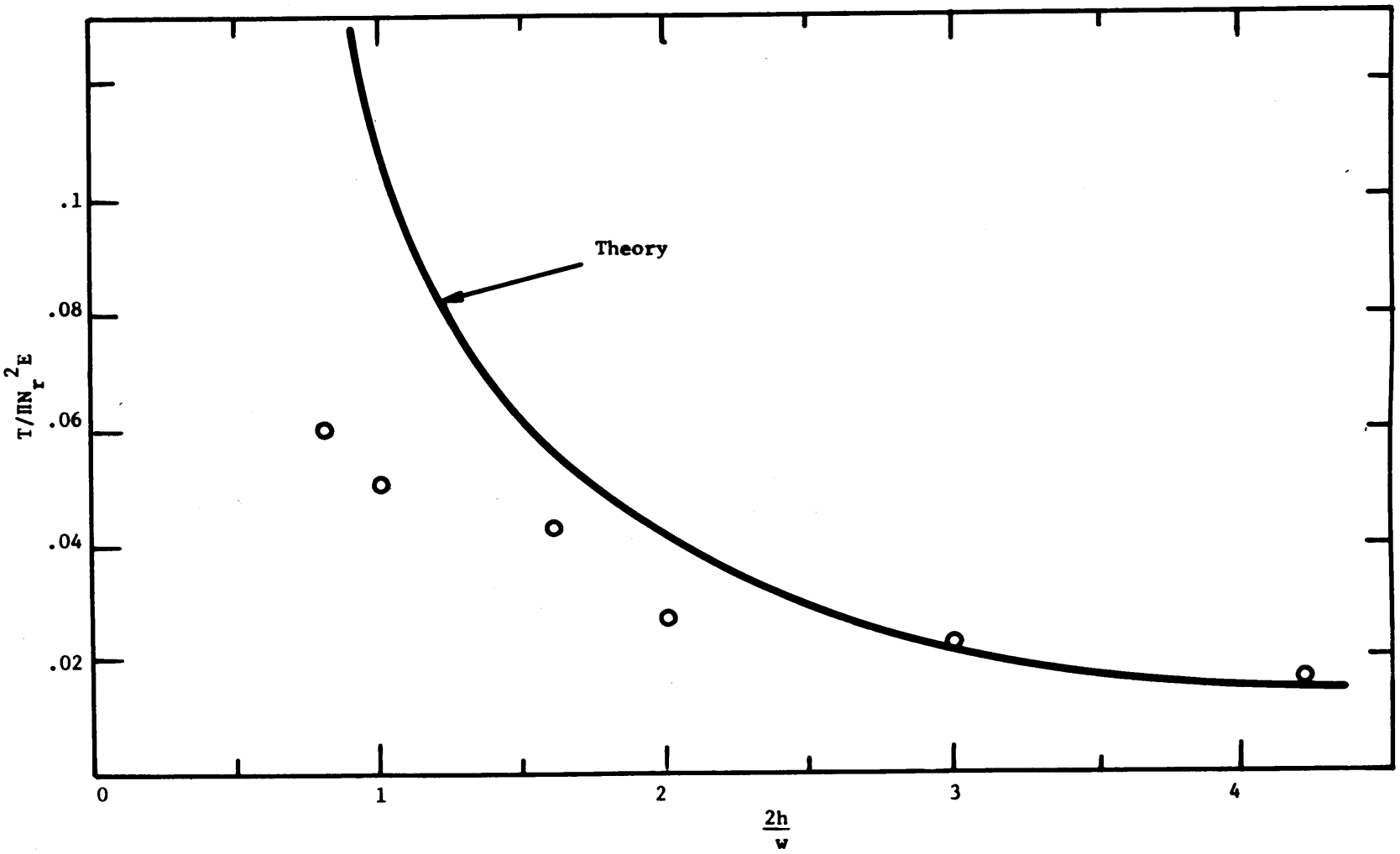

Fig. 7.2 Plot of Equation 7.8 Using a Constant Value for E.

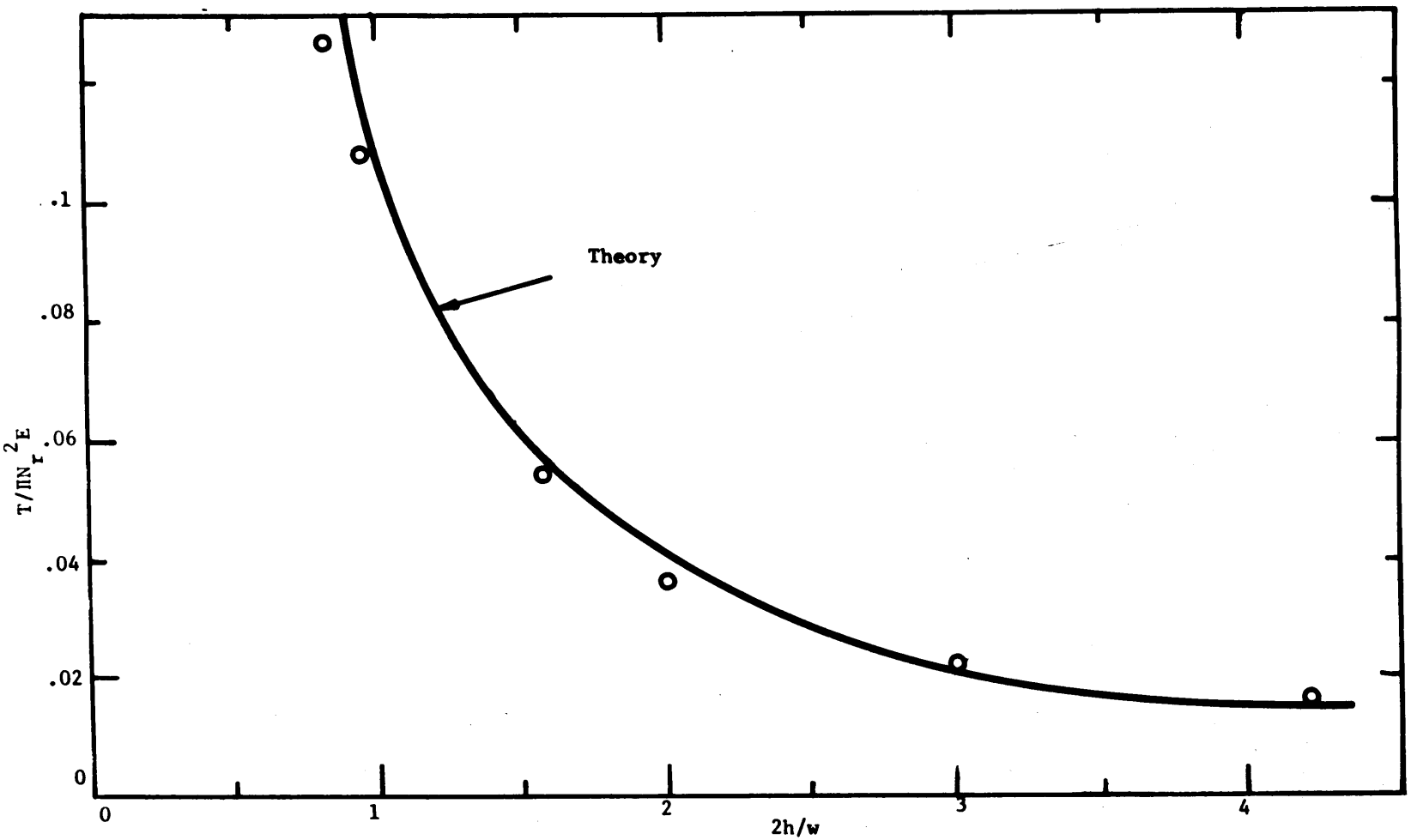

Fig. 7.3 Plot of Equation 7.8, Using Different values for E in the Experimental Data

Appendix B. Method of Calculation of Tension in the Twisting and Winding Zone.

During this investigation the tension in the twisting and winding zone was calculated from DeBarr's equations (5.1 to 5.11) by using the following quantities:

(a) Coefficients of Friction

(1) Friction at Yarn-Traveller and Yarn-Pig Tail Contacts. Table 7.1 represents the values for the coefficient of friction obtained for the different materials used in this thesis.

Table 7.1

Coefficient of Friction at Yarn-Traveller and Yarn-Pig Tail Contacts

Material	Coefficient of Friction	
	At Traveller	At Pig Tail
Viscose Rayon	0.2	.23
Worsted Roving, #1	0.23	.25
Woolen Roving, #2	0.3	.31

These values were obtained by determining the angle to which a yarn (under tension) can be tilted so that the traveller or the pig tail, with a 50 gm. load attached to it, will start sliding down the inclined yarn. The tangent of this angle was taken to be the coefficient of friction.

(2) Friction at Traveller-Ring Contact. The coefficient of friction between the steel ring and the nylon traveller was assumed to be 0.2.

(b) Angles of Wraps of Yarn on Traveller and Pig Tail

(1) At the traveller the angle of wrap was assumed to be π .

(2) At the pig tail the maximum angle of wrap was approximately equal to 60°.

(c) Dimensions of Ring and Bobbin

(1) The bare bobbin diameter used was 2"

(2) The ring radius used was 2.5".

Appendix C. Method of Calculation of Friction-Caused Moments.

The twisting moments caused by friction at both yarn-traveller and yarn-pig tail contacts may be calculated as follows:

(1) Using the tension in the yarn, one can calculate the frictional force "F" at the point of contact using the relation:

$$F = \mu N \qquad 7.9$$

where

μ = Coefficient of friction

N = Normal force at contact point.

(2) Calculate the component "F_m" of this frictional force perpendicular to the yarn axis. The moment of this force around the yarn axis is the friction-caused moment. This force is calculated at the traveller contact from the following expressions:

$$F_m = \frac{F}{\sqrt{1 + \left(\frac{2 V_1}{\omega_T r_y}\right)^2}} \qquad 7.10$$

where

V_1 = Delivery speed (linear)

ω_T = Angular velocity of traveller

r_y = Yarn radius.

However, at the pig tail, Equation 7.10 can be used without the factor 2 appearing in the denominator.

(3) The friction-caused moments (M_f or τ) then can be estimated from the relation:

$$M_f \text{ or } \tau = r_y \cdot F_m \qquad 7.11$$

It is clear from the above relations that the friction-caused moments depend on:

The tension in the yarn,

The coefficient of friction at the contact surface

The radius of the yarn or yarn count, and

The nominal twist inserted, that is the ratio of traveller speed to front roller speed.

In general, these moments will increase with twisting tension, coefficient of friction and yarn radius. They will also increase with decreasing nominal twist.

Appendix D. Variation of Twist along an Irregular Yarn.

Consider a yarn of length L (Fig. 7.4) with n sections having different cross-sectional areas, hence different moments of inertia. We assume that the average cross-sectional moment of inertia of the yarn is I, and that the sections have moments of inertias

$$\alpha_1 I,\ \alpha_2 I,\ \alpha_3 I, \ldots \alpha_i I, \ldots \& \alpha_n I$$

where

$\alpha_i I$ = cross-sectional moment of inertia of the ith section

and

$\alpha_1, \alpha_2, \ldots \alpha_i, \ldots \& \alpha_n$ are constants.

Let us also assume that the lengths of the different sections are

$$S_1, S_2 \ldots S_i \ldots \text{and } S_n$$

where

$$\sum_{i=1}^{n} S_i = L \qquad 7.12$$

Let N be the total number of turns of twist in the yarn of length L. Then the average number of turns/unit length (t) is given by

$$t = N/L \qquad 7.13$$

If we now assume that the torque required to insert the N turns in the yarn is M, then the total energy U (assuming that the yarn is completely elastic) is given by

$$U = \frac{M^2}{2GI} \sum_{i=1}^{n} \int_0^{S_i} \frac{ds_i}{\alpha_i}$$

or

$$U = \frac{M^2}{2GI} \sum_{i=1}^{n} \frac{S_i}{\alpha_i} \qquad 7.14$$

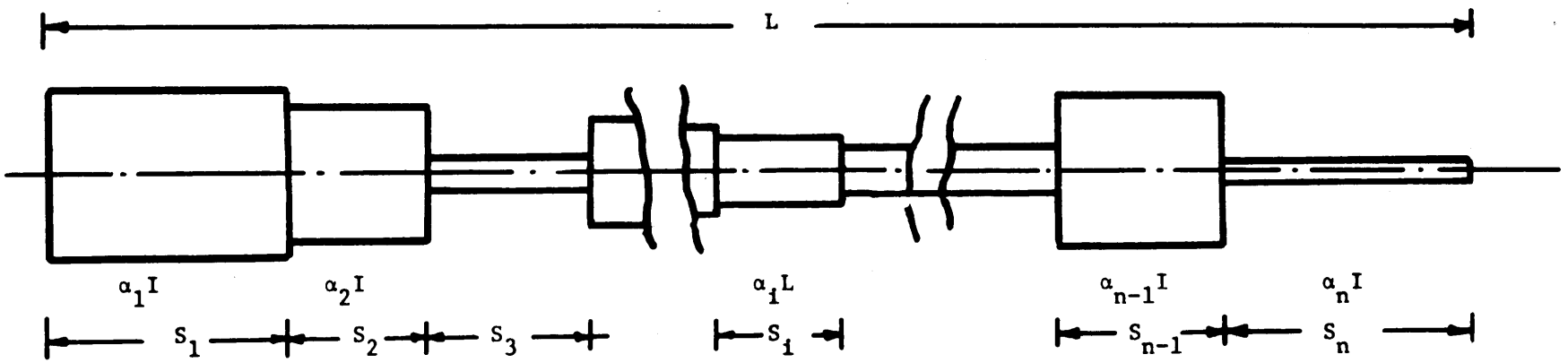

Fig. 7.4 Mathematical Model for an Irregular Yarn

then

$$\frac{\partial U}{\partial M} = 2\pi N \qquad 7.15$$

from which

$$2\pi N = \frac{M}{GI} \sum_{i=1}^{n} \frac{S_i}{\alpha_i} \qquad 7.16$$

or

The local turns/unit length in any section is then given by

$$t_j = \frac{M}{2\ GI\alpha_j} \qquad 7.17$$

where t_j = turns/unit length in the jth section.
Substituting for M from Equation 7.15 into Equation 7.16 we get

$$t_j = \frac{N}{\alpha_j \sum_{i=1}^{n} \frac{S_i}{\alpha_i}} \qquad 7.18$$

From Equation 7.12 and Equation 7.18 we have

$$\frac{t_j}{t} = \frac{L}{\alpha_j \sum_{i=1}^{n} \frac{S_i}{\alpha_i}} \qquad 7.19$$

Equation 7.19 represents the ratio of the local turns/unit length to the average turns/unit length in an irregular yarn.

REFERENCES

1. Martindale
"A Review of the Causes of Yarn Irregularity". Journal Textile Institute 41, 1950, p.p. 340.

2. Cox, D. R. and Ingham, Jr.
"Some Causes of Irregularity in Worsted Drawing and Spinning." Journal Textile Institute 41, 1950, p.p. 376.

3. Annual Conference
"Causes, Measurement and Effects of Yarn Irregularities." Journal Textile Institute 41, 1950, p.p. 335.

4. Hannah, M.
"The Theory of High Drafting." Journal Textile Institute 41, 1950, T 57.

5. Audivert, Hannah, Onions and Townend
"Some Effects of Spinning Conditions on the Irregularity of Yarns Spun on the Ambler Super Draft System." Journal Textile Institute 49, 1958, T1.

6. El-Shiekh, A. H. M.
"On the Dynamics of Wool Spinning." M.I.T. Unpublished S.M. Thesis, 1961.

7. Nissan, A. H. and Wroe, D.
"Some Observations on the Vibration and Whirling of Continuously Loaded Spindles." Textile Research Journal 29, 1959, p.p. 331.

8. Victory, E. L.
"Analysis of Traveller Vibration in Ring Spinning." M.I.T., Unpublished S.M. Thesis, 1958.

9. McNamara, A. B.
"An Investigation of the Drafting and Spinning Processes

in Woolen Ring Frame, Twist Roller Spinning." Leeds University, England, Unpublished Ph.D. Thesis, 1962.

10. Grishin, P. F.
"Balloon Control." Platt Bulletin, Copyright by Platt Bros. (Sales) Limited, Oldham, 1956.

11. DeBarr, A. E.
"A Descriptive Account of Yarn Tensions and Balloon Shapes in Ring Spinning." Journal Textile Institute 49, 1958, T 58.

12. Kyros, W.
"Investigation of Ring Spinning." M.I.T. Unpublished S.M. Thesis, 1957.

13. Fujino, K., Uno, M., Shiomi, A., Yanagawa, Y., and Kitada, F.
"A Study on the Twist Irregularity of Yarns Spun on the Ring Spinning Frame." Journal Textile Machinery Society of Japan 51, 1962.

14. Booth, A. J., Bose, O. N. and Hearle, J. W. S.
"Mechanical Behaviour of Twisted Yarns." Unpublished Final Technical Report, U. S. Army Contract Number DA-91-591-EUC-1833-01-4601-60, October 1962.

15. Bratt, R. L.
"Investigation in Woolen Ring Spinning." Journal Textile Institute 51, 1960, T 1089.

16. Edgerton, H. E., Tredwell, J. and Cooper, K. W. Jr.
"Submicrosecond Flash Sources." Journal of the Society of Motion Picture and Television Engineers, Vol. 70, March 1961.

17. Hearle, J. W. S., and Merchant, V. B.
"Interaction of Position among the Components of a Seven-ply Structure: Mechanism of Migration." Journal Textile Institute 53, 1962, T 537.

18. Peirce, F. T.
"Geometrical Principles Applicable to the Design of Functional Fabrics." Textile Research Journal 17, p.p. 123, 1947.

19. Morton, W. E.
"The Arrangement of Fibers in Single Yarns." Textile Research Journal 26, p.p. 325, 1956.

20. Morton, W. E. and Yen, K. C.
"Fiber Arrangement in Cotton Sliver and Laps." Journal Textile Institute 22, 1952, T 463.

21. Riding, G.
"Filament Migration in Single Yarns." Journal Textile Institute 55, 1964, T9

22. Hearle, J. W. S.
"The Theory of the Mechanics of Staple Fiber Yarns." Pnpublished Report, Textile Division, M.I.T., 1963.

23. Hearle, J. W. S. and El-Shiekh, A. H. M.
"The Mechanics of Wool Yarns." Paper to be published, 1964.

24. Backer, S. and Hearle, J. W. S.
"Structural Mechanics of Textile Materials." Unpublished summer notes, M.I.T., 1964.

25. Anderson, W. W.
"The Dynamic Buckling of Filaments", M.I.T., Unpublished S.M. Thesis, 1964.

26. DeBarr, A. E. and Catling, H.
"Twist Insertion in Ring Spinning and Doubling." Journal Textile Institute, 50, 1959, T 239 and T 424.

27. DuBois, W. F. and Van deRiet, D. F.
"Twist Insertion in Ring Spinning and Doubling." Journal

Textile Institute 50, 1959, T 423.

28. Baird, K.
"Speed of Propagation of Twist in Worsted Yarns." Journal Textile Institute 50, 1959, T 475.

29. Misonow, E. D.
"Die Verbsserung der Arbeitsweise der Spinnmachinen durch Einbau eines Fadenfuhrer--Vibrators." Textil-Praxis, p.p. 782, 1958.

30. Wegener, W. and Landwehrkamp, H.
"Die Drehungsveteilung im Faden beim Spinnprozess." Textil-Praxis, pp 995, 1962.

31. Gessner, W.
"Fadenbruchursachen in der Kammgarnspinnerei." Textil-Praxis, p.p. 58, 1964.

32. Platt, M. M., Klein, W. G. and Hamburger, W.
"Mechanics of Elastic Performance of Textile Materials, Part XIII." Textile Research Journal 28, p.p. 1, 1958.

33. Wegener, W. and Wulfhorst, B.
"Die Drehungsveteilung im Faden beim Spinnprozess." Textil-Praxis, p.p. 1218, 1962.